Calculation of optimum cutting conditions for turning operations using a machining theory

Author:
Meng, Qinghui

Publication Date:
1998

DOI:
https://doi.org/10.26190/unsworks/5335

CALCULATION OF OPTIMUM CUTTING CONDITIONS FOR TURNING OPERATIONS USING A MACHINING THEORY

A thesis submitted in fulfilment of
the requirements for the degree
of Master of Engineering

by

QINGHUI MENG

SUPERVISORS

Dr. Philip Mathew
Dr. Joseph A. Arsecularatne

School of Mechanical and Manufacturing Engineering
University of New South Wales

August, 1998

ABSTRACT

The ever-increasing development and implementation of expensive advanced machines have made the study of machining economics increasingly important. Machining economics is to a great extent about making use of production resources most efficiently and at the lowest possible cost. Since the cost and time of machining are sensitive to the cutting conditions, optimum values have to be determined before a part is put into production. The optimum cutting conditions in this context are those that do not violate any of the constraints that may apply on the process and satisfy the economic criterion. The main objectives of this thesis are to investigate the methodologies and to develop a logical algorithm for predicting the constrained optimum cutting conditions in oblique machining with nose radius tools so that the production cost/time can be calculated and minimised.

Based on a variable flow stress machining theory, a method has been developed for predicting cutting forces, stresses, temperatures, etc. which are then used to check process constraints such as machine power, tool plastic deformation and built-up edge formation, from a knowledge of the work material properties and the cutting conditions. By using the concept of an equivalent cutting edge, the analysis has been extended to the three-dimensional oblique process involving nose radius tools. This method, to a considerable degree, solves the disadvantage of needing a huge amount of preparatory data associated with previous empirical approaches investigated.

A modified form of Taylor tool life equation has been presented and employed in predicting tool life with good accuracy. Using the tool temperatures obtained from the machining theory, a method for determining the constants in this modified Taylor tool life equation has also been developed. This method is shown to reduce the amount of tool life experimental data required considerably.

This work is the first to consider the plastic deformation of the tool as a constraint in the calculation of optimum cutting conditions. To do this, an analytical model has been developed to calculate the stresses inside the cutting edge of a tool. A methodology is described for predicting cutting conditions at which the cutting edge starts to deform plastically when machining with oblique nose radius tools. It is shown how tool stresses and temperatures determined from the machining theory can be used

together with experimental high temperature compressive strength data for the tool material to make these predictions. A series of plastic deformation experiments have been conducted to check the accuracy of the predictions made using the above method. A comparison made between predicted and experimental results for two plain carbon steel work materials and a range of cutting conditions shows good agreement.

Based on economic criteria such as minimum production cost or minimum production time, an optimisation procedure incorporating the above methodologies has been developed to determine the optimum cutting conditions in rough turning with oblique nose radius tools. A C-language computer program has also been developed to predict the constrained optimum cutting conditions. Worked examples are given to validate this optimisation procedure and to demonstrate the effects of cutting conditions, workpiece diameter and carbon content on production cost/time. Further work is proposed for wider applications of this work.

ACKNOWLEDGMENTS

I would like to express my appreciation to a number of people without whom this work would not have been completed. First and foremost, I owe a great debt of gratitude to my supervisors, Dr Joseph A. Arsecularatne and Dr Philip Mathew, who encouraged me to commence this project and then gave me all the support and assistance that I required, especially the financial support in the form of a scholarship, and for these I will always be grateful.

I gratefully acknowledge the valuable help rendered by Professor P.L.B. Oxley during the course of this work , especially during the completion of two papers. His advice and wealth of knowledge brought about many valuable discussions.

The staff in the Industrial Technology and Management Laboratory, especially Ron Fowle, have provided their technical support in the experimental work. Their constant encouragement and guidance is deeply appreciated.

Also I wish to thank A/Prof. R.B. Randall for his understanding and help in my transferring from The University of Newcastle to The University of New South Wales. The same acknowledgment is given to Professor H. Kaebernick who introduced me to my supervisors.

Thanks are also due to BHP (Long Products Division in Newcastle) for providing some of the steels and the Australian Research Council for financial support.

Finally, I would like to express my gratitude to all my friends for their direct or indirect help in both my study and my livelihood in Australia.

TABLE OF CONTENTS

LIST OF FIGURES

LIST OF TABLES

NOMENCLATURE

A, B	constants for tool life equation (Eq.(5-1))
A_t, b_t, c_t , d_t	constants in the modified Taylor tool life equation (Eq.(3-4))
A_{t1}, b_{t1}, c_{t1}, d_{t1}	constants in Taylor tool life equation (Eq.(3-26))
C	total machining cost ($)
C_1	nonproductive cost per component ($)
C_2	cost of machining ($)
C_3	cost due to tool-changing ($)
C_4	tool cost per component ($)
C_5	work-material cost ($)
C_c	the production cost (when work material cost C_5 is neglected) ($)
C_s	side cutting edge angle (deg)
C_{speci}	specific production cost($/$m^3$)
d	depth of cut (mm)
dA	area of undeformed chip section element
dF	frictional force acting on a chip element
d_{max}	maximum allowable depth of cut (mm)
d_{min}	minimum allowable depth of cut (mm)
d_{opt}	optimum depth of cut (mm)
$d_{t\ max}$	maximum depth of cut based on the length of cutting edge of the tool (mm)
$d_{t\ min}$	minimum depth of cut for the operation, tool and work material (mm)
f	feed (mm/rev)
f_{max}	maximum allowable feed (mm/rev)
f_{min}	minimum allowable feed (mm/rev)
$f_{m\ min}$, $f_{m\ max}$	the minimum and maximum available feeds on the machine tool (mm/rev)
$f_{t\ min}$	minimum feed for the operation, tool and work material (mm/rev)

$U_{m\,min}$, $U_{m\,max}$	minimum and maximum available cutting speeds on the machine tool (m/min)
f_{opt}	optimum feed (mm/rev)
F	frictional force at tool-chip interface (N)
F_C	orthogonal force component in direction of cutting (N)
F_R	force component normal to Fc and F_T (N)
F_S	shear force on AB (Fig.2-5) (N)
F_T	orthogonal force component normal to F_C acting in plane normal to cutting edge (N)
i	inclination angle (deg)
k_{AB}	shear flow stress on AB (N/mm^2)
k_{chip}	shear flow stress in chip at tool-chip interface (N/mm^2)
l_e	length of cutting edge (mm)
N	normal force at tool-chip interface (N)
N_{break}	speed at which the power-speed characteristic of the machine changes (rev/min)
P_1 , P_2 , P_3	three mutually perpendicular components of the cutting force when $C_s \neq 0$ (N)
P_{av}	the maximum available power at spindle speed, N_{rq} (kW)
P_{break}	power at which the power-speed characteristic of the machine changes (kW)
r	radial distance of element from cutting edge (mm) (Fig.4-3)
r_w	radius of cutting (m)
r_ε	tool nose radius (mm)
R	resultant force in orthogonal chip formation model (N)
t	production time (min)
t_1	machining time required for the tool to traverse the component (feed engaged) (min)
t_2	actual cutting time (min)
t_3	tool change time (min)
t_c	cut thickness (mm)
t_{ch}	chip thickness (mm)

t_n	nonproductive time (min)
T	tool life (min)
T_f	average temperature on tool flank face (K)
T_{int}	average temperature along tool-chip interface (deg)
T_{max}	maximum allowable tool life (min)
T_{min}	minimum allowable tool life (min)
T_{Tmax}	maximum available torque (Nm)
T_{mod}	velocity modified temperature (K)
T_{opt}	optimum tool life (min)
T_{rq}	machining torque required (Nm)
P_{rq}	machining power required (W)
N_{rq}	spindle speed required (rev/min)
U	cutting speed (m/min)
U_{max}	maximum possible cutting speed (m/min)
U_{opt}	optimum cutting speed (m/min)
$U_{plastic}$	cutting speed which gives plastic deformation of the tool (m/min)
V	chip velocity (m/min)
V_S	shear velocity (m/min)
w	width of cut (mm)
x	operating cost of machine ($/min)
y	cost per cutting edge for a turning tool with an indexable insert ($)
α	tool rake angle (deg)
α_n	tool normal rake angle (deg)
ε	uniaxial (effective) strain
ϕ	shear angle (deg)
η_c	chip flow angle (deg)
η_0	chip flow angle due to the effect of the nose radius measured from the normal to the side cutting edge on the reference plane (deg)
θ	angle made by the tool element with the tool rake face (rad)
σ_1	flow stress (N/mm^2)
$\sigma_{0.05}$	5% proof stress of the tool material (N/mm^2)

σ_f	average normal stress on tool flank-work interface (N/mm^2)
σ_N	average normal stress on tool rake face (N/mm^2)
σ_r	normal stress component in the radial direction (N/mm^2)
σ_θ	normal stress component in the circumferential direction (N/mm^2)
τ_f	average shear stress on flank face (N/mm^2)
τ_{int}	average shear stress at the tool-chip interface (N/mm^2)
τ_{pmax}	the maximum shear stress at P (Fig.4-3) (N/mm^2)
τ_{max}	maximum shear stress in the tool (N/mm^2)
$\tau_{r\theta}$	shear stress component (N/mm^2)
ψ	stress function
*	star sign to indicate angles associated with equivalent cutting edge

CHAPTER ONE - Introduction

1. Introduction

The developed state of a nation can be indicated, generally, by the gross national product (GNP) which can be taken as a measure of material well-being. In most cases, materials are utilised in the form of manufactured goods. Manufacturing, defined as the transformation of materials into goods for the satisfaction of human needs, had claimed the largest single share in GNP, at least until the 1950's (Schey, 1984). Manufacturing is one of the primary wealth-generating activities for any nation---the growth of manufacturing has led to undeniable advances, not only in providing an abundance of material processions, but also in creating the economic basis for genuine improvements in the quality of life. It has been accepted that, in general, the nations intensively engaged in manufacturing enjoy a higher standard of living, as it is expressed by the per capita output of the economy. Manufacturing should be competitive not only locally but also on a global basis since the proportion of manufactured goods in the export trade of a nation can be taken as a measure of the nation's economic development. The only way to make manufacturing competitive is to attain a high level of profit. Since 40% or so of the selling price of a product is manufacturing cost (DeGarmo et al, 1990), maintaining high level of profit often depends on reducing manufacturing cost. Of the manufacturing processes, metal cutting or machining is often claimed to be the most important process in engineering manufacturing because the vast majority of manufactured products require machining at some stage in their production, ranging from relatively rough or nonprecision work, such as cleanup of castings or forgings, to high-precision work involving tolerances of 0.0025 mm or less. In the USA, the yearly cost associated with material removal has been estimated at about 10 per cent of the GNP in 1980's (Shaw, 1984). Now it is estimated that in the United States alone some US$60 billion annually is spent on machining process (DeGarmo et al, 1990). Obviously efficient machining operations with lowest possible machining cost is a key issue of competitive manufacturing and the nation's economy.

1.1 Economics of Machining

With the rapid development and implementation of sophisticated, high cost, numerically controlled machining systems, machining economics becomes more and more important. Machining economics is to a great extent about making use of production resources most efficiently and at the lowest possible cost. The variables affecting the economics of a machining operation are numerous and include material, people and equipment. These interrelated factors in machining must be combined properly in order to achieve low cost, superior quality and on-time delivery. Fig.1-1 shows the components of manufacturing costs (DeGarmo et al, 1990). Particularly, in machining operations, apart from the cost of material that is used, the other costs are:

(i) cost of labour which is measured per unit time that labour is used,

(ii) cost of operating the machine which includes interest on its cost, depreciation, power consumed and the cost of maintaining it in good running condition,

(iii) overhead cost which consists of the cost of establishment such as buildings, land, the cost of general management including salaries,

(iv) the nonproductive cost which includes the cost of loading and unloading the component, the idle time costs and other non-cutting time costs not included in the total cost, and

(v) cost of tool which may include the cost of material of tool and regrinding of tool.

Of the variables affecting the economics of a machining operation, cutting conditions which include the cutting speed, feed and depth of cut have a great effect on the production rate and cost of a machining operation. For example, with cutting speed, if the unwanted material is cut at a very slow speed, the completion time of the operation would increase, resulting in the increase of the cost of labour, the cost of machine operation, and the overhead cost. If the same operation is done at very high speed, the wear of cutting tool would be accelerated, then the tool has to be replaced more frequently, resulting in an increase of the tool cost. Both of these would make the operation costlier. There is a particular speed which is considered as the optimum value where the operation is most economical.

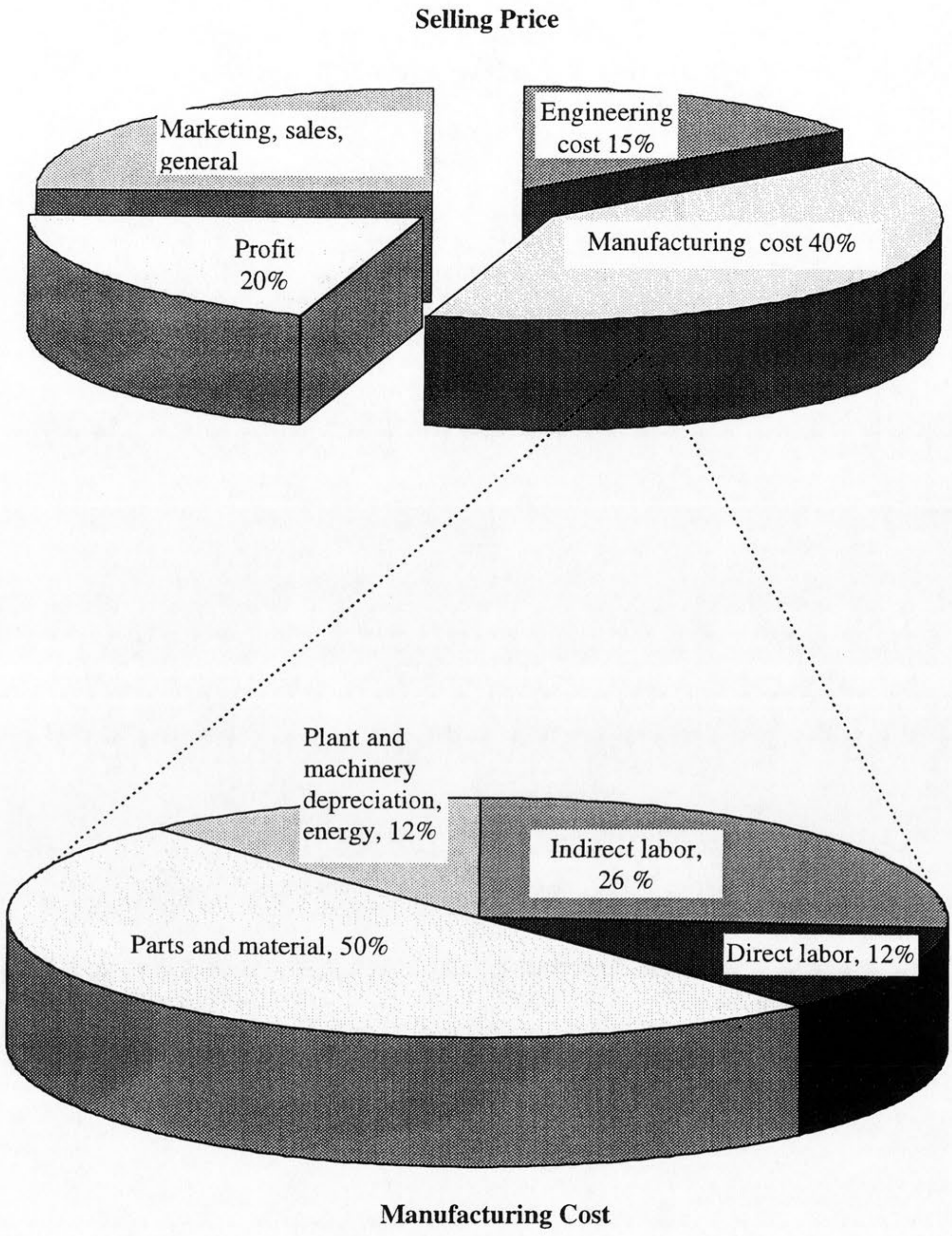

Fig. 1-1 Manufacturing Cost in the Selling Price
(after DeGarmo et al, 1990)

Unfortunately, evidence had confirmed that, even in the aircraft and aerospace industry, the cutting conditions set on computer numerically controlled (CNC) machine tools were far from optimal (Kegg and Zdeblick, 1983). With the continuous increment of financial investment in modern manufacturing systems such as robots, numerically controlled NC/CNC machine tools and computer-integrated-manufacturing systems (CIMS) by manufacturing companies, the use of optimum cutting conditions is definitely essential to offset the massive investment and to improve the efficiency and competitiveness of these companies.

1.2 Optimisation of Cutting Conditions

Since the efficiency and total cost of machining operations are sensitive to the cutting conditions, optimum cutting conditions have to be determined before a part is put into production. Since a manufacturing situation is usually complex and a single machining operation is seldom the only operation carried out on a component by one manufacturer, the true economic optimisation for any one machining operation must take into account the other processes to be performed on the component. The consideration of the production process mix and the production rate at each manufacturing stage will give the greatest return on the overhead investment and the running cost which includes both raw material cost and machining operation cost. The full optimisation should take account of process interactions, the different values of operations at different production rates and possible variation in anticipated sales. Due to the complexity associated with it, the full optimisation is seldom attempted. A procedure that is often adopted is to select machining conditions at each machining operation to give a suboptimised solution. These conditions are then modified, if necessary, after reviewing the process interactions by inspection of the whole production program.

For a machining operation, once the operation planning and the appropriated tools have been determined, its success depends on the optimum cutting conditions. A rational selection (or optimisation) of cutting conditions is the result of taking into account the technical specifications (surface finish, the accuracy of shape and dimensions) listed by the designer, limitations (constraints) of machining processes and production economy. The level of optimisation depends on the extent to which the physical, technical and economic relationship involved in the given machining method are known. Traditionally, the selection of proper cutting conditions has been considered part of the machine operator's duties. Many machining practitioners select cutting conditions by "experience", "rules of thumb", or by reference to tool manufacturers' recommendations or machining data handbook (Metcut Research Associates, 1980). However, for economic selection of the cutting conditions, the required technical and cost data are not readily available to the operator. Consequently an optimum selection can seldom be achieved by this approach.

Attempts have been made to develop other approaches in order to obtain optimum cutting conditions. These approaches broadly fit into two general categories:

(i) predictive methods,

(ii) adaptive control.

Most of the reported work on these methods have not yet reached the stage of practical use. These methods will be discussed in greater detail in the next chapter.

1.3 Objectives of this Work

As noted earlier, since the cost of machining on NC/CNC machines is sensitive to the cutting conditions, optimum values have to be determined before a part is put into production. The optimum cutting conditions in this context are those that do not violate any of the constraints that may apply on the process and satisfy the economic criterion. Since many of the constraints that may apply on the process have to be checked using parameters such as tool life and cutting forces, one has to estimate these parameters with a reasonable degree of accuracy. For a practical machining situation the prediction of the tool life and cutting forces has to be done using empirical equations since no adequate machining theory is available to predict the above parameters. However these empirical equations involve a number of constants which are not readily available. Furthermore these constants depend on many factors thus requiring a huge amount of experimental data for a general workshop situation. To obtain and manage such a huge amount of data is an extremely difficult task. The cost of obtaining the data can exceed the potential savings that might accrue from using that data. Therefore an alternative to the method which uses empirical data to predict cutting forces, tool life, etc. will be of great value.

To overcome the aforementioned difficulties with the empirical approach, the orthogonal machining theory developed by Oxley (1989) and his co-workers has been used in this work to predict tool life, cutting forces, temperatures, etc. and subsequently the constrained optimum cutting conditions. This theory, which takes account of variations in work material flow stress with strain, strain-rate and temperature, has been applied with considerable success in predicting cutting forces, temperatures, etc. from a knowledge of the work material properties and the cutting conditions. Although most of the initial work dealt with the two-dimensional orthogonal process, using the concept of an equivalent cutting edge, the analysis has extended to the three-dimensional oblique process involving nose radius tools (Arsecularatne et al, 1995).

A method for determining the constant and exponents in the extended Taylor tool life equation (Eq.(3-4)) is also discussed. Compared to empirical methods, the developed method, using the temperature information obtained from the machining theory, will considerably reduce the amount of tool life experimental data. Based on the above tool life equation's constant and exponents, the tool life corresponding to a given set of cutting conditions can be predicted.

This work is the first to consider the plastic deformation of the tool as a constraint in the calculation of optimum cutting conditions. To do this, an analytical model is developed to calculate the stresses inside the cutting edge of a tool. This is then used for predicting cutting conditions at which the cutting edge starts to deform plastically when machining with oblique nose radius tools. It is shown how tool stresses and temperatures determined from machining theory can be used together with experimental high temperature compressive strength data for the tool material to make these predictions. A series of plastic deformation experiments are conducted to check the accuracy of the predictions made using the above method. The experiments were made on two plain carbon steel work materials under oblique machining conditions. A comparison is made between predicted and experimental results for a range of cutting conditions which are comparable to those used in practice.

Finally an optimisation procedure is also developed. It incorporates the above models and methods to determine the optimum cutting conditions in rough turning with oblique nose radius tools. This procedure uses a search-methodology to determine the constrained optimum cutting conditions based on economic criteria such as minimum production cost or minimum production time. It can also be used to find the boundary between the feasible and unfeasible depth of cut and feed combinations. A computer program is developed to predict the constrained optimum cutting conditions. The program is written in C-language, which consists of a main function to realise the main logic of the procedure, and some functions to apply the machining theory and to consider the constraints. Worked examples are shown to validate the optimisation procedure, and to demonstrate the effect of cutting conditions on production cost/time.

The above described work is in six chapters. Chapter 1 is the introduction in which the background and the objectives of this research work are described. Also the content of the thesis are summarised. In chapter 2, a literature survey on optimisation criteria and strategies for optimisation are discussed. This survey also reviews the variable flow stress machining theory and its application in oblique machining with nose radius tools. Chapter 3 presents a model for the prediction of constrained optimum cutting conditions. First, the objective functions and constraints of the optimisation are described mathematically. Then the method developed to predict the cutting forces, temperatures, etc. in oblique machining are discussed. A method to determine the constant and exponents in the extended Taylor tool life equation (Eq.(3-4)) is presented. Finally the procedure adopted in this work to determine the optimum cutting conditions for turning operations are given. An analytical model for the calculation of stresses inside the cutting edge of a tool is described in chapter 4. In this chapter a methodology to predict the cutting conditions giving plastic deformation of tools are presented together with a review of previous work on tool plastic deformation. The experimental set-up and procedure for determination of tool plastic deformation are also given together with the comparison between experimental and predicted results. In chapter 5 the computer algorithms for the optimisation are given. Worked examples are also given to validate the optimisation procedure and to demonstrate the effects of cutting conditions, workpiece diameters and carbon content on production cost/time. Conclusions and suggestions for further work are presented in chapter 6.

CHAPTER TWO - Literature Survey

2. Literature Survey

2.1 Optimisation Criteria, Constraints and Strategies

There are unequivocal relationships between the machining conditions and the technical and economic indices of machining. The most important among the variables affecting the economics of a machining operation are the cutting conditions, the machine-tool capacity and the tool material as well as the work material. The most economic machining results would be achieved by the proper combination of the above parameters using some optimisation techniques. The common optimisation techniques attempted so far are predictive methods and adaptive control.

Predictive methods use existing data to determine the optimum cutting conditions before a part is put into production. One of the predictive methods is the data-bank approach. For the last twenty-five years or so many countries have been setting up machinability data banks (C.I.R.P. 1976) for this purpose. Now in industry, optimisation of the machining conditions is often carried out by use of the data bank approach. Machinability data based on past experience or obtained by empirical approach is stored in computers, which is used to estimate the unit production cost when using a variety of tool materials, tool geometrise, feeds, speeds, etc.. The production engineers can estimate the optimum operating conditions for a job by comparing the unit cost for each combination. But the collection of such machinability data especially if they are to be reliable (statistically significant) is extremely time consuming and expensive. Furthermore the optimum result is only approximate since only the most important variables that must be specified to characterise a job are considered. The data-bank approach, although approximate, usually represents a good starting point for the optimisation.

Another approach to optimise cutting conditions is adaptive control (Shaw, 1984), in which performance is monitored and measurements are made during or after a cut, and the cutting conditions adjusted in accordance with a predetermined strategy. Due to the high cost of implementing a hardware control system and the relatively poor performance record to date, the adaptive control methods in turning are not used.

Some researchers (Cook and Goldberger, 1982) have developed a method which is partially predictive, and partially adaptive. The method comprises an attempt to utilise predictive analysis, past experience, and current experience in a way that will give better and better results as time goes on. But this method still uses a reliable data bank as "default" data to enable function in the absence of specific data to a particular operation and it needs a set of logical algorithms for replacing old data with new in a stable fashion, which is still not very clear. It seems that predictive approach is still the most prospective optimisation method.

Considering the ultimate objective of a optimisation process, there exists two kinds of optimisation (Kaczmarek, 1976):

(i) one criterion optimisation,

(ii) multiple criteria optimisation.

The common optimisation criteria used in the one-criterion optimisation are the minimum production cost or the minimum production time (the maximum production rate) (Gilbert, 1950). For a single-pass operation, the machining cost can be written as (Armarego and Brown, 1969)

$$C_T = C_1 + C_2 + C_3 + C_4 + C_5 \qquad (2\text{-}1)$$

where, $C_1 = xt_n$ is the nonproductive cost per component; $C_2 = xt_1$ is the cost of machining where t_1 is the time required for the tool to traverse the component (feed engaged), whether or not the tool is continuously in contact with the work. Neglecting the noncontact time, C_2 can be written as: $C_2 = xt_2$, where t_2 is the actual cutting time per component; $C_3 = xt_3(\frac{t_2}{T})$ is the cost due to tool-changing; $C_4 = y(\frac{t_2}{T})$ is the tool cost per component; C_5 is the work-material cost. When C_5 is neglected, the machining cost becomes

$$C = xt_1 + xt_2 + xt_3(\frac{t_2}{T}) + y(\frac{t_2}{T}) \qquad (2\text{-}2)$$

Obviously, the machining cost C can be reduced by decreasing the nonproductive cost C_1 with the decrease of nonproductive time t_n which includes the loading/unloading time, the idle time, and work-holding time, etc.. Improved tool materials and tool geometry which would give longer tool-life would in turn reduce the total tool costs $(C_3 + C_4)$, resulting in a decrease in the machining cost. Improved work materials with better machinability which gives less tool wear, can also reduce the machining cost. In addition, it may be possible to reduce the machining cost C by decreasing the machining time using high cutting conditions.

Considering the extended Taylor tool life equation (Eq.(3-26)), it should be noted that a high cutting speed (or feed) reduces the machining time, but accelerates the rate of tool wear, resulting in a decrease in tool life. Thus a high cutting speed (or feed) has positive effects on the cost C_2 and opposing effects on the total tool cost $(C_3 + C_4)$. There must be an optimum cutting speed (or feed) which gives the lowest (or minimum) machining cost. It was pointed out that the minimum machining cost occurs as a result of the increasing tool cost as shown in Fig.2-1 (Armarego and Brown, 1969). Obviously the optimum cutting speed can be raised by using improved tool materials which can resist high speeds and give longer tool life values.

Similarly, optimum cutting conditions exist to give the minimum production time (or the maximum production rate), and these optimum values can also be raised by using improved tool materials with greater resistance to high cutting conditions resulting in longer tool life. The production time is given by,

$$t = t_n + t_2 + t_3\left(\frac{t_2}{T}\right) \qquad (2\text{-}3)$$

which can be reduced by decreasing the nonproductive time t_n. Here again, high cutting conditions decrease the actual machining time, but increase the tool changing time. Fig.2-2 shows that the minimum production time occurs with a decrease in machining time and an increase in tool-changing time (Armarego and Brown, 1969).

It has been shown that the cutting speed for minimum production time is higher than the cutting speed for minimum production cost (Armarego and Brown, 1969). The minimum cost criterion would give a lower production rate, while the minimum production time criterion would give a higher cost per component. The overall optimum situation in which both the criteria are considered is usually somewhere between the conditions established by these two criteria.

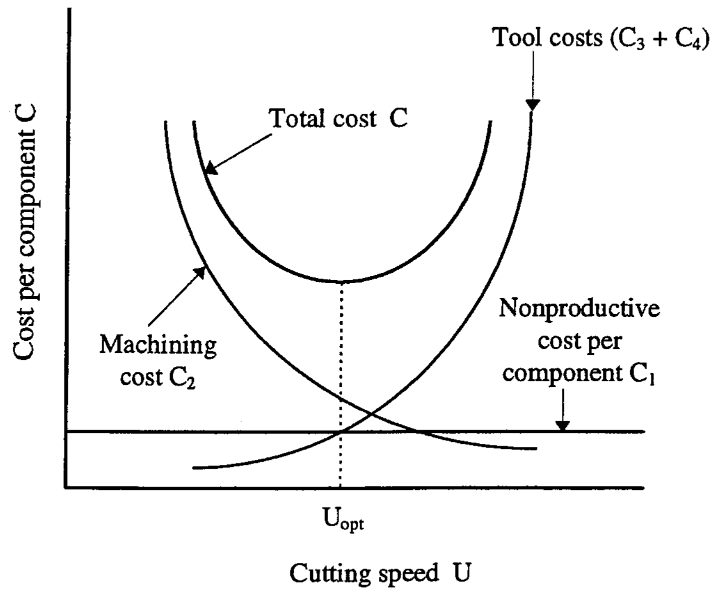

Fig. 2-1 Optimum Cutting Speed based on Minimum Production Cost
(after Armarego and Brown, 1969)

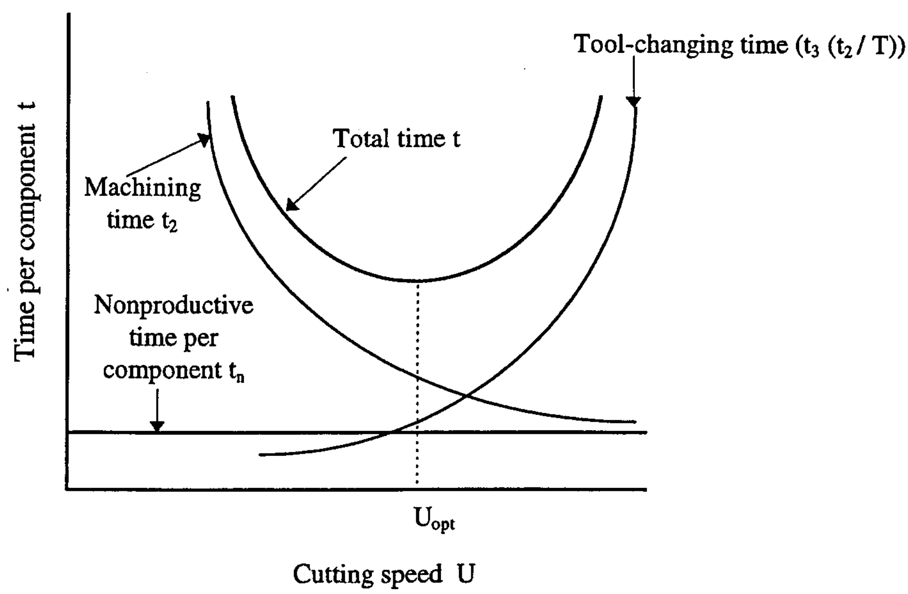

Fig. 2-2 Optimum Cutting Speed based on Minimum Production Time
(after Armarego and Brown, 1969)

It has been argued that a more effective criterion might be needed since the above one-criterion optimisation does not consider the interaction of production cost and production time and vice versa. To take into account production cost, production time and selling revenue, the maximum profit rate criterion was developed in order to maximise the return on the operation per unit time (Armarego and Brown, 1969). The profit rate P_r can be expressed by $P_r = \frac{\text{Income per component} - \text{cost per component}}{\text{Time per component}}$. It has been pointed out that the variables which reduce the production cost and the production time would increase the profit rate. But the optimum conditions determined by the maximum profit rate criterion usually lie close to the minimum production cost conditions unless the profit margin is very high (Armarego and Brown, 1969). Furthermore, the difficulty in obtaining the prerequisite knowledge of the product sale price (or the income per component) needed for the determination of the operation's profit rate makes the criterion difficult to apply.

Agapiou (1992) presented a general multiple-criterion optimisation method which incorporates a combination of the minimum production cost and minimum production time requirements. The key to the applying of this multiple-criterion is the determination of the weight coefficients. However, they are difficult to be estimated due to their uncertainties. So the most popular optimisation criteria are still the minimum production cost and the minimum production time.

Once the theoretical optimum cutting conditions based on the above criteria are obtained, they have to be corrected due to a number of constraints that may apply on the process such as (Colding, 1969):

(i) machine-tool capabilities including maximum/minimum available speeds, feeds, the maximum power/ torque or force, and machine-tool feed and speed steps,

(ii) vibrations due to machine tool structure, set-up conditions and workpiece type,

(iii) surface finish and tolerance requirements,

(iv) cutting tool grade,

(v) diameter or size of the workpiece,

(vi) chip breaking ability,

(vii) maximum chip removal rate due to strength of cutting tool design and tool material, and

(viii) cutting tool geometry.

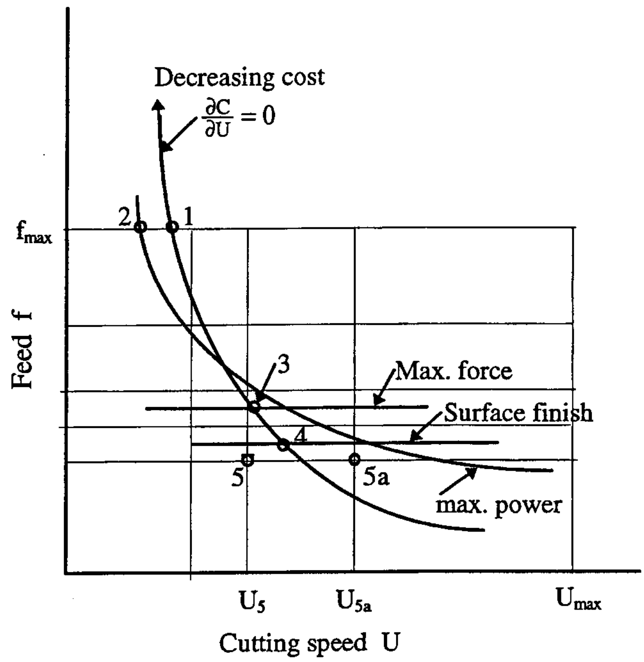

Fig.2-3 Selection of Optimum Cutting Conditions based on Minimum Production Cost when Various Constraints apply
(after Armarego and Brown, 1969)

Armarego and Brown (1969) showed the effects of some constraints on the selection of optimum cutting conditions. According to their work, point 1 (Fig.2-3) is the initial optimum point based on Eq.(2-2) subject to the constraints of the available feed and cutting speed. Then the cutting conditions are modified to satisfy the constraints. First, the cutting conditions are moved to point 2 when the power restriction is considered, then to point 3 to account for the force restriction. Later the surface finish constraint forces the conditions down to point 4. Considering the available feed steps, the conditions have to be moved to the next lower feed step. At this feed step, the available speed steps are checked for the lowest cost until point 5a is found to give the minimum production cost while all the affecting constraints can be satisfied. It was pointed out that the optimisation steps may be varied since the active constraints may vary in different machining processes in practice. For example, in a finishing pass, the most important constraint is the surface finish restriction, so the initial optimum point is checked for the surface finish constraint firstly, then the other constraints such as power and force restrictions can be checked fairly rapidly. In a roughing process, the available maximum feed/depth and power restrictions should be checked firstly, whereas the surface finish restrictions may not apply. In general, the optimal point has to be found within the feasible region defined by constraints. When more practical constraints are incorporated, the complexity of optimisation procedure increases.

A large number of investigations has been carried out to determine the optimum cutting conditions. The procedures reported so far to determine the optimum cutting conditions are based on various nomograms (Brewer and Reuda, 1963), graphical techniques (Colding, 1969), performance envelope (Crookall, 1969), linear programming (Erner and Patel, 1974), geometric programming (Petropoulos, 1973), and search procedures (Hinduja et al, 1985). A comprehensive review of research on optimisation up to 1989 has been given by Arseculаratne (1990). Therefore the following literature survey has been mainly restricted to some selected references published before 1989 and those published after 1989.

Brewer (1958) presented graphs of feed vs velocity with curves of minimum cost to select the optimum velocity and feed for minimum cost per component produced. By adding curves of constant power, he tried to incorporate the constraint of maximum available power into the procedure in determining optimum feed and velocity.

Brewer and Rueda (1963) presented a simplified approach to the selection of optimum cutting conditions by using nomograms. They limited their considerations to turning. First, for a given depth of cut, the maximum feed is determined from experience. Then the most economic cutting speed for this feed is determined using a nomogram. Once the most economic cutting speed is selected, the cutting force and the power consumed are determined using nomograms in order to check the power constraint. The required power for this cut must be within the capability of the motor used. If necessary, the above process is repeated for a lower feed until the optimum values of feed and cutting speed are determined. It should be noted that the nomograms were obtained using empirical data.

Colding (1969) used the chip equivalent concept to describe the tool life relationships, cutting power relationships and productivity for turning, milling and grinding in order to determine the optimum cutting conditions. Chip equivalent is defined as the ratio between the total engaged cutting edge length divided by the chip cross-sectional area. It has been shown that the productivity is proportional to the production rate, but inversely proportional to the production cost or the average production time. When the productivity is a maximum, either the production cost or the average production time is a minimum. In this way, both the production cost and the production rate were incorporated into the optimisation. The relationships between tool life and chip equivalent, the relationships between productivity and tool life, and the relationships between tool life and cutting speed were shown graphically on plots. Then, for constant tool life, the relationships between cutting speed and chip equivalent were plotted. Using the above plot and the economic relationship pertaining to cutting speed versus chip equivalent at constant tool life, the optimum cutting speed was determined.

Brown (1962) presented some general relations for the selection of optimum cutting conditions. By analysing the extended Taylor tool life equation, the machining cost per component and the cutting time per component, he gave the equations for calculating the optimum cutting speed or optimum feed based on minimum production cost, respectively corresponding to constant feed or speed. Consideration was given to single point tools removing material in both one and two passes, and to operations involving more than one tool. He pointed out that, for a single pass operation involving one tool, firstly the maximum permitted feed should be used and an ideal optimum cutting speed could be determined to give the minimum production cost. If the above values of speed and feed violated the available cutting power, then one or both of these values must be reduced which means increasing the cost above the ideal optimum. To make this increase in cost as small as possible, speed and/or feed should be adjusted by as little as is necessary to meet the power restriction. In such situations, the solution for cutting speed should be re-calculated using the maximum available power with the maximum possible feed. In addition, for a single tool operation, he compared the cost of a single pass with the cost of two passes when the total thickness of the material layer to be machined was the same. He pointed out that two passes were not cheaper than one if the single pass did not use maximum power, and a saving using two passes might be obtained when single pass did use maximum power.

The maximum profit criterion has been used by some research workers to determine optimum cutting speed (Okushima and Hitomi, 1964; Wu and Ermer, 1966), or optimum cutting speed and feed (Armarego and Russel, 1966). As noted earlier, one major disadvantage of using this criterion is the difficulty in obtaining the income per component since any particular operation is only one of the many operations needed to manufacture the final product.

To consider the effects of constraints in choosing cutting conditions, Crookall (1969) developed the performance envelope concept for a particular combination of workpiece and tool. The performance envelope can represent simultaneously the many different aspects of performance and behaviour of materials under cut. A performance envelope for a machining process was obtained by superposition of the economical and technological envelopes on a velocity vs feed plane. The economical envelope consisted of minimum production cost and maximum production rate, while the technological envelope consisted of the available maximum power, workpiece rigidity, surface roughness , rapid crating of tool, tool deformation and built-up edge. The economical envelope determined the available technological region. Then the performance envelope gave the feasible machining region, which was used to determine the optimum cutting velocity and feed without violating the above constraints.

Hitomi and Nakamura (1971) used the optimum-seeking machining (OSM) method to obtain the optimum cutting velocity. This method was based on the Taylor tool life equation. Since the constants in the Taylor tool life equation were not known at the initial stage of machining, initial machining conditions were selected based on past experience. A machining operation at the initial machining conditions was conducted and a cutting time up to a tool change was obtained. Using this cutting time as the tool life in Taylor tool life equation, a set of constants was obtained. A new cutting speed was then calculated using Taylor equation with the above constants, and another machining operation at this new speed was conducted and a new cutting time up to a tool change was obtained. Now a new set of constants could be calculated using the above two pairs of practical data (speed and tool life) and a newer cutting speed was calculated. If the tool life is satisfactory from an economical viewpoint, then the optimum cutting conditions were assumed to have been reached. The above procedure was repeated until the velocity between two successive tests fell within ± 5 m/min. It can been seen that, in this method the optimum cutting velocity was determined from data obtained successively in machining tests.

Constraints such as maximum available power, deflection, as well as maximum/minimum available cutting conditions (feeds, speeds and depth of cut) were also considered by Crookall and Venkataramani (1971) in the optimisation of a simple multipass case which consisted of two passes: a roughing and a finishing pass. It was shown graphically that, when the surface finish was considered, the minimum machining time could only be achieved using the two-pass machining instead of a single pass machining.

Armarego and Chia (1980) used a mathematical approach to determine the optimum cutting conditions based on the criterion of maximum production rate for multipass rough turning. In their optimisation strategy, the maximum depth of cut that did not violate the constraints of the maximum available power and the maximum tool force was calculated firstly. Then a minimum number of passes of equal depth of cut was determined. For this depth of cut, the highest allowable feed was selected and finally the optimum cutting speed was determined for every pass.

Nee (1983) used a programmable calculator to perform both optimum analyses and evaluations of machining operations. A single pass operation was considered on a lathe. The surface finish and power were considered as the constraints on optimum machining conditions. The optimisation methodology used in his work can be described as follows. The required data such as available power, estimated drive efficiency, feed and speed ranges, surface finish requirement, economic data, tool nose radius, the available machine, etc., were stored in magnetic cards. An initial relatively high feed and depth of cut was first selected. Then considering the constraint of surface finish, an optimum feed was obtained. For a given tool life, with the above optimum feed and an initial relatively high depth of cut, the cutting speed based on minimum production cost or maximum production rate was then calculated using the Taylor tool life equation. The constraint of power was satisfied by only reducing the initial value of depth from a maximum available power viewpoint. Nee pointed out that such optimum conditions might be quite different to those recommended by handbooks since the handbooks did not account for the different conditions of machine tools as well as dissimilar cost factors in different countries. It was noted that the data required were obtained from cutting tests and from machining handbooks.

Venkatesh (1986) developed systems to determine the cutting conditions using programmable calculators, microcomputers and a main frame computer. In his approach for programmable calculators, machinability ratings, feed values and empirical data for predicting forces, tool life, etc. were retrieved from the data bank available with the calculator for the choice of tool and work materials. For microcomputers, the data system was consisted of generalised empirical equations and a mathematical model. But the equations in the mathematical model were subject to a particular machine used. For the mainframe computer, the data system was built up by storing the experimental data and industrial data in a database. Then these data were analysed statistically and empirical relations were formulated. In the optimisation procedure, Venkatesh used empirical equations to predict tool life, cutting force components, surface finish, rate of crater wear and flank wear. In these equations, in addition to depth of cut, feed and cutting speed, the effects due to nose radius and approach, inclination and normal rake angles were also included. Thus each equation consists of a constant and seven exponents. Using this machinability data base systems in the main frame computer, suitable cutting conditions, which include 'raw data', 'optimum cutting conditions' and 'recommended cutting conditions', can be obtained. The disadvantage of his methods is that the data necessary for these three machinability data base systems are not readily available.

Hinduja et al (1985) used a direct search procedure on the depth-feed (d-f) plane to determine the optimum cutting conditions. This region in the d-f plane gave the depth/feed combinations for adequate chip control. The region was approximated to a quadrilateral and divided into a 20×20 grid, as shown in Fig.2-4. All the points on the grid were checked for the constraints applicable by starting from the point O with the maximum depth. The procedure took into account the changing stiffness of the blank as

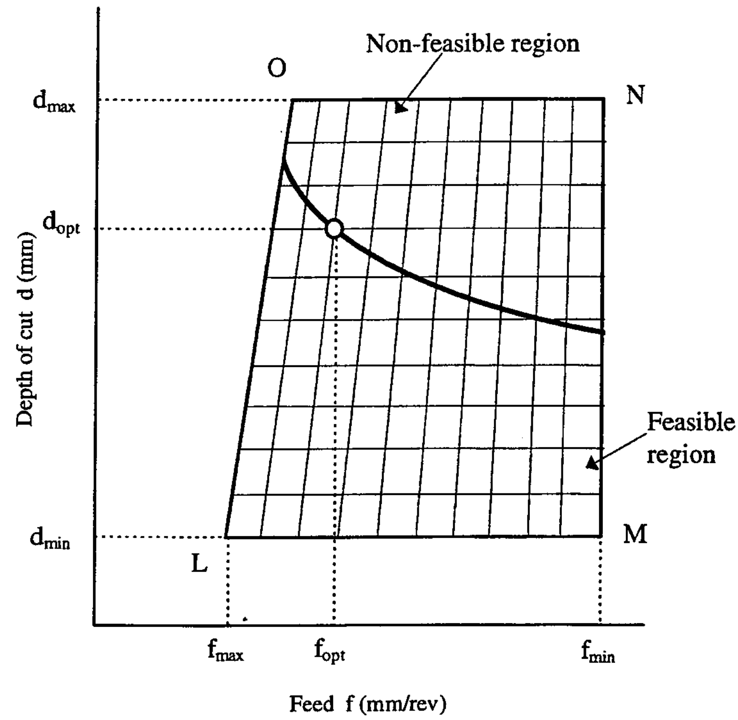

Fig. 2-4 Region on *d-f* Plane for Optimisation
(after Hinduja et al, 1985; Arseculaiatne et al, 1992)

machining proceeds and determined the optimum depth of cut, feed and velocity for each pass in multipass turning. It should be noted that the equivalent chip thickness was used to estimate the force components, which is only suitable for the cutting force component but not for the feed and radial force components (Arseculaiatne, 1993). Moreover, the geometrical data of the component and the blank were read from a file which had to be created before executing the program, which was possible only for relatively simple components with one operation. Since the optimum point always lies on the boundary that separates the feasible and non feasible cutting regions, the search procedure can be restricted to this boundary. This considerably reduces the amount of computation required.

Arseculaiatne et al (1992) used a similar approach in their work. They made the necessary modifications to overcome the above disadvantages. The necessary geometrical information for all the operations was obtained from the output of a process planning module. Optimisation procedures that could be applied in operations such as drilling, grooving, threading and parting-off were also presented. The cutting conditions calculated for each operation were displayed graphically, which could be changed by the user. The geometrical data and the cutting conditions were used to generate the CLDATA, which could be post processed in obtaining the optimum part program. They also developed a method to obtain the necessary data for a particular workpiece/tool combination by measuring the forces on-line using the motor armature current signals of a CNC turning centre.

White and Houshyar (1992) studied the one-dimensional variable optimisation of a single item (i.e. cutting speed as the only decision variable) in single-pass and multi-pass operations. They introduced the concept of quality cost to explore the effects of machining speed on quality. By adding the quality cost of the product to the cost-related objective function, it was shown how roughness of a part would affect its machining cost. They pointed out that quality cost had a measurable effect on choosing the optimum cutting speed under any cost-related criterion.

In order to consider the interactions among the criterion of minimum production cost and the criterion of minimum production time, Agapiou (1992) constructed a combined objective function using the weighted-sums approach. This objective function incorporated both the production cost and production time criteria using different weight coefficients to show the relative importance of each criteria with a constant multiplier for the normalisation of the objective function. The advantage of the combined objective function was shown via numerical examples where the objective function was reduced a two-variable problem (i.e. the cutting speed and feed). The Nelder-Mead simplex method was used to obtain the contours (of the combined objective function and the constraints such as power, force, surface roughness and temperature) on the feed-speed plane for given depth of cut. These contours were then used to determine the optimum cutting conditions. The disadvantage of applying this combined objective function was the determination of the weight coefficients which were difficult to be decided due to their uncertainties.

Da et al (1996) used a multiple criteria optimisation method to determine the optimum cutting conditions and tool inserts for finish turning operations. In order to overcome the disadvantage of the weighted-sums approach, a utility function called 'the tool usage criterion' based on the tool life and material removal rate was constructed by multiplication of these two individual objective functions. Then the goal of the optimisation was to select the cutting conditions resulting in the maximum value given by the above utility function. Constraints such as surface roughness, cutting force, power requirements and chip breakability were considered in determining the optimum values. Nonlinear programming techniques were used to identify optimum process conditions for a given tool insert. Furthermore, comparative analyses of different tool inserts were performed leading to a recommendation of a cutting tool for any special application. However, the calculations of tool life, cutting force and power were still based on empirical equations.

Lee et al (1996) discussed the multiple criteria simulation optimisation problem in their paper. In their approach, a simulation experiment was regarded as a response function from the decision space to the response space. Using a preference function, decision maker can express preferences among the response variables to determine the best compromise solution with a response vector which maximises the preference function. Within the above mathematical framework, the objective of the multiple criteria simulation was to find the best compromise solution. An interactive algorithm for solving the multiple criteria simulation optimisation problem was presented. The method was then applied to the optimisation problem for turning process to show its effectiveness. Optimum values of feed and depth of cut were determined with minimum processing time and good surface finish. However, cutting speed was not considered in this work.

Kilic et al (1993) presented a computer-aided graphical technique to identify the optimum point (feed-speed) for turning operations. By defining a new variable X (X=Uf), the objective function (unit production cost or time) was expressed either in terms of feed f and the variable X or in terms of speed U and the variable X. A method used to determine the variable X was given. By mapping the contours of constraints (tool life, power and surface finish) and the contours of different objective function values (unit production costs or times) in the two-dimensional variable plane of cutting speed vs feed, the optimum combination of cutting speed and feed was obtained.

Gupta et al (1994) attempted to determine the optimum cutting conditions based on maximum profit rate using geometric programming (GP). They proposed that, through modification of the constraint sets (i.e. surface finish, cutting power, tool life and maximum speed and feed), the signomial profit rate function could be converted into posynomial form thus could be solved by GP combined with linear programming (LP). The optimisation problems for single pass and multipass turning were formulated and solved for the maximum profit rate using the GP-LP approach. The optimum cutting parameters were compared with those obtained for minimum production cost or time criteria. Then the following conclusions were arrived at:

'(i) In single as well as multipass turning, the maximum profit rate speed and feed for an individual pass falls in the efficient working range of speed and feed defined by the minimum production cost and maximum production rate criteria.

(ii) The maximum profit rate speed and feed shift towards the minimum production cost speed and feed, respectively, when the revenue is lowered.

(iii) The least number of passes should be used to maximise profit rate or production rate.' The above observations are in agreement with those given by Armarego and Brown (1969). Note that the constants in the modified constraint sets had to be determined using experimental data. In addition, similar to maximum profit criterion, there are difficulties in obtaining the required income per component.

Cus et al (1997), in determining optimum cutting conditions, took into account technological constraints such as the shape of chip, tool life, cutting forces and machine tool power. They suggested that the optimisation based on the above constrains should be achieved by choosing tools which have the geometry that would result in the smallest cutting force for selected cutting conditions. From a tribological viewpoint, they also pointed out that the use of coated cutting tools and the mutually optimum combination of work material, tool material and cooling agent would yield an optimal product for the selected technological values and existing machinery. However the details of the procedure, on how to obtain the required optimum combination of parameters, was not given.

Chen and Rao (1997) argued that the uncertainties encountered in the optimisation process should be considered. These uncertainties were due to the uncertain characteristics of the parameters involved in the formulation of optimum cutting conditions. By rewriting the parameters such as Taylor tool life equation constant and exponents, constraint variables with a transition zone to represent the uncertain nature, they tried to explore and manipulate the uncertainties in the optimisation using fuzzy set theory. A fuzzy optimisation approach was presented for the selection of optimum cutting conditions in the presence of uncertain factors. It was shown that, on the shop floor, there was no substantial difference between the numerical results given by the fuzzy optimisation approach and those given by conventional approach using deterministic constraints. The appropriate application of the fuzzy approach depends on the determination and certainty of the tolerances of parameters involved.

Kee (1995) presented optimisation strategies for selecting optimum cutting conditions in multipass rough turning operations based on minimum production time per component criterion. The constraints considered included available speeds and feeds, maximum force and maximum power. He argued that multipass turning could yield superior production times than single pass turning. In multipass turning the optimal solutions obtained showed that the cutting speeds and feeds were different for each pass although the depths of cut were approximately equal.

Mesquita et al (1995) also presented a model and an interactive program system for the selection of optimum cutting conditions in multipass turning operations. A multiple optimisation criterion based on the weighted-sums approach was used in the optimisation. This multiple criterion was consisted of three criteria: minimum unit production time, minimum unit production cost and minimum number of passes. Constraints such as the available speeds, feeds, depths of cut, cutting forces, occurrence of self-excited vibrations, desired tool life and chip width/thickness ratio were incorporated in the optimisation procedure. But the criterion weights had to be specified by the user in a random way.

In most of the optimisation procedures discussed so far, it has been assumed that the necessary data or empirical equations to calculate parameters such as tool life, cutting forces, etc. are readily available. In fact, the collection of such machinability data is extremely time consuming and expensive therefore not readily available to be used, resulting in the limited application of the above optimisation systems. An alternative to the above empirical approaches is to use machining theories as much as possible to predict tool life, cutting forces, etc. The following sections review the variable flow stress machining theory developed by Oxley (1989) and his co-workers and its application to oblique machining process involving nose radius tools. This theory, which takes account of variations in work material flow stress with strain, strain-rate and temperature, has been applied with considerable success in predicting cutting forces, temperatures, etc. from a knowledge of the work material properties and the cutting conditions.

2.2 Analytical Studies of Machining Process

A large number of investigations has been carried out to investigate the mechanics of the machining process. The well known machining theories are those developed by Merchant (1945), Lee & Shaffer (1951), Shaw et al. (1962) and Kobayashi & Thomsen (1962). These machining theories assume that plastic deformation occurs in the work material at a constant flow stress while the chip formation process can be represented by a shear plane AB (Fig.2-5). It was also assumed that the frictional conditions at the tool/chip interface could be represented by an average coefficient of friction, as for normal sliding friction. So the direction of the resultant cutting force R for a given tool rake angle α is determined by the average friction angle λ (Fig.2-5). Having failed to give an adequate explanation of how work material properties and cutting conditions influence the machining process, the above machining theories have been of little practical help in reducing the amount of empirical results for cutting forces, tool-life, temperatures, surface finish, etc. which are needed in selecting optimum machining conditions.

Fortunately, a more practical machining theory developed by Oxley (1989) and his co-workers is now available for this purpose. In this theory, the aforementioned shear plane model of chip formation is replaced by a shear zone model (Fig.2-5). Therefore, the flow stress of the work material is allowed to vary with strain, strain rate and temperature, and the frictional conditions at the tool/chip interface are described in terms of the shear flow stress in the layer of chip material adjacent to the tool cutting face. In this way, cutting forces and temperatures, which show the influence of cutting

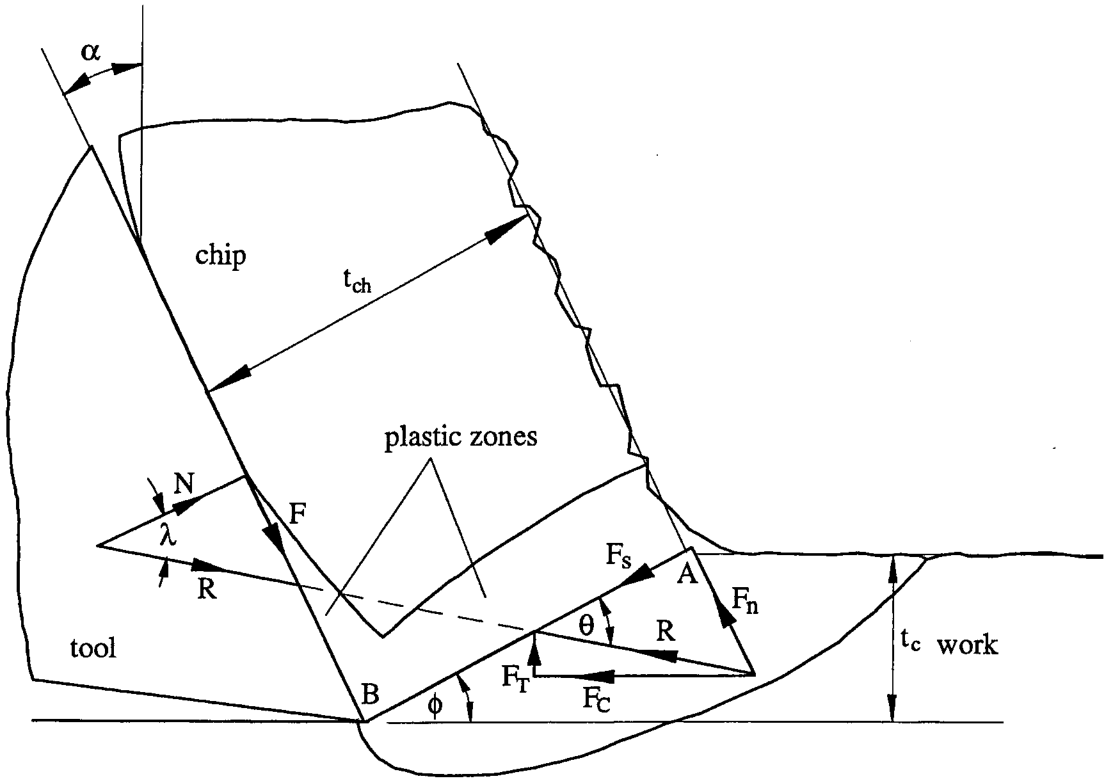

Fig. 2-5 Model of Orthogonal Chip Formation

conditions and work material properties, can be predicted. In addition the method has also been applied successfully to predict parameters such as tool life, tool stresses and the range of cutting conditions in which a built-up edge (which should be avoided in a finishing process) occurs (Arsecularatne et al, 1996). An ability to predict these parameters is essential in the determination of optimum cutting conditions. Although the initial work has mainly been limited to the relatively simple case of orthogonal machining, it has been shown that, by introducing the concept of an equivalent cutting edge, the theory can be extended to the more general case of oblique machining using nose radius tools (Arsecularatne et al, 1995).

2.2.1 The Orthogonal Machining Theory

The machining theory discussed here is for orthogonal machining in which a surface layer of material is removed by a tool with a single, straight cutting edge which is set normal to the cutting velocity, i.e. the angle i in Fig.2-6 is zero. The model of chip formation used in this analysis is given in Fig.2-5. If the undeformed chip thickness t_c is small compared with the width of cut measured along the cutting edge (Fig. 2-5), then the removed chip is formed under approximately plane strain conditions and the analysis is restricted to such conditions. Steady-state conditions (no cracking, no build-up of work material on the cutting tool) are also assumed to apply. The plane AB, near the centre of the chip formation zone, which is found from the same geometric construction as for the shear plane in the well known shear plane model of chip formation, and the tool/chip interface are both assumed to be directions of maximum shear stress and maximum shear strain-rate. It is also assumed that in the chip adjacent to the tool cutting face a boundary layer exists of thickness δt_{ch} across which the velocity changes linearly from zero at the tool surface to the chip velocity V.

The basis of the theory is to analyse the stresses along AB (Fig.2-5) and the tool-chip interface in terms of the shear angle ϕ (angle made by AB with cutting velocity U), work material properties and cutting conditions and then to select ϕ so that the resultant forces transmitted by AB and the interface are in equilibrium - the tool is assumed to be perfectly sharp. Once ϕ is known then the chip thickness t_{ch} and the various components of force can be determined from the following geometric relations:

$$\left.\begin{aligned}
t_{ch} &= \frac{t_c\cos(\phi-\alpha)}{\sin\phi}\\
F_c &= R\cos(\lambda-\alpha)\\
F_T &= R\sin(\lambda-\alpha)\\
F &= R\sin\lambda\\
N &= R\cos\lambda\\
R &= \frac{F_s}{\cos\theta} = \frac{k_{AB}t_c w}{\sin\phi\cos\theta}
\end{aligned}\right\} \tag{2-4}$$

where w is the width of cut, k_{AB} is the shear flow stress along AB.

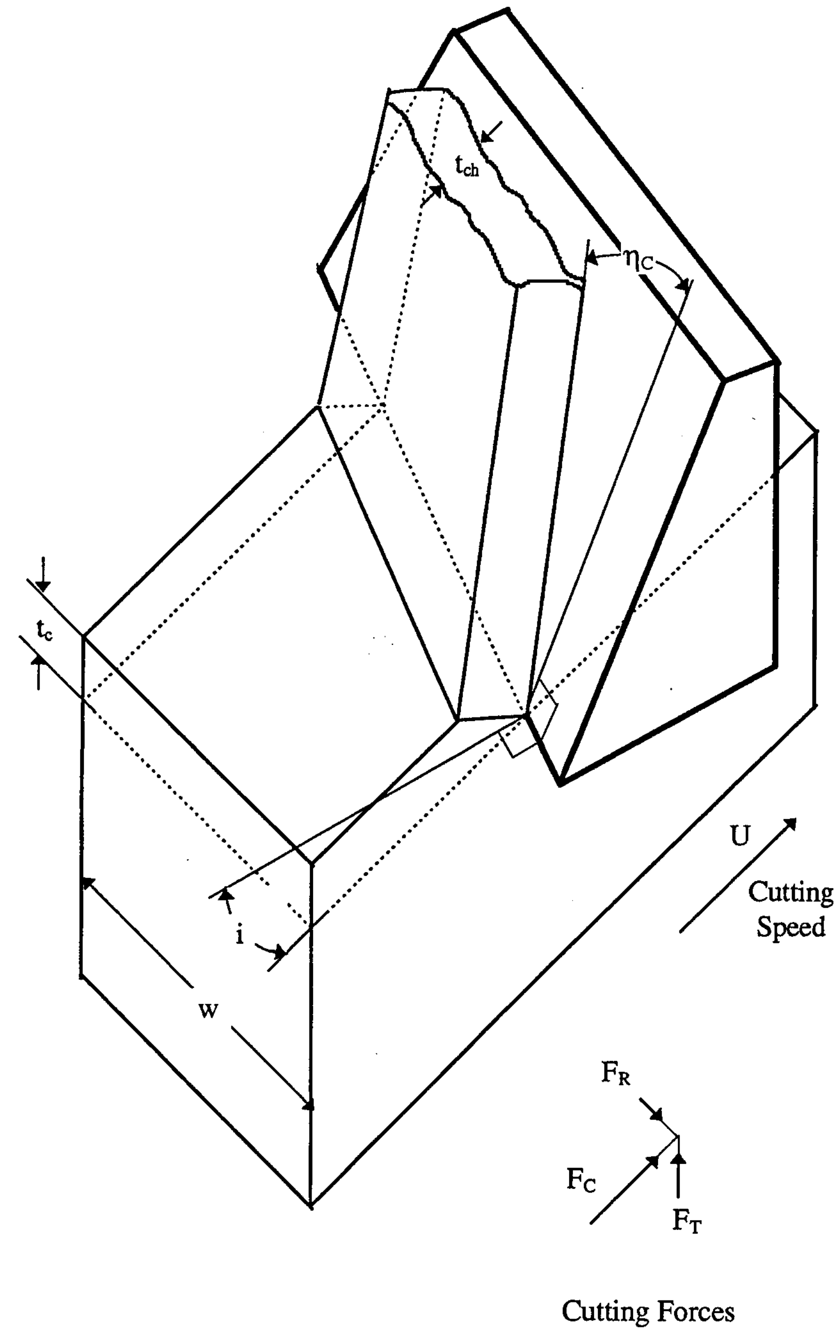

Fig. 2-6 Oblique Machining

The average strain rate along AB can be estimated from the empirical equation (Oxley and Hastings, 1976)

$$\dot{\gamma}_{AB} = C(\frac{V_s}{l}) \tag{2-5}$$

where C is strain rate constant. V_s is the shear velocity and $l = \frac{t_c}{\sin\phi}$ is the length of AB (Fig.2-5).

The stress normal to AB is the hydrostatic stress p and its distribution along AB can be determined by starting at the free surface just ahead of A (assumed to be parallel to the cutting velocity) and by applying the appropriate stress equilibrium equation (i.e. $dp = (dk/ds_1)\,ds_2$, where s_1 and s_2 are distances measured normal to and along AB, k is the maximum shear stress along AB and it is assumed that $k = k_{AB}$). Then it can be shown that for $0 < \phi \le \frac{1}{4}\pi$, the angle θ made by the resultant R with AB is given by

$$\tan\theta = 1 + 2(\tfrac{1}{4}\pi - \phi) - Cn \tag{2-6}$$

where C is the constant in equation (2-5) and n is the strain-hardening index in the empirical stress-strain relation

$$\sigma = \sigma_1 \varepsilon^n \tag{2-7}$$

in which σ and ε are the uniaxial flow stress and strain, σ_1 and n are "constants" which define the stress/strain curve for given values of strain rate and temperature. From the geometry of Fig. 2-5, the angle θ can also be expressed in terms of other angles by the equation

$$\theta = \phi + \lambda - \alpha \tag{2-8}$$

The mean temperature rise in the plastic zone in which the chip is formed is found by considering the plastic work done in this zone and is given by

$$T_{SZ} = \frac{1-\beta}{\rho S t_c w}\frac{F_s \cos\alpha}{\cos(\phi - \alpha)} \tag{2-9}$$

where ρ is the density of the work material and S is its specific heat. The proportion of heat conducted into the work β, which is estimated from the following empirical equations which are based on a compilation of experimental data by Broothroyd (1963):

$$\left.\begin{aligned} &\beta = 0.5 - 0.35\lg(R_T\tan\phi) \quad \text{for} \quad 0.04 \le R_T\tan\phi \le 10.0, \\ \text{and} \quad &\beta = 0.3 - 0.15\lg(R_T\tan\phi) \quad \text{for} \quad R_T\tan\phi > 10.0, \end{aligned}\right\} \tag{2-10}$$

with R_T a non-dimensional thermal number given by

$$R_T = \rho S U t_c / K \tag{2-11}$$

where K is the thermal conductivity of the work material. The limits, $0 \le \beta \le 1$, are also imposed. So the average temperature at AB which is needed, together with the strain rate and strain at AB, to determine k_{AB} and n is taken as

$$T_{AB} = \eta T_{SZ} + T_W \tag{2-12}$$

where T_W is the initial work temperature, η $(0 < \eta \le 1)$ is a factor which allows for the fact that not all of the plastic work of chip formation has occurred at AB.

The average temperature at the tool/chip interface from which the average shear flow stress at the interface is determined is taken as

$$T_{int} = T_{SZ} + T_W + \varphi T_M \tag{2-13}$$

where T_M is the maximum temperature rise in the chip and the factor φ $(0 < \varphi \le 1)$ allows for T_{int} being an average value. Using the results given by Boothroyd (1963), if the thickness of the plastic zone is taken as δt_{ch}, where δ is the ratio of this thickness to the chip thickness t_{ch}, then T_M is given by

$$\lg(\frac{T_M}{T_C}) = 0.06 - 0.195\delta(\frac{R_T t_{ch}}{h})^{\frac{1}{2}} + 0.5\lg(\frac{R_T t_{ch}}{h}) \tag{2-14}$$

where T_C is the average temperature rise in the chip and is given by

$$T_C = \frac{F \sin\phi}{\rho S t_c w \cos(\phi - \alpha)} \tag{2-15}$$

and h is the tool/chip contact length which can be calculated from the equation

$$h = \frac{t_c \sin\theta}{\cos\lambda \, \sin\phi}\left\{1 + \frac{Cn}{3[1 + 2(\frac{1}{4}\pi - \phi) - Cn]}\right\} \tag{2-16}$$

which is derived by taking moments about B of the normal stresses on AB to find the position of R and then assuming that the normal stress distribution at the tool face is uniform so that R intercepts the tool a distance $\frac{1}{2}h$ from B. The maximum shear strain rate at the tool/chip interface, which is also needed in determining the shear flow stress, is found from the equation

$$\dot{\gamma}_{int} = \frac{V}{\delta t_{ch}} \tag{2-17}$$

where V is the rigid chip velocity (Fig.2-5).

Using the above equations, the cutting forces, temperatures etc. can be calculated for given cutting conditions so long as the appropriate work material properties and the values of C in Eqs.(2-5), (2-6) and (2-16) and δ in Eqs.(2-14), (2-17) are known (the methods for determining C and δ will be given later). Briefly, the method used is to calculate for a range of values of ϕ the resolved shear stress at the tool/chip interface from the resultant cutting force obtained from the stresses on AB, that is

$$\tau_{int} = \frac{F}{hw} \tag{2-18}$$

and then for the same range of values to calculate the temperature T_{int} and strain rates $\dot{\gamma}_{int}$ at the tool/chip interface and hence the corresponding values of shear flow stress k_{chip}. The solution is taken as the value of ϕ which gives $\tau_{int} = k_{chip}$ as the assumed model of chip formation is then in equilibrium.

In early applications of the theory C and δ have been assumed to remain constant over a range of cutting conditions. For plain carbon steels they have been taken, on the basis of experimental results, as 5.9 and 0.05 respectively. Oxley and Hasting (1976, 1977) have presented methods to predict C and δ. According to their analysis, for a uniform normal stress at the interface the average normal stress is given by

$$\sigma_N = \frac{N}{hw} \tag{2-19}$$

This stress can also be found from the stress boundary condition at B by working from A along AB. If AB turns through the angle $(\phi - \alpha)$ (in negligible distance) to meet the interface at right angles, as it must do if the interface is assumed to be a direction of maximum shear stress, then it can be shown that

$$\frac{\sigma'_N}{k_{AB}} = 1 + \tfrac{1}{2}\pi - 2\alpha - 2Cn \tag{2-20}$$

and C can be determined from the condition that $\sigma_N = \sigma'_N$. Oxley and Hasting (1976) used 'minimum work' as the criterion in obtaining δ. They proposed that δt_{ch} (the thickness of the plastic zone at the tool/chip interface) can be determined from minimum work considerations. From Eqs.(2-13), (2-14) and (2-17) it can be seen that as δ is reduced, the temperature and strain rate both increase, with T_{int} tending to some finite value and $\dot{\gamma}_{int}$ tending to infinity as δ approaches zero. Usually the flow stress of metals increases with increase in strain rate and decreases with increase in temperature. When this applies it is found that for given cutting conditions a value of δ exists which gives a combination of strain rate and temperature that minimises the shear flow stress k_{chip}. This in turn is found to minimise the rate of both frictional work (FV) and total work ($F_C U$), and it is assumed that in practice δ will take up values satisfying this minimum work condition.

To apply this machining theory to make predictions of cutting forces, temperatures etc., the work material flow stress properties which are expressed in terms of σ_1 and n in Eq.(2-7) have to be determined. For a range of plain carbon steels, this can be done using the high speed compression test results obtained by Oyane et al (1967). The thermal properties used were taken from the experimental measurements of Woolman and Mottram (1964). By introducing the concept of velocity modified temperature T_{mod}

$$T_{mod} = T\left(1 - \frac{\nu \lg \dot{\varepsilon}}{\dot{\varepsilon}_0}\right) \tag{2-21}$$

where T (K) is the temperature, $\dot{\varepsilon}$ is the uniaxial strain rate and ν and $\dot{\varepsilon}_0$ are constants, curves of σ_1 and n against T_{mod} can be plotted (Fig.2-7 shows an example). T_{mod} is a frequently used parameter which combines the effects of strain rate and temperature. To obtain the flow stress for given values of strain, strain rate and temperature from these curves the method used is to determine T_{mod} from the strain rate and temperature and hence the corresponding values of σ_1 and n which can then be substituted together with the strain in Eq.(2-7) to give the stress. In the usual way, uniaxial flow stress results are related to plane strain conditions.

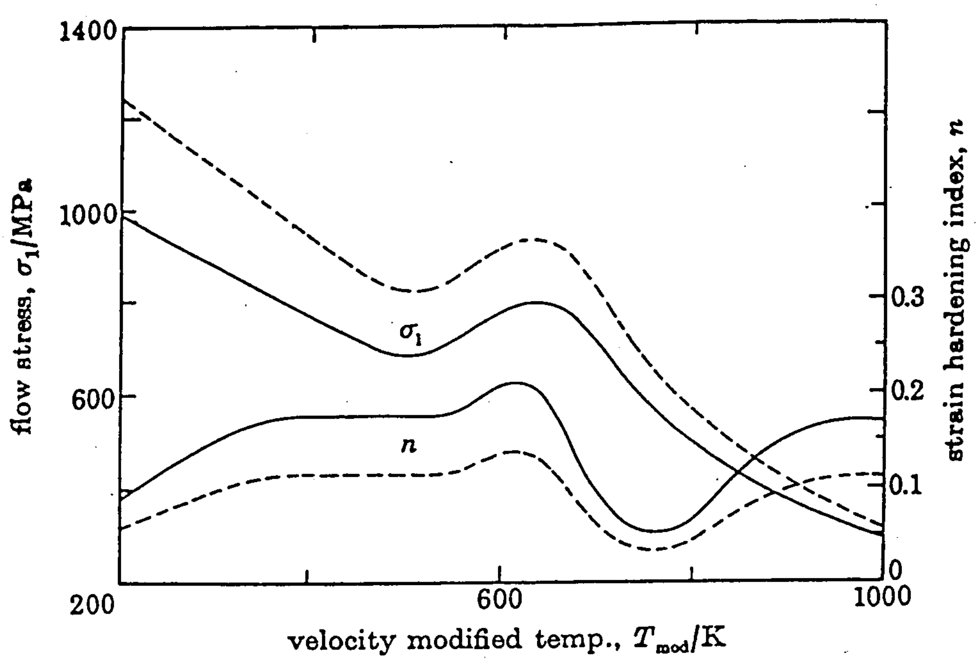

Fig. 2-7 Flow Stress Results Plotted Against Velocity Modified Temperature: ——, 0.2% Carbon Steel; ········; 0.38% Carbon Steel
(after Oxley, 1989)

2.3 Oblique Machining with Nose Radius Tools

The above orthogonal machining theory is extremely useful in relating the physical properties of the work material to its machining characteristics for orthogonal/or approximately orthogonal machining processes. Since most of the practical machining operations are oblique processes (Fig.2-6), it is clear that a theory of oblique machining would be of great value. The oblique process is three-dimensional with the chip flowing across the tool face at an angle η_c (Fig.2-6) which is measured as the angle between the chip velocity and the normal to the cutting edge in the plane of the tool face. In oblique machining, the cutting edge is inclined to the cutting velocity , i.e. $i \neq 0$, where i is the angle between the cutting velocity and the normal to the cutting edge measured in the plane of the machined surface, as shown in Fig.2-6. Considering the extreme complexity of three-dimensional plastic flow of the kind encountered in oblique chip formation, it is not surprising that so far no predictive theory of oblique machining comparable to that for the orthogonal case has been developed.

On the other hand there have been a number of attempts to extend the above orthogonal machining theory to the oblique process. Lin et al (1982) presented a semiempirical approach to do that. They made use of the experimental observations '(a) that, for a given normal rake angle and other cutting conditions, the force component in the direction of cutting and the force component normal to the direction of cutting and the machined surface are very nearly independent of the cutting edge inclination angle and (b) that the chip flow direction approximately satisfies Stabler's flow rule'. They pointed out that the two force components mentioned in (a) could be determined from the orthogonal theory by assuming a zero inclination angle irrespective of its actual value and with the rake angle in the orthogonal theory taken as the normal rake angle. The experiments described by them were made on tubes to ensure that cutting took place only on one edge as assumed in the method developed for predicting forces. Noting that cutting tools were more complex and were normally seen to have two edges that cut simultaneously, Hu et al (1986) made a series of oblique turning tests using sharp nosed tools on a bar to see how the cutting on the end (secondary) cutting edge in addition to cutting on the side (main) cutting edge would influence the cutting forces and chip flow direction. By introducing the concept of an equivalent cutting edge which in essence combines both the side and end cutting edges, they showed how the influence of the latter can be accounted for in predicting the cutting forces.

In the work described above attention was limited to machining with tools without a nose radius. In practice, however. almost all the tools used in industry have a nose radius as it offers a stronger edge, generates a better surface and improves heat transfer, thus reducing the temperature at the cutting edge. Arsecularatne (1995) presented a method by which the chip flow direction and cutting forces etc. can be predicted for oblique nose radius tools using the orthogonal machining theory. This method is now considered.

2.3.1 Chip Flow Direction and Equivalent Cutting Edge

In order to predict the chip flow direction the method adopted for nose radius tools with non-zero rake and inclination angle tools is as follows. The chip flow angle due to the effect of the nose radius is determined first by assuming a tool with zero rake and inclination angles irrespective of their actual values. The equivalent cutting edge for this case is taken to be at right angles to the chip flow direction. The line representing this equivalent cutting edge is now projected onto the face of the tool with non-zero rake and inclination angles with the projected line assumed to represent the equivalent cutting edge for the actual tool. What follows is a review of this method.

2.3.2 Chip Flow Angle due to the Effect of Nose Radius

Young et al (1987) presented a method in which the chip was treated as a series of elements of infinitesimal width. The frictional force component for each element changes in magnitude as well as in direction. These frictional force components were summed up in order to find the resultant and it was assumed that this resultant coincides with the chip flow direction as depicted in Fig.2-8. In this way the resultant chip flow angle due to the nose radius effect, $\overline{\Omega}_0$, measured from the positive Y axis can be determined from the relation

$$\overline{\Omega}_0 = \tan^{-1}\left(\frac{\int \sin\Omega_0 \, dA}{\int \cos\Omega_0 \, dA}\right) \qquad (2\text{-}22)$$

where dA is the area of the undeformed chip element and Ω_0 is the angle a chip element makes with the outward radial direction. The magnitude of the elemental friction force is assumed to vary linearly with the local undeformed chip thickness. Fig.2-8(a) shows

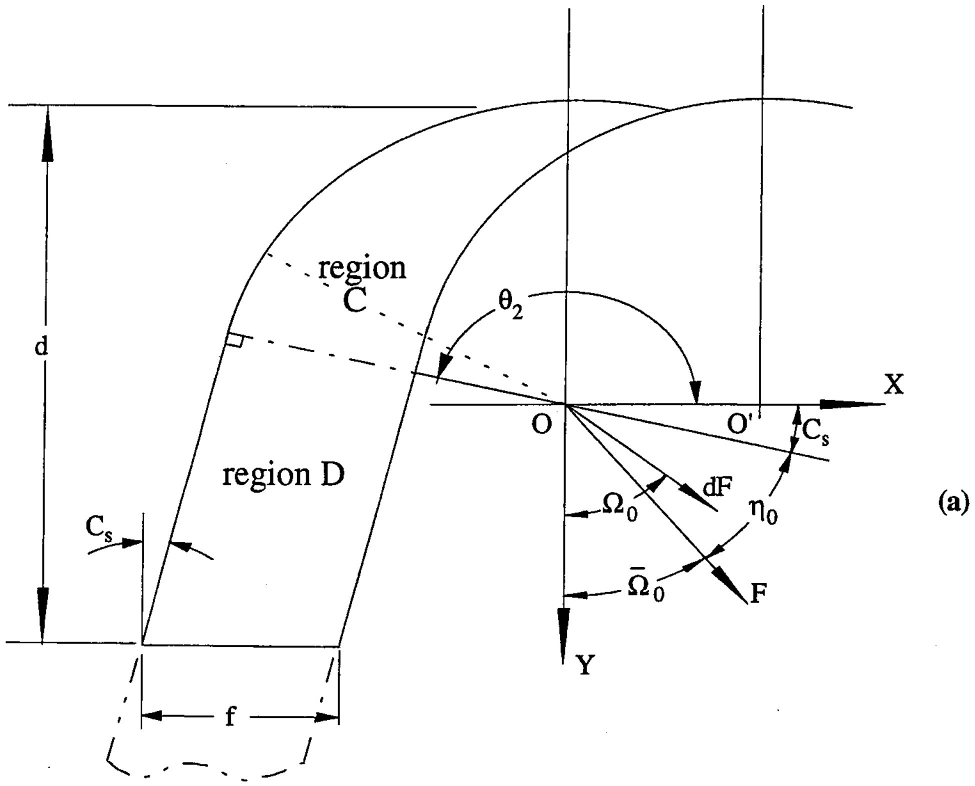

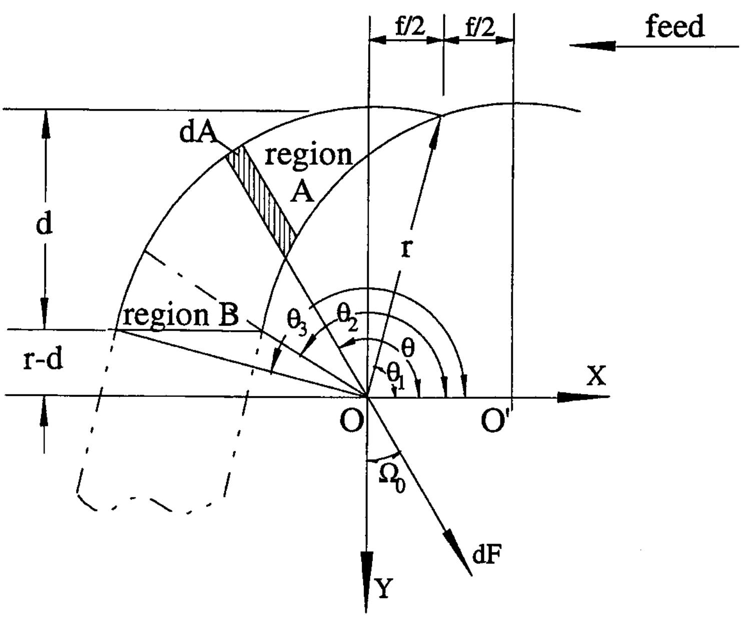

Fig. 2-8 Chip Section Geometries for Chip Flow Model
(after Arsecularatne et al, 1995)

the uncut chip section when the depth of cut is such as to use only the round nose part of the cutting edge. The uncut chip section is given in Fig.2-8(b) is when the cut extends beyond the tool nose to include a part of the straight side cutting edge. By integrating the numerator and denominator of Eq.(2-22) over the entire area of undeformed chip section, the chip flow angle $\overline{\Omega}_0$ is determined. These relations are:

Case 1. When $d \le r(1-\sin C_s)$ as depicted in Fig.2-8(a),

$$NUM = \left[-r\ \sin\theta\right]_{\theta_1}^{\theta_3} + \frac{1}{2}\left[\sin\theta(r^2-f^2\sin^2\theta)^{\frac{1}{2}} + \frac{r^2}{f}\sin^{-1}(\frac{f}{r}\sin\theta)\right]_{\theta_1}^{\theta_2} + f\left[\frac{\sin 2\theta}{4}+\frac{\theta}{2}\right]_{\theta_1}^{\theta_2} + \left[(r-d)\log(\sin\theta)\right]_{\theta_2}^{\theta_3} \qquad (2\text{-}23)$$

$$DEN = \left[-r\ \cos\theta\right]_{\theta_1}^{\theta_3} + \frac{1}{2}\left\{\cos\theta(r^2-f^2\sin^2\theta)^{\frac{1}{2}} + \frac{r^2-f^2}{f}\log\left[(f\cos\theta)+(r^2-f^2\sin^2\theta)^{\frac{1}{2}}\right]\right\}_{\theta_1}^{\theta_2} + \frac{f}{4}(\cos 2\theta)_{\theta_1}^{\theta_2} + \left[-(r-d)\theta\right]_{\theta_2}^{\theta_3}$$

where the limits of integration are

$$\begin{cases} \theta_1 = \cos^{-1}(\dfrac{f}{2r}) \\ \theta_2 = \pi - \tan^{-1}\left[\dfrac{r-d}{(2rd-d^2)^{1/2}-f}\right] \\ \theta_3 = \pi - \sin^{-1}(\dfrac{r-d}{r}) \end{cases}$$

Case 2. When $d > r(1-\sin C_s)$ as depicted in Fig.2-8(b),

$$NUM = \left[-r^2\sin\theta\right]_{\theta_1}^{\theta_2} + \frac{r}{2}\left[\sin\theta(r^2-f^2\sin^2\theta)^{\frac{1}{2}} + \frac{r^2}{f}\sin^{-1}(\frac{f}{r}\sin\theta)\right]_{\theta_1}^{\theta_2} + r\,f\left[\frac{\sin 2\theta}{4}+\frac{\theta}{2}\right]_{\theta_1}^{\theta_2} + \left\{f\left[d-r(1-\sin C_s)\right]-\frac{f^2}{4}\sin 2C_s\right\}\cos C_s \qquad (2\text{-}24)$$

$$DEN = \left[-r^2\cos\theta\right]_{\theta_1}^{\theta_2} + \frac{r}{2}\left\{\cos\theta(r^2 - f^2\sin^2\theta)^{\frac{1}{2}} + \frac{r^2 - f^2}{f}\log\left[(f\cos\theta) + (r^2 - f^2\sin^2\theta)^{\frac{1}{2}}\right]\right\}_{\theta_1}^{\theta_2}$$
$$+\frac{rf}{4}(\cos 2\theta)_{\theta_1}^{\theta_2} + \left\{f\left[d - r(1-\sin C_s)\right] - \frac{f^2}{4}\sin 2C_s\right\}\sin C_s$$

where the limits of integration are $\begin{cases}\theta_1 = \cos^{-1}(\frac{f}{2r}) \\ \theta_2 = \pi - C_s\end{cases}$.

The chip flow direction due to the effect of the nose radius can be written as

$$\overline{\Omega}_0 = \tan^{-1}\left(\frac{NUM}{DEN}\right) \tag{2-25}$$

Therefore the chip flow angle with reference to the normal to the straight side cutting edge of the tool, η_0, can be defined using the angle $\overline{\Omega}_0$ as depicted in Fig.2-8(b) as

$$\eta_0 = \frac{\pi}{2} - C_s - \overline{\Omega}_0 \tag{2-26}$$

2.3.3 Modified Tool Angles and Equivalent Cutting Edge

Using three dimensional geometric analysis the equation for η_0', which is the projection of η_0 on the tool rake face plane as shown in Fig.2-9, is obtained as follows

$$\eta_0' = \cos^{-1}\left(\frac{\sec i - \tan i \tan\eta_0 \tan\alpha_n}{\left\{(\tan i - \tan\eta_0 \tan\alpha_n \sec i)^2 + \sec^2\eta_0\right\}^{\frac{1}{2}}}\right) \tag{2-27}$$

The same technique and η_0' are then used to obtain the equations for the equivalent cutting edge normal rake angle, α_n^*, inclination angle i^* and side cutting edge angle C_s^* which are given below

$$i^* = \sin^{-1}\left(\cos\eta_0' \sin i - \sin\eta_0' \sin\alpha_n \cos i\right)$$

$$\alpha_n^* = \sin^{-1}\left(\frac{\sec\eta_0' \sin i - \sin i^*}{\tan\eta_0' \cos i^*}\right) \tag{2-28(a)}$$

$$C_s^* = C_s + \eta_0$$

For a typical nose radius tool, modified tool angles associated with the equivalent cutting edge and the general tool angles are shown in Fig.2-9.

In summary, a tool with a nose radius r_ε and side cutting edge angle C_s, inclination angle i and normal rake angle α_n can be replaced by a tool having a single straight cutting edge, ie., the equivalent cutting edge, with a side cutting edge angle C_s^*,

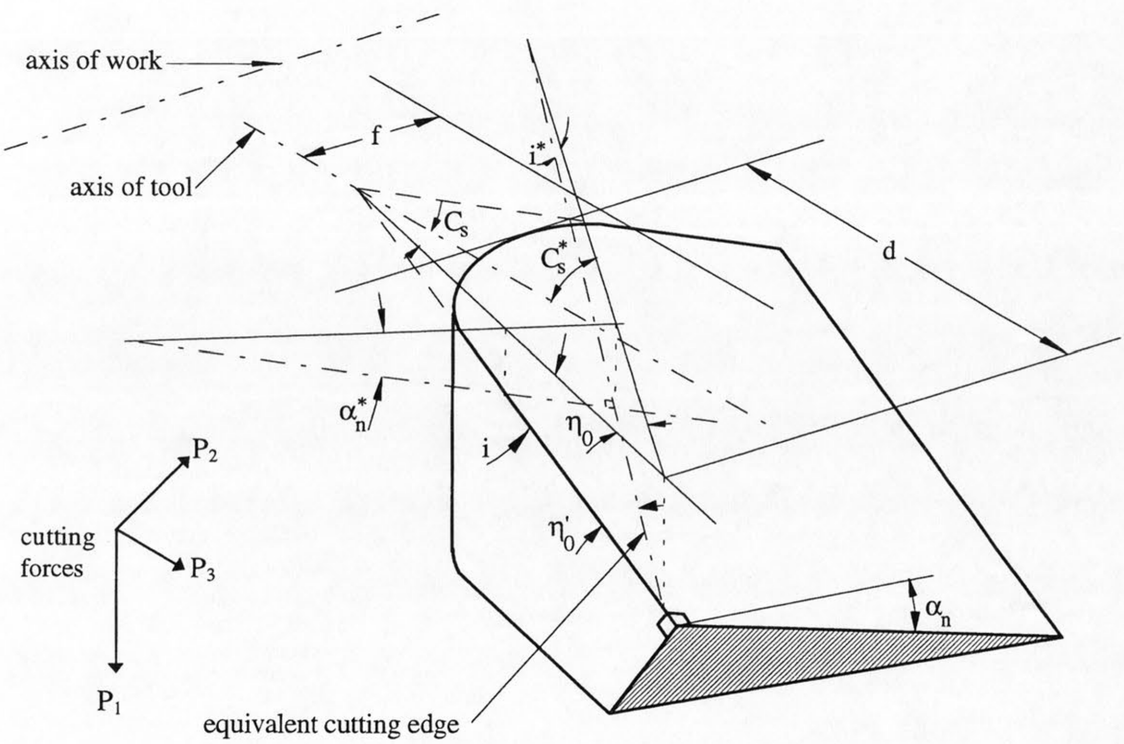

Fig.2-9 Equivalent Cutting Edge and Tool Angles
(after Arseculаratne et al, 1995)

inclination angle i^* and normal rake angle α_n^*. Assuming that the chip flow direction satisfies Stabler's flow rule, the chip flow angle η_c^*, which is measured as the angle between the normal to the equivalent cutting edge and the chip flow direction in the rake face plane, is given by

$$\eta_c^* = i^* \qquad (2\text{-}28(b))$$

2.4 Cutting Forces and Tool Temperatures in Oblique Machining

Once the geometry of the equivalent cutting edge is known, the same procedure as described by Hu et al (1986) is used to determine the cutting force components. This work is based on original analysis of Lin et al (1982) for a single straight cutting edge in oblique machining and uses the following experimental observations:

1. For a given normal rake angle α_n^* and other cutting conditions, the force component in the direction of cutting, F_C, and the force component normal to the direction of cutting and machined surface, F_T, are nearly independent of the cutting edge inclination angle, i^*.
2. The chip flow direction satisfies Stabler's flow rule over a wide range of conditions.

It is assumed that F_C and F_T can be determined from the orthogonal machining theory by assuming zero inclination angle irrespective of its actual value and with the rake angle in the orthogonal theory taken as α_n^*. The tool angles associated with the equivalent cutting edge given by Eq.(2-28(a)), together with the predicted values of F_C and F_T and the value of η_c^* determined from Eq.(2-28(b)), are then used to determine F_R the force normal to F_C and F_T, which results from a non-zero inclination angle, from the relation

$$F_R = \frac{F_C(\sin i^* - \cos i^* \sin\alpha_n^* \tan\eta_c^*) - F_T \cos\alpha_n^* \tan\eta_c^*}{\sin i^* \sin\alpha_n^* \tan\eta_c^* + \cos i^*} \qquad (2\text{-}29)$$

For a tool with a non-zero side cutting edge angle, the force components F_R and F_T no longer act in the feed and radial directions. Therefore, the force components are redefined as P_1, P_2 and P_3, of which the positive directions are taken as the velocity, negative feed and radially outward directions as shown in Fig.2-6. For the equivalent cutting edge these are given by the following equations

$$\begin{aligned} P_1 &= F_C \\ P_2 &= F_T \cos C_s^* + F_R \sin C_s^* \\ P_3 &= F_T \sin C_s^* + F_R \cos C_s^* \end{aligned} \tag{2-30}$$

It is important to note that the force in the direction of cutting remains equal to F_C. As it is F_C which determines the power expended in chip formation, it can be seen that with this model, the oblique tool temperature can be taken as being equal to the temperature calculated from the orthogonal theory.

Until now, it has been shown that the orthogonal machining theory can be extended to predict the chip flow direction, cutting forces and temperatures in oblique machining with nose radius tools by introducing the concept of an equivalent cutting edge. In chapter 3, it will be shown that these predicted tool temperatures can be used to determine the built-up edge formation range and tool life.

It is clear that the above methodologies for predicting cutting forces, tool life, etc. for oblique nose radius tools using as a basis the variable flow stresses machining theory can be used in obtaining the optimum cutting conditions. This will overcome the disadvantages of the empirical approach used in the previous optimisation procedures discussed in this literature survey. It should be noted that the plastic deformation of cutting tools has not been considered as a constraint in the determination of optimum cutting conditions in all the optimisation procedures discussed so far. This is partially due to the lack of a methodology for predicting cutting conditions at which the cutting edge of a tool starts to deform plastically; and partially due to the difficulty in calculating the stresses inside the cutting edge. A survey on plastic deformation of tools will be given in chapter 4, with a methodology and an analytical model. As a result, a more practical optimisation procedure incorporating the above methodologies to determine optimum cutting conditions is now available. All of these will be discussed in greater detail in the following chapters.

CHAPTER THREE - Modelling of the Optimisation of cutting conditions

3. Modelling of the Optimisation of Cutting Conditions

The operations that can be performed on a NC/CNC turning centre include turning, drilling, grooving, threading and parting-off. They can be further classified as roughing operation or finishing operation. As stated earlier, for each operation, a optimisation procedure should be adopted in order to obtain the required pay-back. In view of machining economics, rough turning on a NC/CNC machine is by far the most important operation since large amounts of material are removed thus increasing possible savings. Rough turning is also the most complex operation since the process often involves multiple passes, therefore feed, speed and depth of cut for each pass have to be optimised. This chapter mainly considers the optimisation methodologies for turning operations.

3.1 Economic Consideration and Objective Functions of a Single-Pass Turning Operation

The ultimate objective of the optimisation of cutting conditions is to make the cutting most economic by decreasing production cost and/or production time. The production cost and time are given by Eq.(2-2) and Eq.(2-3) respectively. When considering the effect of cutting conditions on cost and/or time, nonproductive cost C_I and work material cost C_5 can be neglected. Then the production cost can be written as (Arsecularatne et al, 1992)

$$C_c = x\left[t_2 + t_3(\frac{t_2}{T})\right] + y(\frac{t_2}{T}) \qquad (3\text{-}1)$$

where y is the cost per cutting edge for a turning tool with an indexable insert which is determined using the following equation

$$y = \frac{\text{cost of holder}}{400} + \frac{\text{cost of insert}}{0.75 \times \text{number of cutting edges}} \qquad (3\text{-}2)$$

while the production time is given by

$$t = t_2 + t_3(\frac{t_2}{T}) \qquad (3\text{-}3)$$

From Eq.(3-1) and Eq.(3-3), it can be seen that tool life T is one of the parameters which affect the production cost/time. It may be stated that in any operation, when a tool material with higher tool life T is used while the other parameters (i.e. x, y, t_2 and t_3) are held constant, the number of tool changes (or the number of cutting edges needed) $\frac{t_2}{T}$ will be reduced, then the production cost/time will decrease.

Using a modified form of extended tool life equation, the tool life can be expressed as

$$T = \frac{A_t}{U^{b_t} t_c^{c_t} w^{d_t}} \tag{3-4}$$

where t_c and w are cut thickness and width of cut (Fig.2-5) with reference to the equivalent cutting edge (t_c and w can be calculated using f, d and the equivalent cutting edge angle C_S^* for a oblique process using (Eq.(3-25)). It should be noted that this form of tool life equation (Eq.(3-4)) is used in this work because, as will be seen later, the constant A_t, as well as exponents b_t, c_t and d_t do not depend on a number of tool geometrical parameters thus substantially reducing the amount of empirical tool life data required.

Using t_c and w, the volume of metal removed can be calculated as

$$W = t_2 U t_c w \tag{3-5}$$

In developing the necessary equations the minimum cost criterion is considered as shown below. From Eqs.(3-1), (3-3) and (3-5), the cost per unit volume of metal removed (that is specific cost) can be obtained as

$$C_{speci} = \frac{C_c}{W} = \frac{x}{U t_c w} + \frac{(xt_3 + y) U^{b_t - 1} t_c^{c_t - 1}}{A_t w^{1-d_t}} \tag{3-6}$$

By simplifying Eq.(3-6) further

$$C_{speci} = \frac{1}{U t_c w}\left[x + \frac{(xt_3 + y) U^{b_t} t_c^{c_t} w^{d_t}}{A_t}\right] \tag{3-7}$$

By eliminating U in Eq.(3-7) using Eq.(3-4)

$$C_{speci} = \frac{1}{A_t^{1/b_t} t_c^{(b_t - c_t)/b_t} w^{(b_t - d_t)/b_t}}\left[x T^{\frac{1}{b_t}} + (xt_3 + y) T^{\frac{1}{b_t} - 1}\right] \tag{3-8}$$

According to Eq.(3-6), for given values of U and t_c, the specific cost decrease continuously as w increases. Thus a given amount of material can be removed most economically by using the maximum available width/depth of cut. From Eq.(3-8) the optimum value of tool life T for minimum specific cost can be obtained as

$$T_{opt} = (b_t - 1)\left(t_3 + \frac{y}{x}\right) \qquad (3\text{-}9)$$

Similarly, by setting x=1 and y=0 in the above relevant equations, the time per unit volume of metal removed (that is specific time) can also be obtained as

$$t_{speci} = \frac{1}{Ut_c w}\left(1 + \frac{t_3 U^{b_t} t_c^{c_t} w^{d_t}}{A_t}\right) \qquad (3\text{-}10)$$

while the optimum value of tool life T for minimum specific time can be obtained as

$$T_{opt} = (b_t - 1)t_3 \qquad (3\text{-}11)$$

For given values of w and T, it can be shown that material can be removed more economically by using a higher t_c and low cutting speed (ArseculAratne et al, 1992). Using Eqs.(3-4), (3-9) and (3-11), for given values of w and t_c, the optimum cutting speed for minimum specific cost/time is given by

$$U_{opt} = \left(\frac{A_t}{T_{opt} t_c^{c_t} w^{d_t}}\right)^{\frac{1}{b_t}} \qquad (3\text{-}12)$$

It should be noted that, for different optimisation criteria, T_{opt} in Eq.(3-12) is calculated using a different equation (Eq.(3-9) or Eq.(3-11)).

3.2 Optimisation Procedure

Using the objective functions discussed in section 3.1 and the constraints that will be discussed in section 3.3, the optimum cutting conditions can be obtained using the optimisation procedure given below.

The cutting conditions that need to be optimised are depth of cut, feed and cutting speed. The method adopted here, in order to determine the optimum depth of cut and feed, is a direct search procedure on the d-f plane. The d-f plane is defined by the minimum and maximum values of depth of cut and feed available for the given operation, tool, machine and work material. Alternatively these values can be specified by the user. To start with, the d-f plane is divided into a grid. For machine tools which have infinitely variable feeds and speeds, the grid can be determined by the user, say 10×20, as shown in Fig.3-1. For conventional machine tool, the d-f plane is divided into a grid determined by the limited number of feed steps, i.e. only the available discrete feed provided by the machine can be used. Some of the grid points will not be feasible since certain constraints will limit the material removal process (section 3.3). The feasible region is usually separated from the non-feasible region by the arrows, as shown in Fig.3-1. The specific cost/time of machining at each of the feasible points can be determined. However, the point at which the cost/time is a minimum always lies on the boundary separating the feasible and non-feasible regions (Hinduja et al, 1985; Arsecularatne et al, 1992). Therefore, it is not necessary to consider all the points on the d-f plane. This will considerably reduce the amount of calculations.

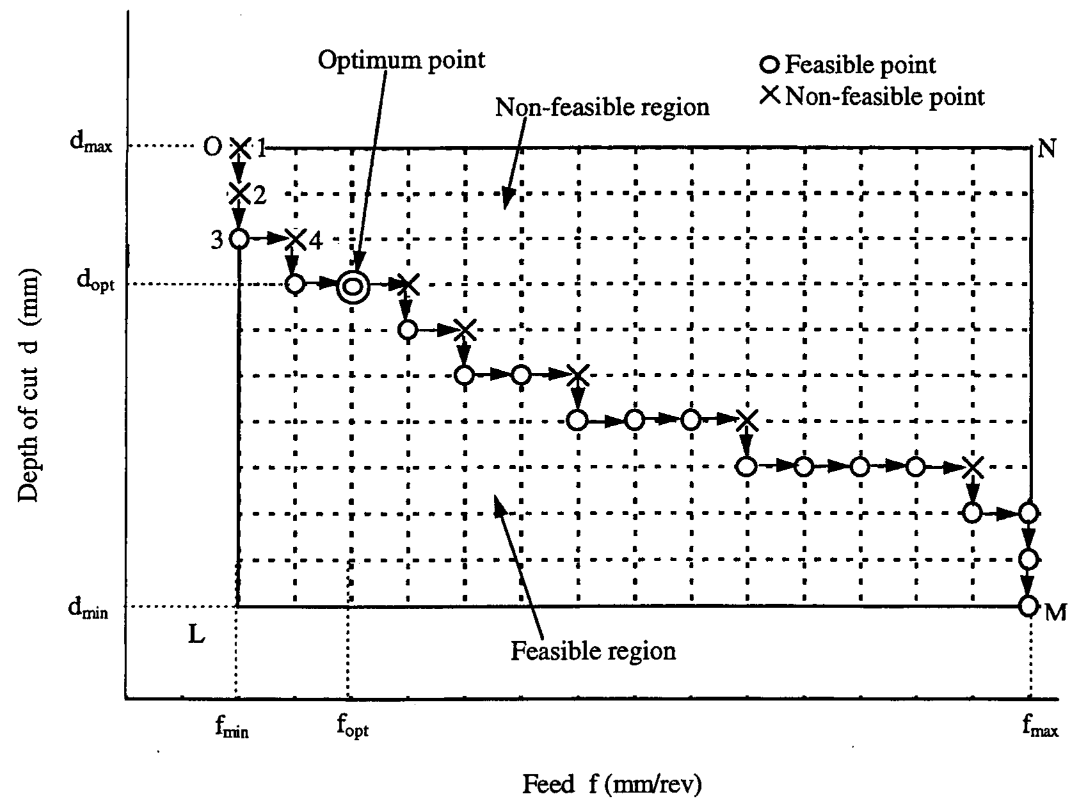

Fig. 3.1 Region for Optimisation and Search for the Optimum Point

The search procedure starts from point O in Fig.3-1 and the steps involved are:

Step 1. Determine the equivalent cutting edge geometry for the given oblique nose radius tool, depth of cut and feed as discussed in section 2.3.3 (Eq.(2-25)). Then determine the corresponding cut thickness t_c and width of cut w with reference to the equivalent cutting edge (Eq.(3-25)).

Step 2. For a grid point defined by (d_i, f_j) the optimum cutting speed is calculated using Eq.(3-12). T_{opt} is the tool life calculated using the appropriate objective criterion (i.e. minimum cost or maximum production rate). If the user do not have the relevant cost and time data (required for the economic criterion) then he/she can specify the tool life directly.

Step 3. The optimum cutting speed calculated in step 2 is checked for the tool plastic deformation and power constraints discussed in section 3.3. If it violates these constraints then the point may still be feasible but a sub-optimum speed U_0 is calculated to satisfy these constraints. If it is non-feasible (eg. Point 1 in Fig.3-1) then the point with the next lower depth but with the feed on the same line (point 2) is tested and the method returns to step 1.

Step 4. The optimum/sub-optimum speed calculated in step 2 is checked for built-up edge (B.U.E.) constraint. If it violates this constraint or the resulting tool life is unacceptably high then the point becomes non-feasible. If it is non-feasible then the point with the next lower depth of cut but with the same feed is tested and the method returns to step 1.

Step 5. If it is feasible (point 3) the specific cost/time of machining is calculated for this point using the appropriate values t_c and w (with reference to d, f) and U (Eqs. (3-7), (3-10)). The point on the grid with the same depth but a higher feed is considered next (point 4) and the method returns to step 1.

Step 6. Steps 1 to 5 are repeated until the first non-feasible point on the lowest depth line or point M is met. The optimum depth of cut, feed and cutting speed are given by the point at which the specific cost/time is a minimum.

It should be noted that the parameters such as cutting forces, stresses, temperatures, etc., which are needed for checking the above constraints (section 3.3), should be recalculated every time when any of the cutting conditions (i.e. depth of cut or feed or cutting speed) are changed.

3.3 Constraints

Due to relatively higher depths and feeds and hence resulting high cutting forces, rough turning operations are generally affected by a number of constraints including available power and tool strength which are influenced directly by cutting forces generated. It is true that, in practice, the specific production cost and/or the specific production time should be minimised by choosing optimum cutting conditions while satisfying a number of practical constraints which limit the permissible values of cutting conditions. The determination of optimum cutting conditions becomes increasingly complex as more technological constraints such as available feeds and speeds, maximum depth of cut, cutting edge plastic deformation as well as available torque and power of machine tool are incorporated. All the pertinent constraints should not be violated in the obtaining of optimum cutting conditions. The methods used to check these constraints are discussed in the following sections.

3.3.1 Tool Plastic Deformation

Cutting tools have a tendency to deform plastically under the influence of the high compressive stresses and temperatures encountered during machining at high speeds and feeds. Plastic deformation of the tool changes the geometry of the cutting edge which in turn causes accelerated rates of tool wear, resulting in a decrease in tool life and in the machined surface quality, as well as catastrophic tool failure. In obtaining the optimum cutting conditions it is important to predict the conditions that cause the cutting edge's plastic deformation and avoid them.

The starting point for predicting the conditions giving plastic deformation of the cutting edge is to calculate the maximum shear stress τ_{max} in the region of the tool adjacent to the cutting edge. τ_{max} can be determined using the stress analysis method presented in chapter 4 (Eq.(4-5)). If the boundary stresses of σ_N, τ_{int}, σ_f, τ_f (Fig.4-3) are known, τ_{max} can be determined. Using the failure criterion (Eqs.(4-6) and (4-7)) and high temperature uniaxial compression test data such as that given by Trent (1968), the cutting speed $U_{plastic}$ (for given feed and depth of cut) which gives plastic deformation of the tool in oblique machining, can be determined if the temperature T_{int} (Section 2.2, machining theory) are known. The stress analysis model for the determining τ_{max} and the methodology for predicting cutting conditions at which the cutting edge of a tool starts to deform plastically will be given in greater detail in chapter 4.

Obviously, for any selected cut thickness t_c and width of cut w (or: feed f and depth d), the selected cutting speed U should satisfy

$$U < U_{plastic} \tag{3-13}$$

3.3.2 Machine Tool Torque/Power

The available torque/power in the machine tool is also one of the most important constraints that must be considered in obtaining optimum cutting conditions, especially in rough machining. For a given radius of cutting r_w and selected cutting speed U , the machining torque T_{rq} and power required P_{rq} in a turning process are given by

$$T_{rq} = F_c r_w \tag{3-14}$$

$$P_{rq} = F_c \frac{U}{60} = \frac{2\pi\, r_w N_{rq} F_c}{60} = 2\pi \frac{N_{rq}}{60} T_{rq} = \frac{\pi\, N_{rq} T_{rq}}{30} \tag{3-15}$$

where F_c is the corresponding force component in direction of cutting, N_{rq} is the spindle speed given by $N_{rq} = \frac{U}{2\pi\, r_w}$. It can be seen that, for given r_w and U, both the required machining torque T_{rq} and power P_{rq} will only depend on cutting force F_c. These parameters are interrelated because one can be derived from the other.

The consumed power in rough turning depends on cutting speed and cutting force (Eq.(3-15)). The cutting force mainly depends on the selected cut thickness t_c and width of cut w (or: feed f and depth d). Hence the cutting power involves all the three cutting parameters, i.e. cutting speed U, cut thickness t_c and width of cut w (or: feed f and depth of cut d). Consequently, the available power would have severe restrictions on the choice of feed (or cut thickness t_c) and cutting speed, particularly for rough turning operations in which the tendency is to use the maximum allowable feed f_{max} (or the maximum allowable value of cut thickness t_c).

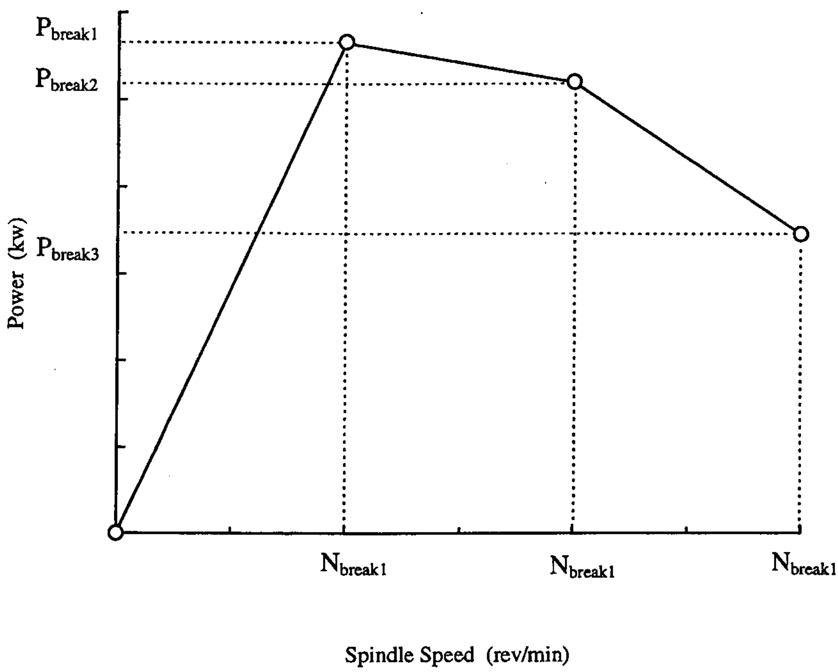

Fig. 3-2 Power-Speed Characteristics of the Machine

Fig.3-2 shows the power/speed characteristics of a typical D.C. motor drive used in a CNC turning centre. It should be noted that there are three speed ranges in Fig.3-2. When the workpiece is cut on such a CNC turning centre, the required torque/power must satisfy the requirements of this power/speed characteristics. For example, in the speed range 0 to N_{break1} available torque is a maximum and is given by

$$T_{Tmax} = \frac{1000 \times P_{break\,1}}{2\pi (N_{break\,1}/60)} = \frac{30 \times 1000 \times P_{break\,1}}{\pi N_{break\,1}} = \frac{30000 \times P_{break\,1}}{\pi N_{break\,1}} \tag{3-16}$$

For given value of feed f and depth of cut d (or, cut thickness t_c and width of cut w) and U, if the required torque to machine the component is greater than T_{Tmax} , the grid point of f and d (Fig.3-1) becomes non-feasible. If the cutting conditions f, d (or, t_c, w) and

U are feasible, the power required to machine the component which can be determined using Eq.(3-15) should meet

$$P_{rq} \leq P_{av} \qquad (3\text{-}17)$$

where P_{av} is the maximum available power at spindle speed, N_{rq}. It should be noted that, if $P_{rq} > P_{av}$ and $N > N_{break\,1}$ then the point f and d may still be feasible but a new value for U should be calculated so that $P_{rq} = P_{av}$. At cutting speed $U = 2\pi r_w N_{break1}$, if $P_{rq} > P_{break\,1}$ then the grid point of f and d becomes non-feasible.

3.3.3 Minimum and Maximum Tool Life Values

It is assumed that tool life equation (Eq.(3-4)) is valid for T only in the range $T_{min} \leq T \leq T_{max}$. For given t_c, w and U the tool life is calculated using Eq.(3-4). If this value of tool life is less than T_{min} cutting speed is reduced so that $T = T_{min}$. If, on the other hand, tool life is greater than T_{max}, the corresponding combination of f and d is considered to be non-feasible.

3.3.4 Available Feeds and Speeds of the Machine Tool Used, as well as the Minimum and Maximum Feeds/Depths for Tool and Workpiece

The optimum cutting speed calculated based on the economic criterion may not be available on the machine tool used because speeds are provided in a limited number of steps, unless the machine is provided with continuous variation of speed in which case the calculated speed can be used. The same applies to feed. For machine tools which have infinitely variable feeds and speeds, the selected feed f and the calculated speed U must lie within the available range of feed and the available range of speed respectively. For a conventional machine tool, only the available discrete feed and speed which are closest to the selected feed and the calculated speed can be used. The selected feed f and the calculated speed U must satisfy

$$f_{m\,min} \le f \le f_{m\,max} \tag{3-18}$$

$$U_{m\ min} \le U \le U_{m\ max} \tag{3-19}$$

where $f_{m\,min}$, $f_{m\,max}$, $U_{m\,min}$ and $U_{m\,max}$ are the minimum or maximum available feeds and speed provided by the machine tool.

A given combination of d and f also must satisfy

$$d_{t\,min} \le d \le d_{t\,max} \tag{3-20}$$

$$f_{t\,min} \le f \le f_{t\,max} \tag{3-21}$$

where $d_{t\,min}$ and $f_{t\,min}$ depend on the operation, tool and work material. For a turning tool with a noise radius, most tool manufacturers recommend that $d_{t\,max}$ and $f_{t\,max}$ could be calculated as follows

$$d_{t\,max} = \frac{2}{3} l_e \tag{3-22}$$

$$f_{t\ max} = 0.8\, r_\varepsilon \tag{3-23}$$

Alternatively $d_{t\,max}$ and $f_{t\,max}$ can be specified by the user. So the selected feed must satisfy

$$f_{t\,min} \le f \le f_{max} \tag{3-24}$$

where, f_{max} = min ($f_{t\,max}$, $f_{m\,max}$). The region for optimisation in Fig.(3-1) is obtained using these values of $d_{t\,min}$, $d_{t\,max}$, $f_{t\,min}$ and f_{max}.

3.3.5 Built-up Edge Formation

Under some machining conditions the chip material welds itself to the tool face and then forms a built-up edge (B.U.E.). Often the B.U.E. continues to grow and then breaks down when it becomes unstable, the broken pieces being carried away by the underside of the chip and the new work piece surface. This cycle of building up and breaking of B.U.E. happens periodically and the machined surface gets dotted with portions of the broken built-up edge. With an unstable B.U.E., the highly strain-hardened fragments which adhere to the chip undersurface and the new work piece surface, can increase the tool-wear rate by abrading the tool faces. A B.U.E. can also contribute to sudden tool failures when tools with carbide inserts are used. For example, when a tool is suddenly disengaged, a portion of built-up edge may be torn off, taking with it a fragment of tool material.

It was also pointed out that (Armarego and Brown, 1969) B.U.E. formation can be a periodic effect which excites vibration of the machining system, irrespective of the natural frequencies of the machining system. So it can be concluded that B.U.E. is one of the principal factors affecting surface finish, tool wear, tool failure and the vibration of a machining system, etc..

Since cutting conditions play a considerable part in the formation of the B.U.E., the prediction of the cutting conditions giving a B.U.E. is most important. Generally speaking, changes in depth, feed or speed that would reduce the tool chip interface temperature, increase the tendency to form a B.U.E.. For a given work and tool material combination, the ranges of speed and feed causing B.U.E. can be determined using the experimental graphs such as that prepared by Trent (1968).

For plain carbon steels it has been shown (Oxley, 1989) that when the values of T_{mod} at the tool-chip interface are higher than (approximately) 700K it follows that the layer of chip material adjacent to the interface that has the highest temperature in the chip is the weakest; therefore deformation should occur in this layer. However, as a result of dynamic strain ageing this is not true for values of T_{mod} in the range (approximately) $500K < T_{mod} < 700K$, and for such cases the chip will generally be weaker some distance from the interface where the temperature is lower. Noting this and the experimental results obtained from machining tests it was proposed that (Oxley, 1989)

(i) if $T_{mod} > 700K$ then there would be no built-up edge but that for lower values there will be,

(ii) even if $T_{mod} < 700K$ there will be no built-up edge if $T_{int} > 1000K$.

Using the experimental results obtained from bar turning tests it has been shown that the built-up edge range can be predicted exceptionally well using the above two criteria. These experiments were carried out under orthogonal conditions (Oxley, 1989) and under oblique conditions using nose radius tools (Arsecularatne et al, 1996).

The parameters such as tool life, cutting forces and temperatures, etc. that can be used are limited by the above constraints, therefore it is necessary to estimate these parameters with a reasonable degree of accuracy. The following sections describe the methods used to calculate the above parameters in oblique machining with nose radius tools.

3.4 Prediction of Cutting Forces, Temperatures, Stresses, etc. in Oblique Machining With Nose Radius Tools

As stated in chapter 2, for given cutting conditions and with a knowledge of the work material properties, the variable flow stress machining theory, which takes account of variations in work material flow stress with strain, strain-rate and temperature, can be used to predict cutting forces, temperatures, etc. for the relatively simple case of orthogonal machining (plane strain). It was also pointed that, by introducing the concept of an equivalent cutting edge (Arsecularatne et al, 1995), this theory can be extended to the more general case of oblique machining.

In chapter 2 it was pointed out that a tool with a nose radius r_ε and side cutting edge angle C_s, inclination angle i and normal rake angle α_n can be replaced by a tool having a single straight cutting edge, ie., the equivalent cutting edge, with a side cutting edge angle C_s^*, inclination angle i^* and normal rake angle α_n^*. Since the force component in the direction of cutting, F_C, and the force component normal to the direction of cutting and machined surface, F_T, are nearly independent of the cutting edge inclination angle (Oxley, 1989), it is assumed that F_C and F_T can be determined from the orthogonal machining theory (Eq(2-4)) by assuming zero inclination angle irrespective of its actual value and with the rake angle in the orthogonal theory taken as α_n^*. Then F_R, the force normal to F_C and F_T which results from a non-zero inclination angle, can be determined using Eq.(2-26). It should be noted that, for a tool with a non-zero side cutting edge angle, the force components are redefined as P_1, P_2 and P_3 which can be determined using Eq.(2-27). The force in the direction of cutting, P_1 remains equal to F_C. Noting this and that the power expended in chip formation is determined by F_C, it was proposed that with this model, the oblique tool temperature can be taken as being equal to the temperature calculated from the orthogonal theory.

The above approach for predicting cutting forces, temperatures, stresses, etc. in oblique machining with nose radius tools (a tool with a nose radius r_ε and side cutting edge angle C_s, inclination angle i and normal rake angle α_n) can be described briefly as follows.

For given cutting conditions (f, d and U) and with a knowledge of the work material properties,

(i) calculate the angles associated with the equivalent cutting edge, i.e. side cutting edge angle C_s^*, inclination angle i^* and normal rake angle α_n^*, using Eq.(2-25).

(ii) calculate the corresponding cut thickness t_c and width of cut w (Fig.2-5) using f, d and the equivalent cutting edge angle C_S^* for a oblique process

$$\begin{aligned} t_c &= f \cos C_s^* \\ w &= \frac{d}{\cos C_s^*} \end{aligned} \tag{3-25}$$

(iii) by assuming zero inclination angle irrespective of its actual value and with the rake angle taken as α_n^* (Eq.(2-25)) as well as the corresponding cut thickness t_c and width of cut w (Eq.(3-25)), using the equations in the orthogonal theory, the cutting forces (Eqs.(2-4), (2-26) and (2-27)), temperatures (Eqs.(2-12), (2-13) and (2-15)) and stresses (Eqs.(2-18) and (2-19)) can be predicted for the oblique machining process with nose radius tools.

The parameters obtained using the above method are sufficient to consider the constraints (section 3.3) in determining optimum cutting conditions in oblique machining with nose radius tools.

It will be seen that the temperatures determined using the above method can also be used to predict tool life for oblique machining with nose radius tools.

3.5 Prediction of Tool Life in Oblique Machining

In order to determine the optimum cutting conditions it is necessary to estimate the tool life. For this purpose, the extended Taylor equation (Eq.(3-26)) is normally used.

$$T = \frac{A_{t1}}{U^{b_{t1}} f^{c_{t1}} d^{d_{t1}}} \tag{3-26}$$

In this equation the influence of operator controllable variables d, f and U on tool life is independently considered. Although this type of equation can be used to obtain good estimates of tool life, one major disadvantage is that the constants A_{t1}, b_{t1}, c_{t1}, and d_{t1} depend on many parameters such as work material, tool material and tool geometrical parameters that include rake angle, nose radius and side cutting edge angle. Thus, every time any one of the above parameters changes, a new set of constants will be required, hence a huge amount of experimental tool life data will be needed.

In order to overcome this problem the modified form of extended tool life equation (Eq.(3-4)) is used in this work. Based on the machining theory, a method which greatly reduces the reliance on experimental data has been developed to obtain the constants for Eq.(3-4). This method will be discussed in greater detail in chapter 5 with an example to illustrate the method.

A computer program which incorporates all the methods and optimisation procedure discussed in this chapter has been completed to determine the optimum cutting conditions in oblique machining with nose radius tools. This program will also be presented in greater detail in chapter 5.

CHAPTER FOUR- Prediction of Cutting Conditions Giving Plastic Deformation of the Tools in Oblique Machining

4. Prediction of Cutting Conditions Giving Plastic Deformation of the Tools in Oblique Machining

4.1 Introduction

The tendency of cutting tools to deform plastically under the influence of the high compressive stresses and temperatures encountered during machining at high speeds and feeds has been discussed by a number of researchers. Plastic deformation of the tool changes the geometry of the cutting edge which in turn causes accelerated rates of tool wear, resulting in a decrease in tool life and in the machined surface quality. Plastic deformation can also cause catastrophic tool failure which can damage the component, the tool and/or machine tool and thus interrupt the machining process substantially. In obtaining the optimum cutting conditions it is important to determine the conditions that cause tool plastic deformation and avoid them.

This chapter presents a method by which the cutting conditions giving plastic deformation of a tool can be predicted in turning with oblique nose radius tools using as a basis the orthogonal machining theory developed by Oxley (1989) and his co-workers. As stated early, this theory, which takes account of variations in work material flow stress with strain, strain-rate and temperature, has been applied with considerable success in predicting cutting forces, temperatures, etc. from a knowledge of the work material properties and the cutting conditions.

4.2 Review of Previous Work

One of the weakest elements in a machining system is the cutting tool being used. The efficiency and reliability of an advanced machining system involving greater capital investment depend on the degree of failure resistance of the cutting tool. It is generally assumed that one of the main causes of ending the life of a tool is gradual wear. Plastic deformation of the cutting edge due to the extreme working conditions of high stresses and temperatures tends to accelerate tool wear, chipping of the cutting edge and/or the breakage of the tool.

The phenomena of plastic deformation of a tool has been discussed in a number of papers. Cook and Goldberger (1982) have outlined a method of selecting the feed to give maximum metal removal rate using the results obtained from tool life tests when machining 4340 steel using carbide (Carbaloy 370) tools. For a given feed, tests were made at a number of cutting speeds and the results were cross-plotted to determine the speed which would give a flank wear land width of 0.25 mm after 10 minutes of cutting. When plotted on a log (speed) versus log (feed) graph they were able to represent the tool life results by two straight lines with the line for the higher feed range steeper than that for the lower feed range. It was also shown that the feed corresponding to the maximum metal removal rate is given by the feed value at the intersection of the two lines (referred to as f'_{max}). Cook and Goldberger have shown how this f'_{max} value decreases as the hardness of the 4340 steel is increased. They also carried out a series of tool-life tests to determine the feed required to actually break the tool-tip. It was found that the value of f'_{max} (based on wear) was substantially less than the feed required for fracture. Cook and Goldberger offered no explanation of why their results show that it is necessary to reduce the cutting speed far more rapidly with increase in feed above f'_{max} in order to maintain the same tool life. Nachev and Oxley (1985) in considering this observation suggested that f'_{max} corresponds to those conditions where the cutting edge starts to deform plastically. This is also consistent with the experimental results of Trent (1968) and Kuljanik (1992) which show that accelerated rates of flank wear can occur when the flank face is bulged outwards by the high stresses acting on the rake face.

Trent (1968) pointed out that cutting tools were subjected to localised stresses, largely compressive, near the cutting edge at the high temperatures. When machining steels, the normal stresses on the tool rake face were frequently of the order of 770 MPa or higher, and the temperatures in this region were 1000 °C or higher, so the most frequently observed plastic deformation was a depression of the rake face and a bulge on the clearance face of the tool close to the cutting edge. Fig.4-1 shows diagrammatically the shapes of plastic deformation of cemented carbide tools in use. Considering the factors which affect the tool deformation,Trent pointed out that high

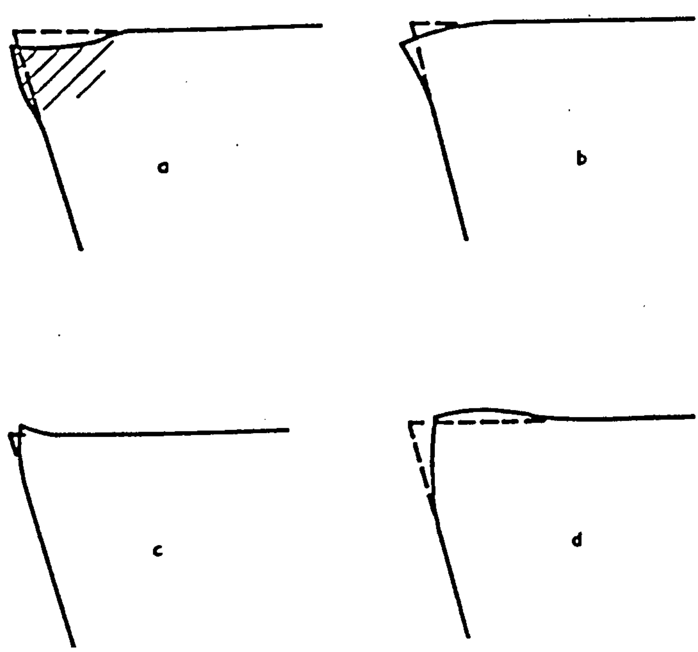

Fig. 4-1 Shapes of Plastic Deformation of Carbide Tools in Use
(after Trent, 1968)

cutting speeds and/or feeds tend to cause tool plastic deformation, and that the high temperature compressive strength of the tool material was one of the factors controlling deformation of the tool. A method was given for measuring the compressive strength of tool materials under conditions up to 1300 °C or higher. Trent found that carbide tools could be plastically deformed by 5% to 10% without visible fracture damage to the structure. He measured the 5% proof stress for a range of carbide cutting tool materials. To an appreciable extent, the 5% proof stress could be used to represent the high temperature strength of tool materials. He also suggested that the high rates of metal removal attainable with carbide tools results mainly from their ability to resist plastic deformation of the cutting edge at high temperatures.

Kujanic (1992) investigated the phenomenon of the macro plastic deformation of the carbide tools. He found that the macro plastic deformation took place approximately three seconds after the start of a cut when an extensive flank wear and vibrations appeared. Since the force component in feed direction had the highest increase when the macro plastic deformation occurred, it was considered as the most sensitive force by which the macro plastic deformation could be detected. He pointed out that the macro plastic deformation of the cutting edge should be considered in determining the cutting conditions under which a tool would be utilised at its maximum. He also proposed a method to avoid the tool macro plastic deformation by first decreasing the cutting speed followed by feed and depth of cut, respectively. But a quantitative method for determining the required decrease in either cutting speed or feed or depth of cut to avoid macro plastic deformation of the cutting tool was not given.

Nachev and Oxley (1985) presented a method to predict those cutting conditions giving plastic deformation of the cutting edge using the tool stresses and temperatures predicted from machining theory together with the high temperature compressive strength data of the tool material given by Trent (1968). Their approach is now considered. In predicting those conditions which will cause plastic deformation of the cutting edge the factors of interest are the tool stresses and temperatures. The machining theory used, assumes a perfectly sharp tool with no forces acting on the clearance face and provides values of average stresses and temperatures on the tool rake face. Nachev and Oxley assumed that the average tool-chip interface temperature, T_{int}

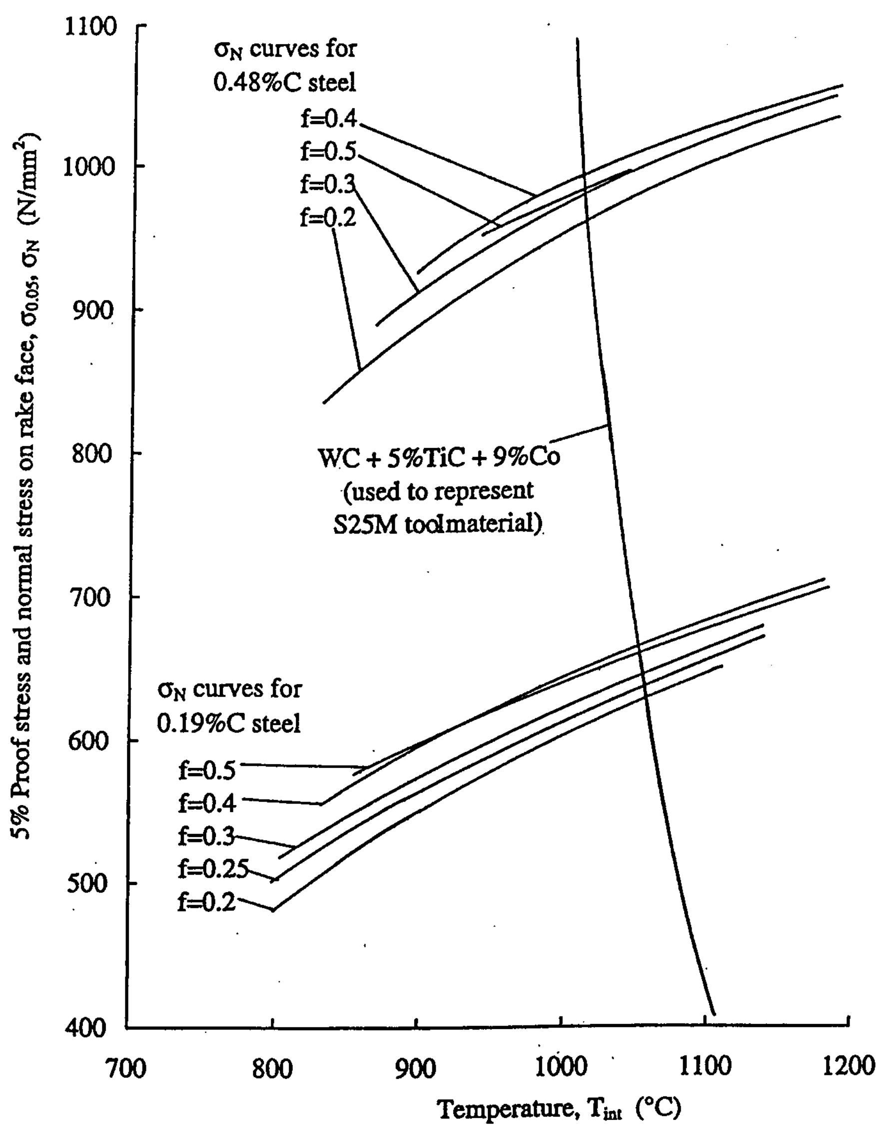

Fig. 4-2 Curves of Tool Material (S25M) Hot Compressive Strength and Predicted Tool Stresses and Temperatures
(after Nachev & Oxley, 1985)

can be taken to represent the cutting edge temperature and that the average normal stress at the interface σ_N would be the stress that causes deformation of the cutting edge. They calculated the values of σ_N and T_{int} from the machining theory for two plain carbon steels (0.19%C and 0.48%C) for feeds in the range 0.2 to 0.5 mm/rev and cutting speeds in the range 100 to 500 m/min. Calculations were made for only one rake angle, i.e. α=5°, which was the rake angle of the tips used in the subsequent tests. The predicted results for σ_N and T_{int} were then plotted (Fig.4-2) together with the curve which was assumed to represent the hot compressive strength properties of the tool material. The σ_N lines given in Fig.4-2 are lines of constant feed with cutting speed increasing along the lines from left to right. The intersections of the σ_N curves with the curve representing the compressive strength of the tool material were assumed to give the feed/speed combinations at which the tool starts to deform plastically. In order to determine the accuracy of these predictions Nachev and Oxley carried out bar turning tests using similar work and tool materials as used in making the predictions. In the tests, the feeds used were the same as those used in making predictions and the starting cutting speed in each test was selected to be approximately the same as the speed at which deformation was predicted to occur. By varying the speed in subsequent tests, they were able to determine the speed at which the tool starts to deform plastically within 50 m/min. When the predicted results were compared with the experimental results, reasonable agreement was found to exist.

It should be noted that the estimation of the stresses generated in a cutting tool during machining is the first step in predicting conditions that would cause tool failure due to chipping, plastic deformation, fracture, etc. of the cutting edge. There also have been a number of attempts to determine these stresses and these are now considered.

Tlusty and Masood (1978) studied chipping and fracture of carbide tools. They carried out interrupted and continuous turning tests using C6 and C7 grade carbide tools on three steel work materials (AISI-1040 steel and two AISI-4340 steels with 217 BHN and 380 BHN respectively). After examining the chipped surfaces of the tool tips they suggested that chipping was accompanied by some plastic flow and concluded that chipping is a ductile failure due to high shear stresses at the cutting edge. The fractured surfaces were found to indicate brittle failure occurring as a result of tensile stresses. A stress analysis in the tool carried out using a finite element method was found to support the above findings. Shear stress maxima were found close to the cutting edge at levels corresponding to the shear flow strength of the tool materials used. A local maximum tensile stress with a magnitude corresponding to the transverse rupture strength of the tool materials was noted at a distance which coincided with the origin of the experimentally observed fracture.

Sampath et al (1984), in their study of fracture probability for tungsten carbide (6%Co) tools turning AISI-4340 steel under steady state cutting conditions, microscopically examined fractured surfaces (fractography) produced by tensile failure and shear failure of tool specimens. They found that the difference in appearance of shear and tensile fracture surfaces was not sufficiently distinctive to enable the character of the fracture to be accurately identified based on fractography alone. It should be noted that above findings conflict with the observations of Tlusty and Masood.

Kronenberg (1966) investigated the stresses generated in a tool using the equation for radial stress derived for a wedge with a force applied at the apex. This equation, when applied to a point at the apex where r=0, gave an infinite radial stress. He pointed out that this would indicate immediate breakdown of the cutting edge unless an edge radius was used. Assuming that the stresses generated at the tool face are of primary interest in determining the conditions of tool failure due to stresses, he simplified the above equation to determine the stresses in the tool face. He used this equation to determine the angle of the resultant cutting force with reference to the bisector of the tool wedge (θ_{max}) that would cause zero stress in the tool face. He argued that if the angle of the resultant cutting force caused by tool geometry, cutting conditions, etc. was greater than θ_{max} there would be tension in the tool face, which is undesirable for carbide tools. If the angle is smaller than θ_{max} the tool face would be under compression, which is desirable. He also used the same analysis to show that the chance of generating tension in the tool face was considerably less for tools with negative rather than positive rake angles. The above analysis, however, did not consider the effects of increased tool temperatures during machining.

In this work, in order to predict the conditions giving plastic deformation of the cutting edge, a method similar to the one presented by Nachev and Oxley (1985) will be used. In the method developed by Nachev and Oxley (1985) the shear stress acting on the tool rake face and the normal and shear stresses on the flank face were not taken into account, and it was assumed that the average normal stress on the tool rake face was the stress that causes deformation of the cutting edge. In their work, attention was also limited to approximately orthogonal conditions. Therefore, in this present work more realistic account is taken of the mode of cutting edge failure under the action of all of the stresses acting by considering a criterion of failure based on the maximum shear stress at the cutting edge. The analysis is also extended to oblique conditions for a tool having a nose radius.

4.3 Calculation of Stresses Inside the Cutting Edge of a Tool

4.3.1 Stress Analysis in the Cutting Edge Region of a Tool

The starting point for predicting the conditions giving plastic deformation of the cutting edge is to make a stress analysis of the region of the tool adjacent to the cutting edge. As stated earlier, although Kronenberg (1966) has done this previously, he limited his attention to a wedge under the action of a single load acting at the wedge apex. In the present work account is taken of the stress distributions at the rake and flank faces of the tool rather than reducing these to a single force.

It was well known that the tool may deform plastically due to the cutting forces acting on it. When the physical stresses inside the cutting edge satisfy a critical stress condition, the cutting edge starts to deform plastically. There are three basic internal stresses in a cutting tool: compression, tension and shear stresses (Nash, 1994). The values and distributions of these internal stresses vary with the stress distributions on the tool-chip interface and the flank face of the tool, which are the boundary conditions in the stress analysis.

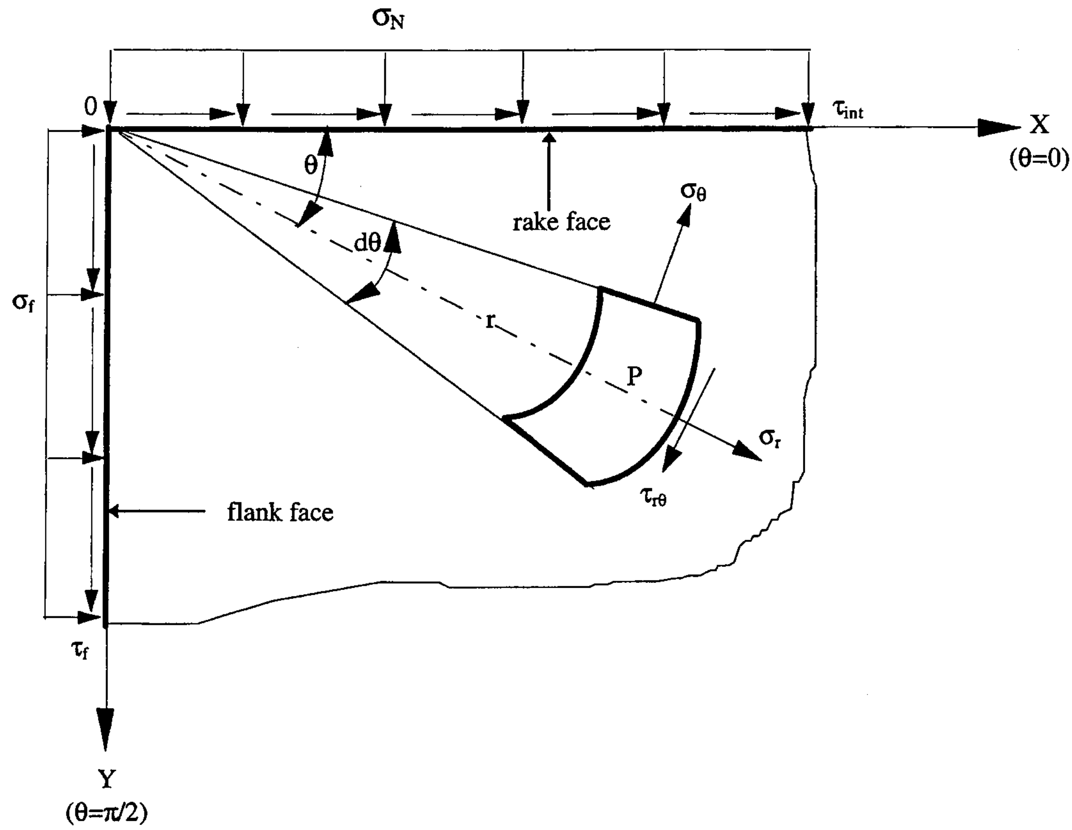

Fig. 4-3 Stresses Acting on an Element and on Rake and Flank Faces of a Tool

It is advantageous to use polar coordinates in analysing stresses inside the cutting edge of a tool which can be considered as a wedge loaded along the faces. Fig.4-3 shows the stresses assumed to act at the cutting edge in the analysis. For the sake of simplicity the rake and clearance angles of the tool are assumed to be zero which is reasonable for carbide tools. The normal and shear stress distributions on the rake face are assumed to be uniform. In support of this it should be noted that Arsecularatne (1997) who reviewed the experimental methods used to determine rake face stress distributions and the reported results concluded that, for a sharp tool, shear and normal stresses reach constant values as the cutting edge is approached. At this stage, and lacking more detailed information it also seems reasonable to assume uniform stress distributions on the flank face.

Consider the equilibrium of the element P at r, θ (Fig.4-3). The normal stress components in the radial and circumferential directions are denoted by σ_r and σ_θ while the shear stress component is denoted by $\tau_{r\theta}$. From the equilibrium of the element P in the circumferential and radial directions (neglecting the body force), the general form of relations for the stress components can be obtained as shown by Timoshenko and Goodier (1987) in the form

$$\sigma_r = \frac{1}{r}\frac{\partial \psi}{\partial r} + \frac{1}{r^2}\frac{\partial^2 \psi}{\partial \theta^2}$$
$$\sigma_\theta = \frac{\partial^2 \psi}{\partial r^2} \qquad (4\text{-}1)$$
$$\tau_{r\theta} = \frac{1}{r^2}\frac{\partial \psi}{\partial \theta} - \frac{1}{r}\frac{\partial^2 \psi}{\partial r \partial \theta}$$

where ψ is the appropriate stress function.

For the boundary conditions given in Fig.4-3, the following equations for these stress components can be obtained using the expression for ψ given by Timoshenko and Goodier (1987).

$$\sigma_r = \frac{1}{2}[(\cos 2\theta - 1)\sigma_N - (\cos 2\theta + 1)\sigma_f$$
$$-(\sin 2\theta + \frac{\pi}{2}\cos 2\theta - 2\theta + \frac{\pi}{2})\tau_{int} - (\sin 2\theta - \frac{\pi}{2}\cos 2\theta + 2\theta - \frac{\pi}{2})\tau_f]$$

$$\sigma_\theta = \frac{1}{2}[-(\cos 2\theta + 1)\sigma_N + (\cos 2\theta - 1)\sigma_f \qquad (4\text{-}2)$$
$$+(\sin 2\theta + \frac{\pi}{2}\cos 2\theta + 2\theta - \frac{\pi}{2})\tau_{int} + (\sin 2\theta - \frac{\pi}{2}\cos 2\theta - 2\theta + \frac{\pi}{2})\tau_f]$$

$$\tau_{r\theta} = \frac{1}{2}[(\sin 2\theta)\sigma_N + (\sin 2\theta)\sigma_f$$
$$+(\frac{\pi}{2}\sin 2\theta - \cos 2\theta - 1)\tau_{int} - (\frac{\pi}{2}\sin 2\theta + \cos 2\theta - 1)\tau_f]$$

The maximum shear stress at P, τ_{pmax} can be obtained in terms of the above stress components as

$$\tau_{p\max} = \sqrt{\tau_{r\theta}{}^2 + \left(\frac{\sigma_\theta - \sigma_r}{2}\right)^2} \qquad (4\text{-}3)$$

To get the maximum shear stress τ_{max} i.e. the maximum value of τ_{pmax}, differentiate τ_{pmax} (Eq.(4-3)) with respect to θ and set it to zero, then the maximum shear stress inside the cutting edge of a tool τ_{max} occurs at a value of θ given by

$$\tan 2\theta = -\frac{(\sigma_f - \sigma_N) + \frac{\pi}{2}(\tau_{int} - \tau_f)}{\tau_f + \tau_{int}} \quad (4\text{-}4)$$

with τ_{max} then given by

(i) when $[(\sigma_f - \sigma_N) + \frac{\pi}{2}(\tau_{int} - \tau_f)] \geq 0$:

$$\tau_{max} = \frac{1}{2}(\tau_f - \tau_{int}) + \frac{1}{2}\frac{[(\sigma_f - \sigma_N) + \frac{\pi}{2}(\tau_{int} - \tau_f)]^2}{\sqrt{[(\sigma_f - \sigma_N) + \frac{\pi}{2}(\tau_{int} - \tau_f)]^2 + (\tau_{int} + \tau_f)^2}} + \frac{1}{2}\frac{(\tau_{int} + \tau_f)^2}{\sqrt{[(\sigma_f - \sigma_N) + \frac{\pi}{2}(\tau_{int} - \tau_f)]^2 + (\tau_{int} + \tau_f)^2}},$$

and

(ii) when $[(\sigma_f - \sigma_N) + \frac{\pi}{2}(\tau_{int} - \tau_f)] < 0$:

$$\tau_{max} = \frac{1}{2}(\tau_f - \tau_{int}) - \frac{1}{2}\frac{[(\sigma_f - \sigma_N) + \frac{\pi}{2}(\tau_{int} - \tau_f)]^2}{\sqrt{[(\sigma_f - \sigma_N) + \frac{\pi}{2}(\tau_{int} - \tau_f)]^2 + (\tau_{int} + \tau_f)^2}} - \frac{1}{2}\frac{(\tau_{int} + \tau_f)^2}{\sqrt{[(\sigma_f - \sigma_N) + \frac{\pi}{2}(\tau_{int} - \tau_f)]^2 + (\tau_{int} + \tau_f)^2}}, \quad (4\text{-}5)$$

Note that the maximum shear stress in the tool τ_{max} does not depend on r. This is due to the assumption of uniform shear and normal stress distributions on the rake and flank faces of the tool near the cutting edge. Beyond this region τ_{max} will depend on r. However, since deformation is mainly restricted to the cutting edge region, as will be seen later, it is sufficient to consider τ_{max} in the region where constant boundary stresses apply.

Note that when considering plastic deformation of a tool working at high temperatures, the failure criterion can be taken as (Nash, 1994)

$$\left|\tau_{max}\right| \geq \left|\frac{\sigma_{comp}}{2}\right| \tag{4-6}$$

where σ_{comp} is the uniaxial compressive strength of the tool material at the onset of plastic deformation. In practice, it is assumed that when τ_{max} reaches a value of $\sigma_{0.05}/2$, i.e. when

$$\left|\tau_{max}\right| \geq \left|\frac{\sigma_{0.05}}{2}\right| \tag{4-7}$$

the tool starts to deform plastically where $\sigma_{0.05}$ is the 5% proof stress for the tool material determined from high temperature uniaxial compression test data such as that given by Trent (1968).

Thus τ_{max} and hence the cutting edge plastic deformation conditions can be determined if σ_N, τ_{int}, σ_f, τ_f and T_{int} are known. σ_N, τ_{int} and T_{int} can be predicted using the methodology described in section 3.3. σ_f, τ_f can be calculated using the method described in the following section.

4.3.2 Stresses on the Tool Flank-Work Interface

As mentioned earlier, when the cutting edge radius is small enough to be neglected, it is reasonable to assume uniform shear and normal stress distributions on the tool flank-work interface as shown in Fig.4-3. Based on an investigation on the contribution of the tool flank wear to cutting forces in orthogonal machining, Li (1991) pointed out that the tool flank-work interface shear stress τ_f and normal stress σ_f can be obtained using the empirical relations:

$$\begin{aligned} \sigma_f &= \frac{0.0528 F_T}{t_c} \\ \tau_f &= \frac{0.0671 F_C}{t_c} \end{aligned} \tag{4–8}$$

where t_c, F_C and F_T are cut thickness, cutting force and feed force, respectively.

4.4 Prediction of Cutting Conditions Giving Plastic Deformation of the Cutting Edge of a Tool

4.4.1 Load Conditions of a Tool

In predicting the conditions which give plastic deformation of the tool, the maximum shear stress in the tool was determined from Eq.(4-5). In making the calculations the following three cases of tool loading were initially considered:

Case I, when $\sigma_N \neq 0$, $\tau_{int} \neq 0$, $\sigma_f \neq 0$, and $\tau_f \neq 0$.

Case II, when $\sigma_N \neq 0$, $\tau_{int} \neq 0$, and $\sigma_f = \tau_f = 0$.

Case III, when $\sigma_N \neq 0$ and $\tau_{int} = \sigma_f = \tau_f = 0$.

It can be seen that Case III is that considered by Nachev and Oxley (1985) in which case as shown by Eq.(4-9),

$$\tau_{max} = \frac{\sigma_N}{2} \tag{4-9}$$

It should be noted that in considering cutting edge deformation only the stresses acting on element P as shown in Fig.4-3 have been taken into account. This neglects the possible influence of the stresses normal to the plane in Fig.4-3. Preliminary calculations show that this will only introduce an error in Case II and that this error is relatively small.

4.4.2 Prediction Methodology

In applying the above three cases to predict the cutting speeds which will cause plastic deformation of the cutting edge the method used was basically the same as that depicted in Fig4-2 and described earlier in section 4.2. However, as the maximum shear stress τ_{max} is now used as the failure criterion, Trent's curve is plotted in terms of maximum shear strength which is taken as half the value of the corresponding hot compressive strength. The predicted cutting speeds giving plastic deformation are then taken to be the values at the intersections of this curve with the τ_{max} curves calculated from the machining theory and Eq.(4-5).

A computer program written in C-language is used in the present work to make all of the necessary calculations (chapter 5). The input data to the program includes: work material composition, tool geometrical data (rake angle, inclination angle, side-cutting edge angle and nose radius), high temperature shear strength of tool material, feed and depth of cut and an assumed initial cutting speed value. The steps involved are:

(i) Determine the equivalent cutting edge geometry for the given oblique nose radius tool, depth of cut and feed.

(ii) For this equivalent cutting edge and the assumed cutting speed, determine the forces F_C, F_T, temperature T_{int} and tool stresses using the methods described in chapter 3.

(iii) Calculate the maximum shear stress τ_{max} for the appropriate case from Eq.(4-5).

(iv) Determine the cutting speeds corresponding to the intersections of the two curves using a bi-section search method (Yakowitz, 1990).

4.4.3 Comparison Between Predicted and Experimental Plastic Deformation Conditions in Approximately Orthogonal Machining

In order to determine which of the three loading cases described in section 4.4.1 is the most appropriate in predicting cutting conditions giving plastic deformation of the cutting edge, the predicted results for each case were compared with the experimental results of Nachev (1983) and Nachev and Oxley (1985) obtained from approximately orthogonal machining tests. These workers determined the experimental plastic deformation conditions for two plain carbon steel work materials using P25 grade (Seco-Titan S25M) carbide tools. Although the S25M carbide tool has 6.5%TiC, it was considered by Nachev and Oxley to be near enough to the alloy of chemical composition WC + 5%TiC + 9%Co tested by Trent (Fig.4-4) to justify using Trent's curve for this material to represent the hot strength properties of the S25M carbide used in their machining tests. In what follows this was again assumed to be the case. Using the Matlab package, Trent's curve can be obtained using the curve-fitting method (Yakowitz, 1990) as: $\sigma_{0.05} = 5.048 \times 10^{38} \times T^{-11.8468}$, where $\sigma_{0.05}$ is the 5% proof stress

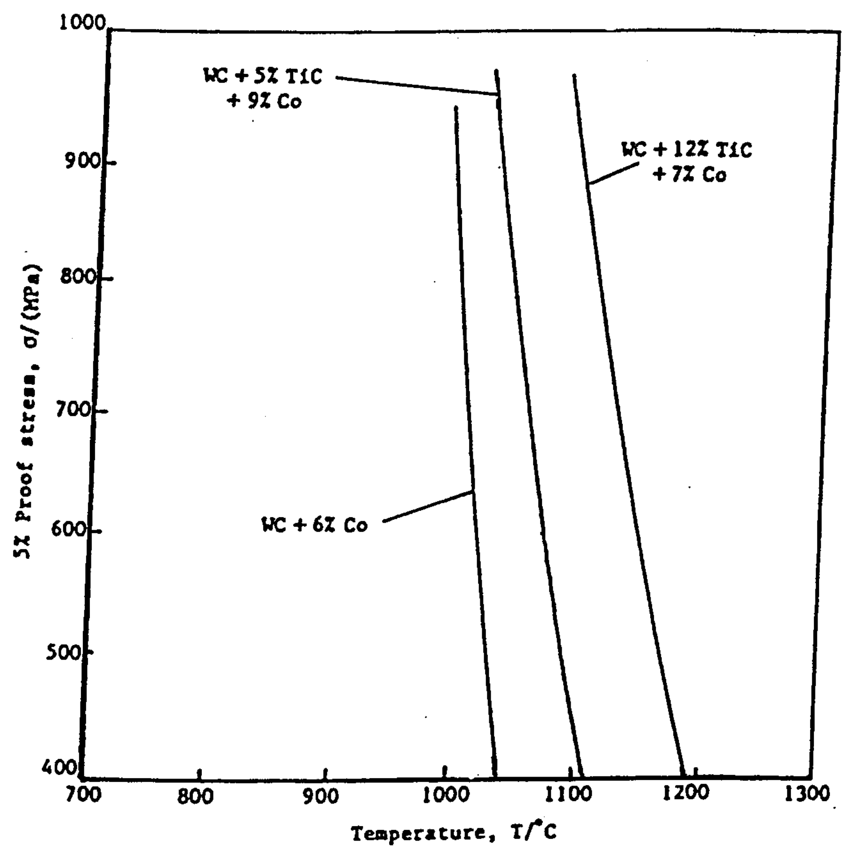

Fig. 4-4 Proof Stress Values Obtained by Trent for Cemented Carbide Tool Materials (after Trent, 1968)

in N/mm^2, T is temperature in °C. The machining parameters used by Nachev and Oxley are summarised as follows:

(a) *Work materials.* (BHP) K1022 plain carbon steel bar of chemical composition 0.19%C, 0.021%P, 0.88%Mn, 0.27%Si, 0.02%Ni, 0.085%Cr, 0.005%Mo was used as one work material. The other material used was a (BHP) K1045B plain carbon steel bar with a chemical composition of 0.48%C, 0.019%P, 0.80%Mn, 0.30%Si.

(b) *Tool material and tool geometry.* Uncoated P25 grade (Seco-Titan S25M) TPGN-220408 carbide tools with a chemical composition WC + 6.5%TiC + 9.5%Co + 14.5%(TaC + NbC) were used. The tool geometrical parameters were normal rake angle α_n= 5 degrees, inclination angle i = 0 degrees, nose radius r_ε= 0.8 mm, side cutting edge angle C_s= 0 degrees.

(c) *Cutting conditions.* Feeds f = 0.2, 0.25, 0.3, 0.4 and 0.5 mm/rev and depth of cut d=2.5 mm were used. The initial cutting speed in each test was selected to be approximately the same as the speed at which deformation was predicted to occur.

Using the computer program mentioned in section 4.4.2 with the above machining parameters, the plastic deformation cutting speeds for the three cases of tool loading were predicted respectively.

The predicted and experimental results are plotted on a log-log basis in Fig.4-5(a) for the 0.19%C steel and in Fig.4-5(b) for the 0.48%C steel. The filled-in symbols indicate the cutting speeds for which plastic deformation was observed and the open symbols indicate cutting speeds 50 m/min lower for which no plastic deformation was observed. The predicted results for the three cases (section 4.4.1) are given by the lines.

However, the predicted results can be seen to overestimate the cutting edge's ability to resist plastic deformation with the smallest overestimation corresponding to Case I which takes into account the shear and normal stresses acting on both the rake and flank faces of the tool. Case I represents the most realistic tool edge loading conditions and it is not surprising that this gives the best predictions.

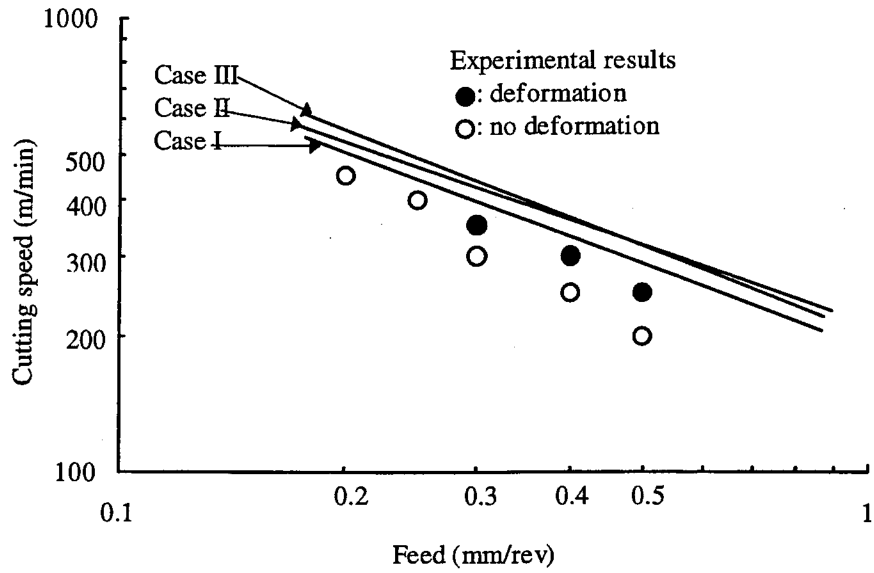

(a)

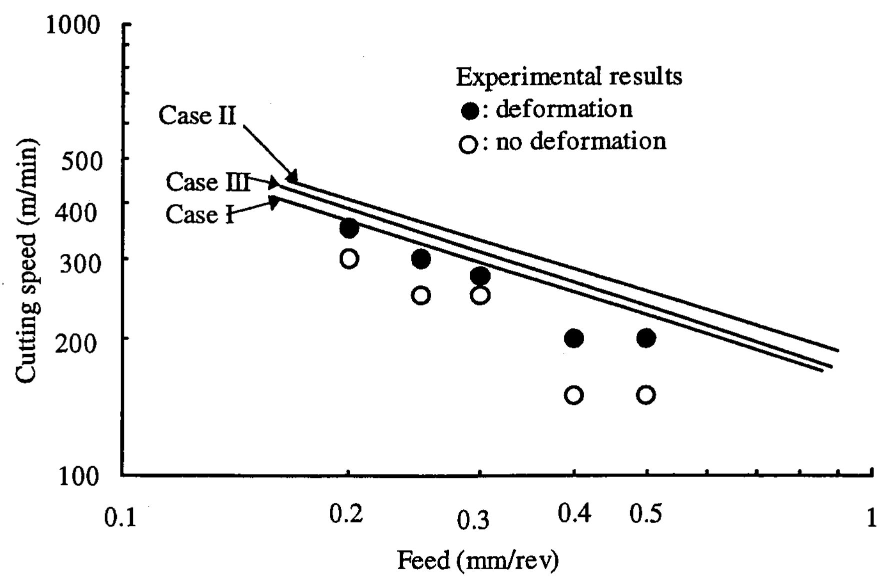

(b)

Fig. 4-5 Comparisons between Predicted and Experimental Plastic Deformation Cutting Conditions for (a): 0.19%C Steel; (b): 0.48%C Steel

4.4.4 Prediction of Plastic Deformation Conditions in Oblique Machining

To check the effectiveness of the above proposed method when extended to oblique machining conditions, predictions and experiments were also carried out on another two plain carbon steels: 0.30%C steel and 0.45%C steel using the uncoated P25 grade DNGA-150408 carbide inserts (without chipbreaker groove) with a chemical composition 7.6-8.4%TiC + 3.5%Co + 11-12%TaC. The ranges of each machining parameter listed in section 4.5 were used in both the predictions and the experiments. The predictions are discussed in this section, while the experiments will be discussed in section 4.5.

4.4.4.1 Determination of High Temperature Shear Strength Data for the Tool Material

In order to predict the tool plastic deformation conditions it was first necessary to determine the high temperature shear strength curve for the P25 grade carbide tools used in the experiments. It is preferable to carry out Trent (1968) type compression tests on the tool material considered. But due to the lack of the facilities for these tests, a tool material whose chemical composition is similar to those tested by Trent was selected. From the data given by Trent (1968) it is clear that the hot compressive strength is directly related to the TiC content of the tool material with, at a given temperature, the 5% proof stress increasing with increase in TiC content. Since the P25 grade carbide used in the tests had 7.6-8.4%TiC, it was assumed that the curve representing its hot compressive strength would lie in the middle of the curves given by Trent (1968) for tool materials of chemical composition WC + 5%TiC + 9%Co and WC + 12%TiC + 7%Co. (Fig.4-6). Using the Matlab package, this curve can be obtained using the curve-fitting method (Yakowitz, 1990) as: $\sigma_{0.05} = 4.497 \times 10^{33} \times T^{-10.135}$, where $\sigma_{0.05}$ is the 5% proof stress in N/mm^2, T is temperature in °C.

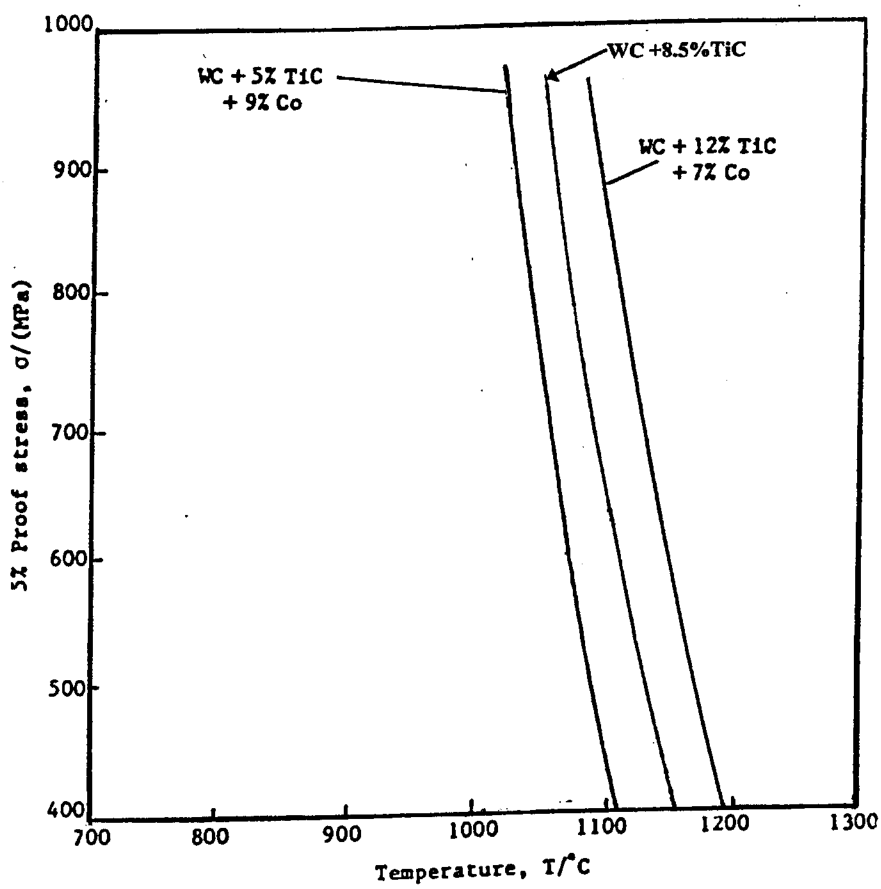

Fig. 4-6 Proof Stress Values for Carbide Tool Materials

4.4.4.2 The Predicted Results

Using the computer program discussed in section 4.4.2 and the predictive method discussed in section 4.4.2 with the machining parameters given in section 4.5, the plastic deformation cutting speeds for Case I tool loading conditions were predicted. These predicted values are given in Table 4-1 for the 0.30%C steel and in Table 4-2 for the 0.45%C steel. In these tables, Case I, CaseII and Case III represent the three cases of tool loading (section 4.4.1), while $U_{plastic}$ is the predicted cutting speed where the tool starts to deform plastically, T_{int} is the calculated tool-chip interface temperature corresponding to $U_{plastic}$, and τ_{max} is the corresponding calculated maximum shear stress inside the cutting edge.

Table 4-1 Predicted plastic deformation cutting conditions for 0.30%C steel (d=2.5 mm)

	Loading conditions								
	Case I			Case II			Case III		
Feed (mm/rev)	$U_{plastic}$ (m/min)	T_{int} (°C)	τ_{max} (MPa)	$U_{plastic}$ (m/min)	T_{int} (°C)	τ_{max} (MPa)	$U_{plastic}$ (m/min)	T_{int} (°C)	τ_{max} (MPa)
0.2	484	1082.1	-393.4	493	1085	-386	446	1059.5	-488.9
0.25	431	1081.6	-394.9	436	1085.8	-380	398	1060.6	-484
0.315	370	1082.2	-394.2	380	1087	-376	342	1061.4	-479
0.4	332	1082.3	-395.4	338	1088.9	-372	303	1062.1	-476
0.45	306	1082.1	-394.2	315	1088.8	-370	284	1062.9	-474

Table 4-2 Predicted plastic deformation cutting conditions for 0.45%C steel (d=2.5 mm)

	Loading conditions								
	Case I			Case II			Case III		
Feed (mm/rev)	$U_{plastic}$ (m/min)	T_{int} (°C)	τ_{max} (MPa)	$U_{plastic}$ (m/min)	T_{int} (°C)	τ_{max} (MPa)	$U_{plastic}$ (m/min)	T_{int} (°C)	τ_{max} (MPa)
0.2	421	1061.6	-478.1	435	1069.2	-447	390	1044.2	-569.5
0.25	376	1061.8	-478.1	390	1069.9	-443	349	1044.5	-564.9
0.315	327	1062.5	-476.6	335	1070.9	-438	304	1045.8	-559.9
0.4	286	1062.7	-474.1	297	1071.9	-435	265	1046.1	-555
0.45	269	1062.9	-473	275	1071.9	-433	249	1046.9	-553

4.5 Experimental Procedure

Plastic deformation experiments on the above two plain carbon steel bars were carried out on a lathe using a bar turning process under dry conditions. For each test condition, it was necessary to measure the plastic deformation of the cutting edge after machining for a predetermined time interval. Tool plastic deformation is affected by the work material, tool material, tool geometrical parameters, cutting conditions, etc. In order to keep the experiments to a manageable number, priority was placed on the parameters having greatest relevance to the present investigation. The selected ranges of each parameter are given below.

(a) *Work materials.* A nominal AISI-1045 plain carbon steel bar of chemical composition 0.45%C, 0.01%P, 0.66%Mn, 0.053%Si, 0.031%S, 0.01%Ni, 0.02%Cr, 0.01%Mo, 0.01%Cu and 0.001%Al was used as one work material. The other material used was a nominal AISI-1030 plain carbon steel bar with a chemical composition of 0.30%C, 0.013%P, 0.68%Mn, 0.26%Si, 0.011%S, 0.02%Ni, 0.01%Mo, 0.02%Cu and 0.025%Al.

(b) *Tool material and tool geometry.* Uncoated P25 grade DNGA-150408 carbide inserts (without chipbreaker groove) with a chemical composition 7.6-8.4%TiC + 3.5%Co + 11-12%TaC were used on a PDNNR2525 tool holder. The tool geometrical parameters were normal rake angle α_n= -6 degrees, inclination angle i = -6 degrees, nose radius r_ε = 0.8 mm, side cutting edge angle C_s = 27 degrees and clearance angle 6 degrees.

(c) *Cutting conditions.* Feeds f = 0.2, 0.25, 0.315, 0.4 and 0.45 mm/rev and depth of cut d = 2.5 mm were used. The initial cutting speed in each test was selected to be approximately the same as the speed at which deformation was predicted to occur.

The machine tool used for the tests was a 37 kW Heidenreich and Harbeck VDF precision lathe having a variable speed motor with speeds 0-5600 rev/min. The available feed range was 0.01 to 0.71 mm/rev. The original DNGA-150408 inserts were provided with all faces ground by the manufacturer. The flank face of each cutting edge was checked for flatness using the same method adopted for checking plastic deformation which is to be described in the following section. Finally each cutting edge was numbered and randomly assigned to a test in order to minimise the influence of variations in work and tool material properties, etc.

After the steel bar was mounted in the lathe, a clean-up cut was made along its length with a tool to remove scale and to ensure that the work surface was clean and uniform along its length. Then the tool holder was placed in the tool post and firmly secured.

For each test, the carbide insert was first placed in the tool holder and the feed rate for this test was set. The machining was carried out at a cutting speed which was selected to be approximately the same as the speed at which deformation was predicted to occur (Tables 4-3 and 4-4). An approximate cutting speed was selected using the gear box and the correct speed was reached with the help of the variable speed motor and a Veeder Root Digital Tachometer (Model 6611) which was placed on the rotating surface which was to be machined. The depth of cut was then set and cutting commenced. The duration of each cut was controlled by using a stopwatch. If in this initial test no deformation was observed further tests were made with the speed increased in increments of 40 m/min until deformation was observed. If deformation was observed further tests were made with the speed decreased in increments of 40 m/min until no deformation was observed. This procedure was continued until for each feed a cutting speed was found at which the tool will deform plastically and will not deform at all other speeds below it. It should be noted that each cutting edge of the inserts was used to cut the workpiece only once. In all tests it was found that 20s machining time was sufficient for steady state conditions to be achieved.

After a cut, the insert used was removed from the tool holder. Then the cutting edge was examined for plastic deformation using the method described in the next section.

4.5.1 Method Used for Determining Plastic Deformation

Although a number of methods were tried for measuring the plastic deformation of the cutting edge, the following method, although one of the simplest, gave the best results.

The flank face of the tool which was expected to bulge outwards when plastic deformation has occurred was carefully cleaned to remove any adhering steel, etc. The flank face was then held firmly on a polished surface and the two surfaces were placed in front of a strong light and examined from the front. If deformation had not occurred the flank surface was flat and in close contact along its length with the polished surface thus there was no gap between the two surfaces and hence no light could be seen. If deformation had occurred then light could be seen through the resulting gap between the two surfaces which was formed due to the bulged out flank face near the cutting edge. With this method it was possible to detect even small amounts of plastic deformation occurring in the nose radius part of the tool flank face. The results obtained using this method are given in Table 4-3 for 0.30%C steel and in Table 4-4 for 0.45%C steel.

When the deformed inserts were further examined it was found that bulging out of the flank face had occurred in a small region near the cutting edge. This justifies the use of the equation for τ_{max} (Eq.(4-5)) which was derived for the region where uniform boundary stresses were assumed to apply.

Table 4-3 Plastic deformation experimental results for P25 grade carbide tool used to machine 0.30% carbon steel (d = 2.5 mm)

Test No.	Feed (mm/rev)	Speed (m/min)	Experimental results
1	0.45	290*	Deformation
2	0.45	250	No deformation
3	0.315	310*	Deformation
4	0.315	270	No deformation
5	0.4	310*	Deformation
6	0.4	270	No deformation
7	0.25	400	Deformation
8	0.25	360*	Deformation
9	0.25	320	No deformation

Note: * star sign to indicate the lowest cutting speeds at which tool plastic deformation was observed.

Table 4-4 Plastic deformation experimental results for P25 grade carbide tool used to machine 0.45% carbon steel (d = 2.5 mm)

Test No.	Feed (mm/rev)	Speed (m/min)	Experimental results
1	0.315	310	Deformation
2	0.315	270*	Deformation
3	0.315	230	No deformation
4	0.25	310*	Deformation
5	0.25	270	No deformation
6	0.25	250	No deformation
7	0.2	360*	Deformation
8	0.2	320	No deformation
9	0.45	250*	Deformation
10	0.45	210	No deformation
11	0.4	275*	Deformation
12	0.4	235	No deformation

Note: * star sign to indicate the lowest cutting speeds at which tool plastic deformation was observed.

4.6 Results and Discussion

The predicted and experimental results from Tables 4-1, 4-2, 4-3 and 4-4 are also plotted on a log-log basis in Fig.4-7(a) for the 0.19%C steel and in Fig.4-7(b) for the 0.48%C steel. These results are now considered in detail.

The lines given in Fig.4-7(a) and Fig.4-7(b) represent predicted speed/feed combinations for the 0.30%C and 0.45%C steels respectively at which the tool starts to deform plastically. The predictions were made with the tool stresses corresponding to assumed Case I. Considering the relatively small inclination angles used with carbide tools it was also assumed that the two-dimensional stress analysis (section 4.3.1) is applicable to oblique machining. Again the experimental results are given by the symbols with the filled in symbols indicating the cutting speeds at which plastic deformation was observed and the open symbols indicating cutting speeds 40 m/min lower at which no plastic deformation was observed. From Fig.4-7 it can be seen that the predicted plastic deformation speeds show the same trends as the experimental results with reasonably

good quantitative agreement. In particular the speeds which cause tool deformation can be seen to decrease with increase in feed and, at a given feed the speed which cause tool deformation can be seen to decrease with increase in carbon content of the steel work material. However the predictive method tends to overestimate cutting edge's resistance to plastic deformation, particularly at feeds below 0.4 mm/rev. One reason for this overestimation of the plastic deformation cutting speed is due to possible underestimation of the stresses acting on the tool flank face. Another reason is that the actual high temperature shear strength of the tool material could have been lower than that given by the assumed curve, which is for a tool material with approximately 8.5%TiC while the P25 grade tool material used in the tests had 7.6-8.4%TiC. The results given in Fig.4-7 also confirm that it is necessary to take into account the stresses acting on both the rake and flank faces (Case I) of the tool
in determining the plastic deformation conditions as Case II and Case III were found to result in greater overestimations (Tables 4-2 and 4-3).

4.7 Concluding Remarks for this Chapter

In this chapter it has been shown how the cutting conditions that cause tool cutting edge plastic deformation can be predicted for oblique nose radius tools from a knowledge of the hot compressive strength of the tool material using machining theory combined with an analysis of the tool stresses. It is expected that the present level of agreement between predicted and experimentally observed deformation conditions will be sufficiently accurate for most practical applications including the prediction of optimum cutting conditions.

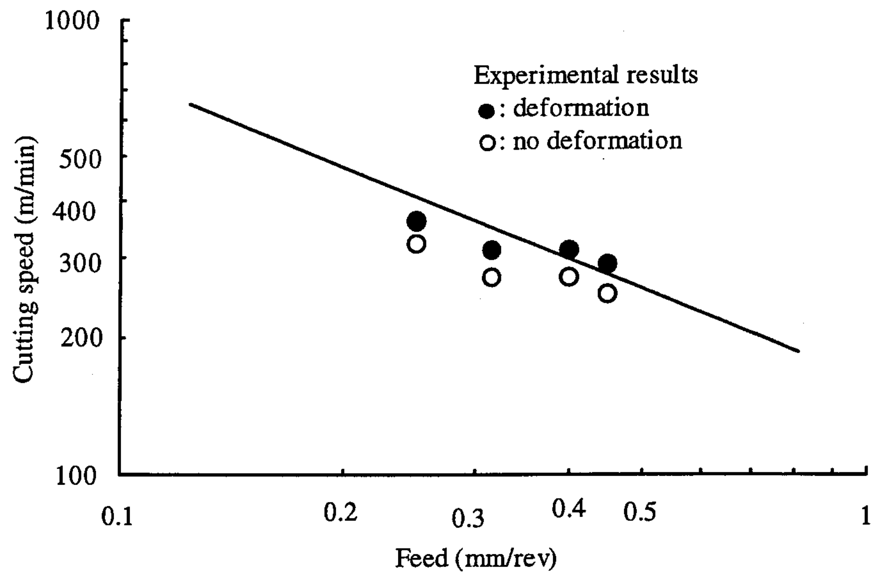

(a)

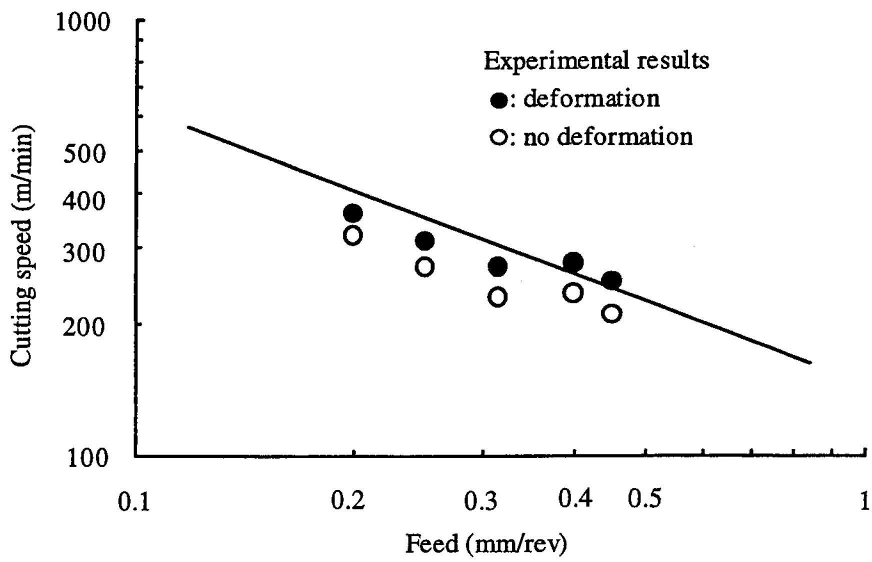

(b)

Fig. 4-7 Comparisons Between Predicted and Experimental Plastic Deformation Cutting Conditions for (a): 0.30%C Steel; (b): 0.45%C Steel

CHAPTER FIVE - Computer-aided Optimisation of Cutting Conditions and Worked Examples

Chapter 5 Computer-aided Optimisation of Cutting Conditions and Worked Examples

5.1 The Computer Program

A computer program for the prediction of optimum cutting conditions in oblique machining with nose radius tools has been developed for microcomputers (PCs). The program is written in ANSI C. It is well known that C has proven to be a pleasant, expressive, and versatile language for a wide variety of programs. Since C is not tied to any particular hardware or system, the program developed will run without change on any machine that supports C.

The typical way of getting something done in a C program is to call a function to do it. Defining a function is the way to specify how an operation is to be done. This optimisation program consists of a main function to perform the main task of the optimisation procedure as stated in section 3.2 and a number of functions to perform the tasks such as the determination of cutting parameters with reference to the equivalent cutting edge, the calculations of tool life and the optimum cutting speed for a given feed and depth of cut, the calculations relevant to the machining theory, the consideration of constraints, the calculations of specific production cost/time, the final optimum cutting conditions for the minimum specific production cost/time, etc.. While the program is being executed, the input data, temporary data and the output data are stored, read and transferred by opening/closing a number of data files.

The construction of the computer program is shown in Fig.5-1. Before the program starts to work, the input data files which will provide the necessary input data have to be built up. The input data to the program are:

(i) Work material composition.

(ii) Tool geometrical data (rake angle, inclination angle, side-cutting edge angle and nose radius).

(iii) Economic data (operating cost of machine and cost of cutting edge).

(iv) Tool life equation data (constants for Eq.(3-4)).

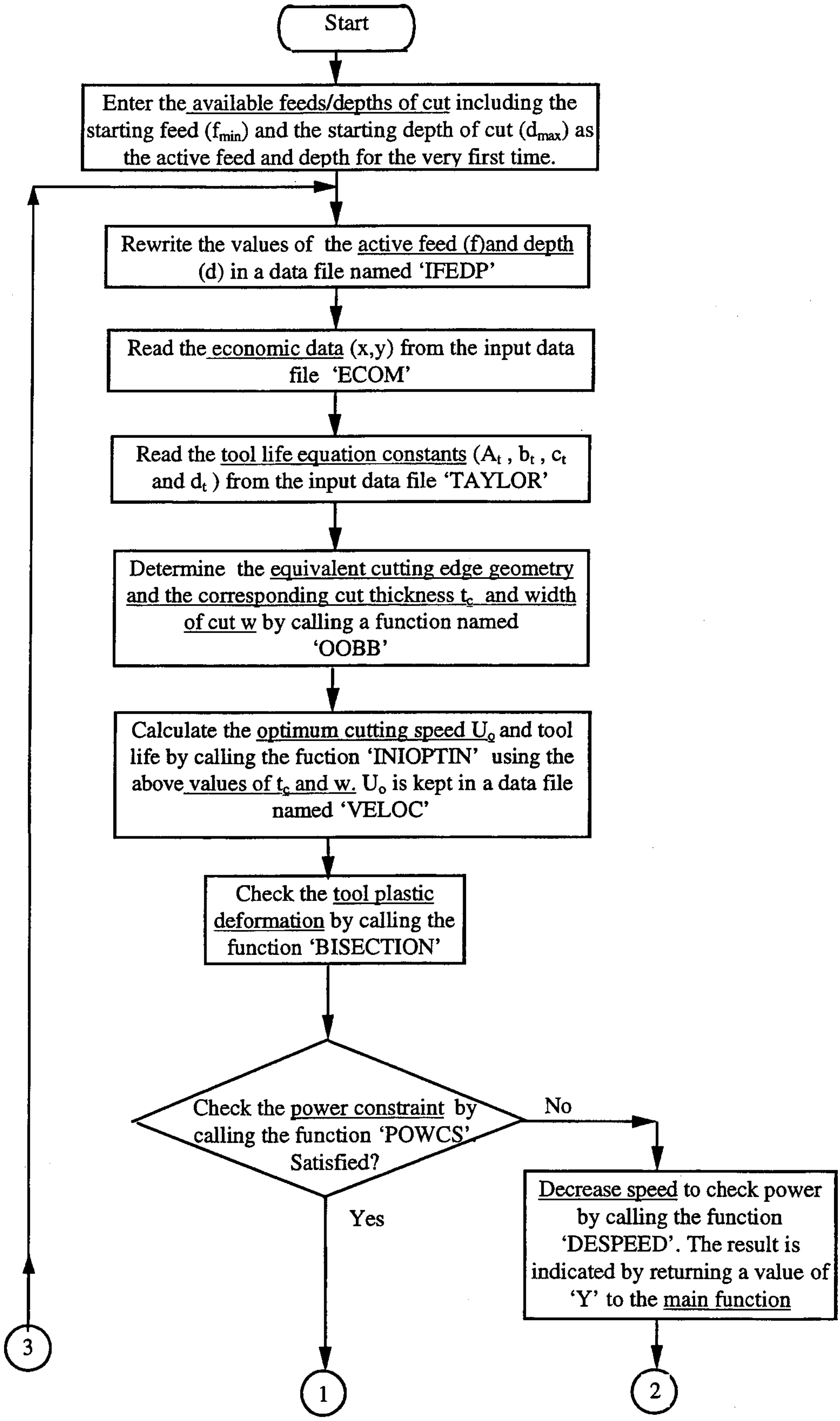
Start
Enter the available feeds/depths of cut including the starting feed (f_{min}) and the starting depth of cut (d_{max}) as the active feed and depth for the very first time.
Rewrite the values of the active feed (f)and depth (d) in a data file named 'IFEDP'
Read the economic data (x,y) from the input data file 'ECOM'
Read the tool life equation constants (A_t , b_t , c_t and d_t) from the input data file 'TAYLOR'
Determine the equivalent cutting edge geometry and the corresponding cut thickness t_c and width of cut w by calling a function named 'OOBB'
Calculate the optimum cutting speed U_o and tool life by calling the fuction 'INIOPTIN' using the above values of t_c and w. U_o is kept in a data file named 'VELOC'
Check the tool plastic deformation by calling the function 'BISECTION'
Check the power constraint by calling the function 'POWCS'. Satisfied?
No
Yes
Decrease speed to check power by calling the function 'DESPEED'. The result is indicated by returning a value of 'Y' to the main function
3
1
2

(Fig. 5-1)

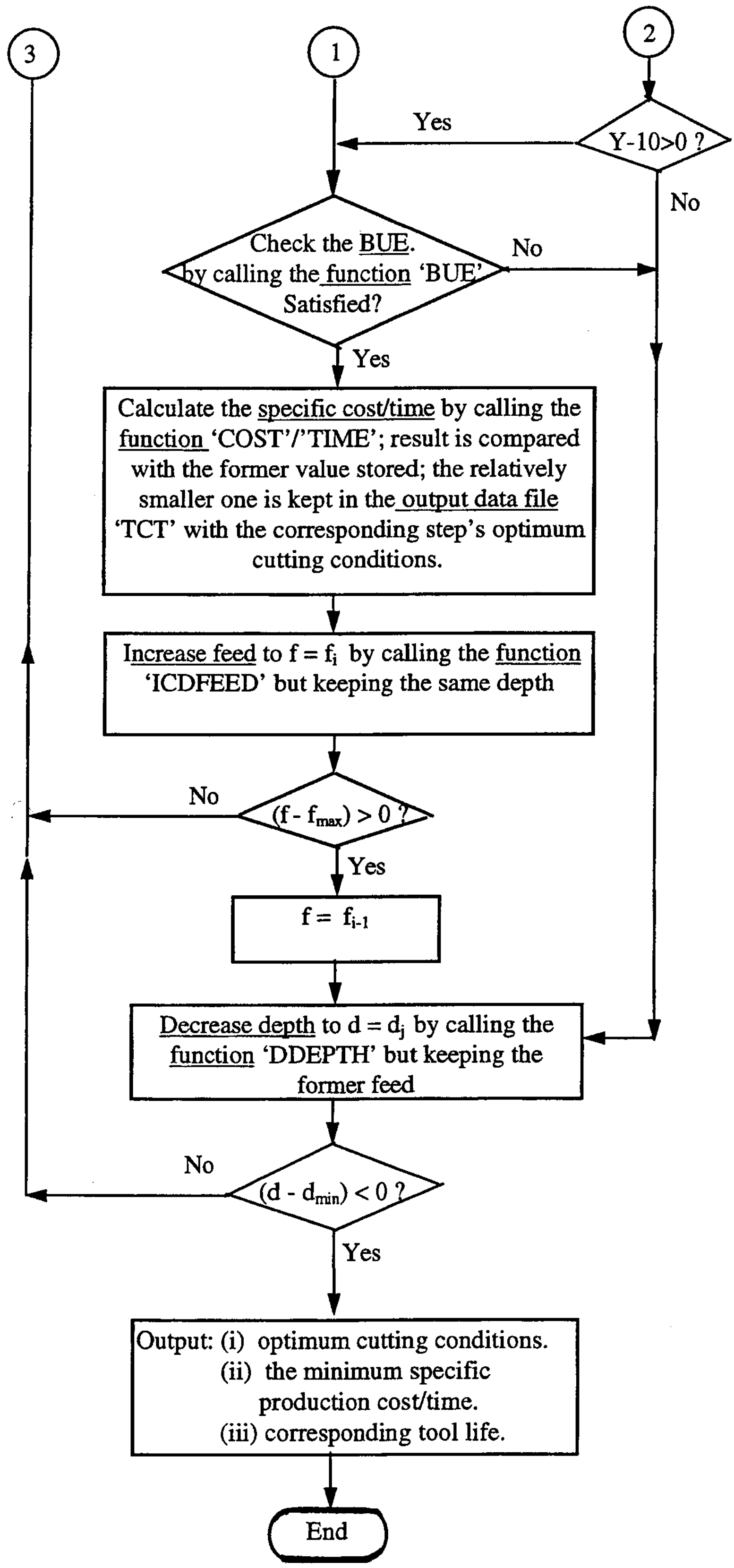

Fig.5-1 Flowchart for the Optimisation Procedure

(v) Available feeds and speeds of the machine tool used, the minimum and maximum feeds and depths for tool and workpiece (if applicable), or the predetermined minimum/maximum feed and predetermined maximum depth of cut.

(vi) Radius of cutting (workpiece diameter).

(vii) High temperature shear strength data for the tool material.

(viii) machine tool's power/torque-speed characteristics.

After settling up the above input data files, the program can be started by executing the main function. The main function's task can be explained by the help of the flow chart in Fig.5-1. The optimisation procedure has been given in section 3.2. What is discussed here is only a brief outline of the optimisation program.

First the information on feeds/depths of cut are read from an input data file. The minimum feed (f_{min}) and the minimum depth (d_{min}) can be read from the data file, while the maximum feed (f_{max}) and the maximum depth (d_{max}) will be either read from a data file or calculated by calling a function named 'MAXFEEDEPTH'. Then the starting feed (f_{min}) and the starting depth of cut (d_{max}) are written in the 'active' feed/depth data file for calculating the corresponding cut thickness t_c and width of cut w. It should be noted that the active values of feed and depth will be changed when a new point on the d-f plane is considered (Fig.3-1). Also the economic data and the tool life equation data are read from the corresponding input data files. The equivalent cutting edge geometry for the given oblique nose radius tool and the corresponding cut thickness t_c and width of cut w are calculated by calling a function named 'EQUEDGE'. The initial optimum cutting speed is calculated by calling the function named 'INIOPTIM', while the required tool life is calculated or obtained from the user. The tool plastic deformation is checked by calling the function 'BISECTION', and the power constraint is checked by calling the function 'POWCS'. The function 'BUE' is called to check the built-up edge constraint. The grid point with the next lower depth but with the feed on the same line is obtained by calling the function 'LOWDEPTH'. If all the constraints are satisfied, the specific production cost/time is calculated and compared by calling the function 'COST/TIME' and the present smallest value is kept in the output data file with the corresponding cutting conditions and tool life. Lastly the optimum cutting conditions with the smallest values of specific production cost/time

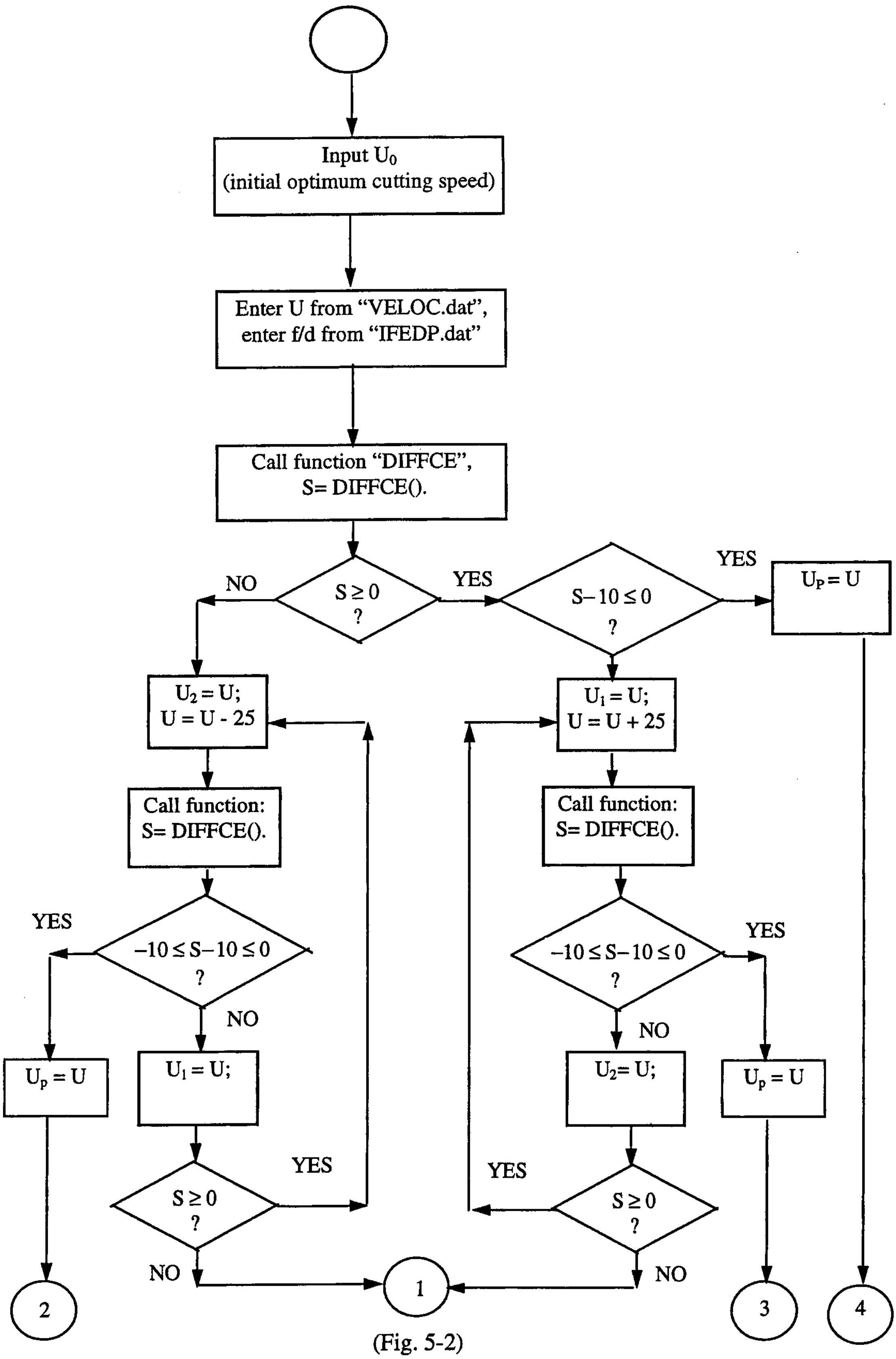

Input U_0
(initial optimum cutting speed)
Enter U from "VELOC.dat",
enter f/d from "IFEDP.dat"
Call function "DIFFCE",
S= DIFFCE().
$S \geq 0$?
NO
YES
$S - 10 \leq 0$?
YES
$U_P = U$
$U_2 = U$;
$U = U - 25$
$U_1 = U$;
$U = U + 25$
Call function:
S= DIFFCE().
Call function:
S= DIFFCE().
YES
$-10 \leq S - 10 \leq 0$?
NO
$-10 \leq S - 10 \leq 0$?
YES
NO
$U_p = U$
$U_1 = U$;
$U_2 = U$;
$U_p = U$
YES
$S \geq 0$?
YES
$S \geq 0$?
NO
NO
1
2
3
4

(Fig. 5-2)

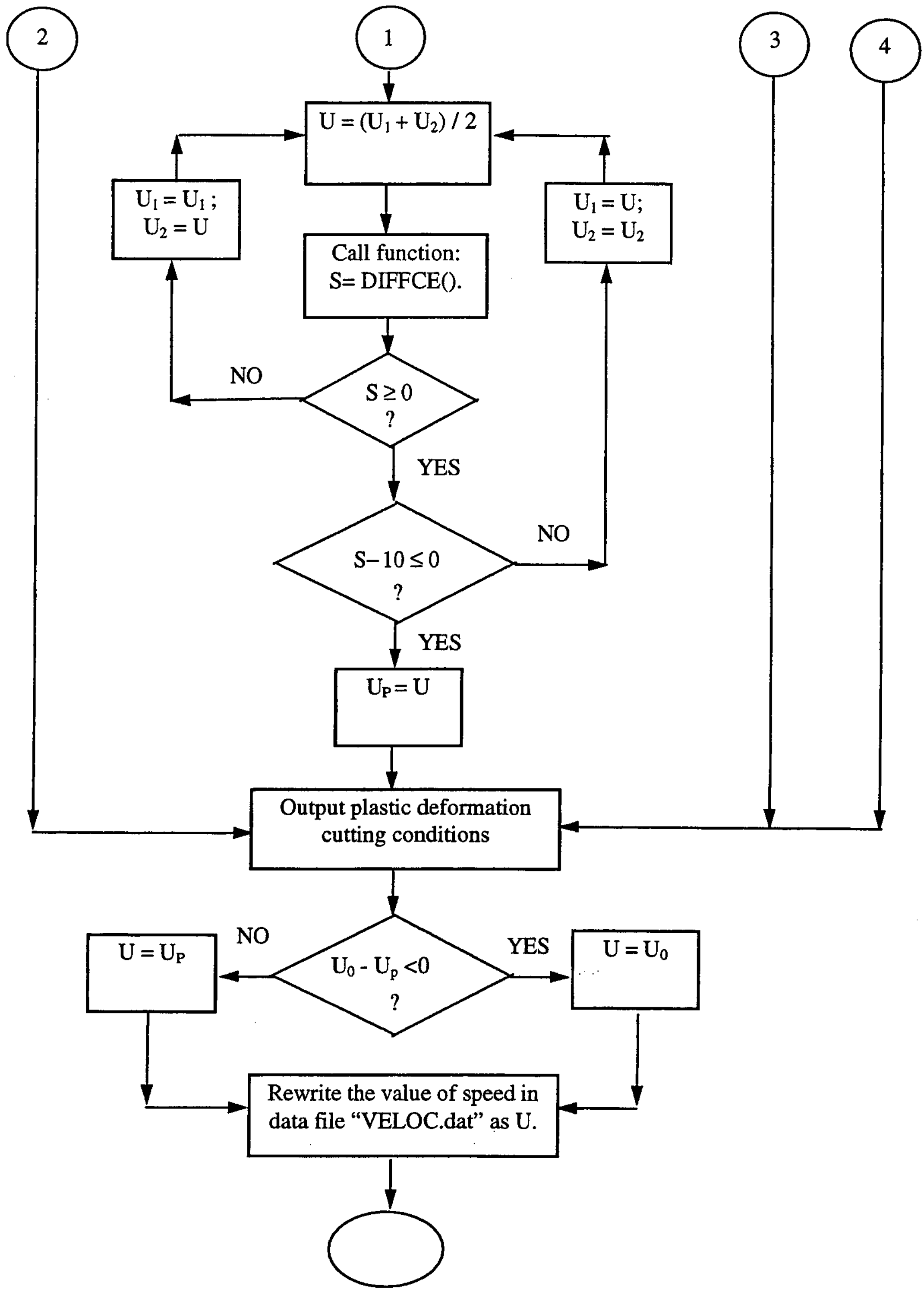

Fig. 5-2 Flowchart for Function void BISECTION(double U_0)

are obtained and stored in the output data file. The program is user friendly and flexible because there are many options available to the user. The user is able to get the required data such as the tool plastic deformation cutting conditions, cutting forces, required power, temperatures, stresses, etc. by opening the corresponding data files. The user can stop the executing of the program after obtaining the required data. Since most of the tasks are performed by using functions, it is very convenient for expanding or modifying the program which can be achieved by adding new functions or modifying the necessary functions.

A summary of the optimisation procedure is given by the flow chart in Fig.5-1. Fig.5-2 gives a flow chart for the function 'BISECTION' which is used to check the tool plastic deformation constraint. In Fig.5-2, a function named 'DIFFCE' is called to calculate the difference between the predicted maximum shear stress, τ_{max} in the tool and half of the proof stress, $\frac{\sigma_{0.05}}{2}$ of the tool material for a given set of cutting conditions.

5.2 Results and Discussion

As stated earlier in chapter 3, in order to obtain the optimum cutting conditions it is necessary to estimate the tool life. To do so a modified Taylor tool life equation (Eq.(3-4)) is used in this work instead of the extended Taylor equation (Eq.(3-27)). Thus the constants in Eq.(3-4) have to be determined before determining the optimum cutting conditions.

5.2.1 Determination of Tool Life Equation Constants

Considering a machining process involving a tool with a single straight cutting edge, the extend Taylor tool life equation (Eq.(3-27)) can be modified as Eq.(3-4). In the modified form of Taylor equation (Eq.(3-4)), cut thickness t_c and width of cut w referred to equivalent cutting edge are used instead of f and d. Since the tool geometrical parameters such as nose radius and side cutting edge angle have been taken into account in determining the equivalent cutting edge, the constants A_t, b_t, c_t, and d_t do not depend on these tool geometrical parameters. This will considerably reduce the amount of tool life data required. However, these constants will still depend on work material, tool material and tool rake angle. Due to above reason, Eq.(3-4) has been used in estimating the tool life in this work. What follows is a brief description of the method used to obtain the tool life equation (Eq.(3-4)) constants for the two carbide grades (uncoated P25 and coated P15) used in the present work.

For the uncoated P25 grade tool material, in order to obtain the constants of Eq.(3-4) the approach used is as follows. Taking account of the observation that when machining with cutting tool temperatures above 800 °C, which would generally be the case for carbide tools in the normal cutting speed range for turning operations, the main wear mechanism is diffusion which is a temperature controlled rate process (Oxley, 1989). Therefore, if the appropriate temperature can be determined and the relationship between tool wear rate/ tool life and temperature is known then it should be possible to predict tool life with far less effort than by purely empirical means.

When the tool life is defined in terms of flank wear, the relationship between tool life, T and tool flank temperature, T_f can be written as (Oxley, 1989; Arsecularatne et al, 1996)

$$T = 10^{A}\, T_f^{-B} \tag{5-1}$$

where A, B are constants. It has also been shown that T_f can be determined from the relation (Oxley, 1989)

$$T_f = 0.9\, T_{int} \tag{5-2}$$

where T_{int} is the interface temperature determined using the machining theory (Eq.(2-13)) and the temperatures are in Kelvins. The above relationship gives good agreement with experimental results not only when tool life is defined in terms of flank wear but also when crater wear is used as the tool failure criterion (Oxley, 1989). In applying the method of predicting tool life based on Eq.(5-1), care should be taken to ensure that the temperatures are sufficiently high for diffusion to be the predominant wear mechanism.

First the constants A and B in Eq.(5-1) were determined from a small number of tool life experimental results obtained for near orthogonal conditions. In these experiments nose radius tools with zero inclination angles were used. For the same cutting conditions the corresponding values of T_f were determined from the machining theory. When plotted on a $\log(T_f)$ versus $\log(T)$ graph the results fell close to a straight line and the corresponding equation was (Arsecularatne, 1998)

$$T = 10^{35.323}\, T_f^{-11.872} \qquad (5\text{-}3)$$

In order to obtain the constants A_t, b_t, c_t, and d_t in Eq.(3-4), fifteen combinations of width of cut/cut thickness/cutting speed values were first selected from ranges w = 1.5 to 4.5, t_c = 0.1 to 0.4 mm and U = 100 to 200 m/min respectively. For each combination of cutting conditions T_{int} values were determined from machining theory. The rake angle of the actual tool which was -6° was used in calculations. The corresponding T_f values and tool life values were then determined from Eqs.(5-2), (5-3). Finally the values of w, t_c , U and T were used to determined the constants A_t, b_t, c_t, and d_t using the multiple linear regression analysis provided in the SPSS package (Norusis, 1992). These constants are given below:

$A_t = 281104$ $\qquad$ $b_t = 2.56319$ $\qquad$ $c_t = 1.66511$ $\qquad$ $d_t \approx 0.0$.

As noted earlier the constants A_t, b_t, c_t, and d_t will depend on work material, tool material and tool rake angle. However, for a given tool material, to account for variations in rake angle and work material composition, additional experimental data will not be required since these variations can be taken into account in calculating T_{int} using the machining theory. Only when the tool material changes will it be necessary to obtain a new set of constants A and B for Eq.(5-2) which can be done using a relatively small number of machining tests. Thus with the described method for determining the constants A_t, b_t, c_t, and d_t reliance on experimental results has been minimised.

For the coated P15 grade tool, since the constants of Eq.(3-27) can be obtained from the work of Arsecularatne et al (1992), the constants A_t, b_t, c_t, and d_t were determined using a different procedure. For fifteen combinations of width of cut/cut thickness/cutting speed values selected from ranges d = 1.5 to 4.5, f = 0.1 to 0.4 mm and U = 100 to 200 m/min respectively, tool life values were determined using Eq.(3-26). The constants A_{t1}, b_{t1}, c_{t1}, and d_{t1} used were those given in the above reference and are given below:

$A_{t1} = 343283296$ $\qquad$ $b_{t1} = 3.023$ $\qquad$ $c_{t1} = 1.153$ $\qquad$ $d_{t1} = 0.258$

Then for each combination, using depth of cut, feed and tool geometry, w and t_c values with reference to the equivalent cutting edge were determined. The values of w, t_c ,U and T were then used to determine the constants A_t, b_t, c_t, and d_t using the SPSS package and are given below:

$A_t = 278351778$ $\qquad$ $b_t = 3.0$ $\qquad$ $c_t = 1.2$ $\qquad$ $d_t = 0.22$.

In order to check the above method using the modified Taylor tool life equation (Eq.(3-4)), the experimental tool life results of a tool material (Seco S4 tool) obtained by Arsecularatne (1998) were used. The corresponding predicted tool life results were calculated using the same machining conditions as that used in obtaining the experimental results. The full data required are shown in appendix A. A comparison between the predicted tool life and the experimental tool life is given in Table 5-1, where U, f and d are the cutting conditions used, C^*_s is the corresponding equivalent side cutting edge angle, t_c and w are the corresponding cut thickness and width of cut, T_{pred} is the predicted tool life while T_{exp} is the experimental tool life. As seen in Table 5-1, the predicted results are in good agreement with the experimental results.

Table 5-1 Comparison between Predicted and Experimental Tool Life (Tool: Seco S4 tool, rake angle: 10 deg. Work material: AISI 1022 steel

U (m/min)	f (mm/rev)	d (mm)	C^*_s (deg)	t_c (mm)	w (mm)	T_{pred} (min)	T_{exp} (min)	$\frac{T_{pred} - T_{exp}}{T_{exp}} \times 100\%$
290	0.2	2	20.747	0.1870	2.1386	18.723	22.8	-17.87872543
200	0.2	2	20.747	0.1870	2.1386	56.034	43.2	29.7092506
350	0.2	2	20.747	0.1870	2.1386	10.751	9.1	18.14301323
290	0.2	2	16.513	0.1917	2.0860	17.960	18.1	-0.76970584
240	0.315	1	33.275	0.2633	1.1961	18.574	18.6	-0.138849916
290	0.315	1	33.275	0.2633	1.1961	10.627	9.2	15.51973993
350	0.315	1	33.275	0.2633	1.1961	6.1024	7.4	-17.53470489
220	0.2	1	16.513	0.1917	1.0430	41.160	34.2	20.35275037
330	0.2	1	16.513	0.1917	1.0430	12.444	13.8	-9.821572748
270	0.2	1	16.513	0.1917	1.0430	22.495	25.5	-11.78346271

From the results obtained, it can be seen that the modified Taylor tool life equation can be used to obtain good estimates of tool life for various work/tool material combinations. In the following sections the modified Taylor tool life equation is used for selecting the optimum cutting conditions.

5.2.2 Worked Examples

In this section the optimisation procedure discussed so far is illustrated with examples which were obtained by executing the optimisation program (Fig.5-1(a), (b))

In these examples the tools used are the two carbide grades (uncoated P25 and coated P15). The tool life equation constants for these tool materials have been given in section 5.2.1. The cost rate of the machine used is assumed to be \$150 per hour. The maximum depth d_{max} is assumed to be 2.5 mm. The maximum feed f_{max} when calculated as described in section 3.3 is 0.64 mm/rev. The minimum values for depth and feed, d_{min} and f_{min} are assumed to be 0.5 mm and 0.2 mm/rev respectively. These values of d_{min}, f_{min}, d_{max} and f_{max} define the d-f planes (Fig.5-3, 5-6 and 5-8) for the optimisation procedure. All the remaining data used in these examples are given in the Appendix B.

Example 1

It is assumed that a 50 mm diameter AISI-1045 steel bar has to be machined using a P25 grade carbide tool (Holder: PDNNR2525; Insert: DNGA150408). The search for the optimum cutting conditions is confined to the d-f plane and the optimisation procedure starts from the top left corner as shown in Fig.5-3.

Fig.5-4(a) shows the variation of optimum cutting speed at the considered grid points while Fig.5-4(b) shows the variation of specific cost at these grid points. These results were obtained using the optimisation program discussed above using minimum cost as the economic criterion. The optimum tool life calculated is 6.12 min. At the first grid point (d = 2.5 mm and f = 0.2 mm/rev) the optimum cutting speed corresponding to a 6.12 min tool life is 209 m/min. The maximum speed that can be used without violating plastic deformation constraint is 390 m/min. Therefore this constraint is satisfied. The estimated power required at speed 209 m/min is 4.33 kW. Since the available power at that speed is 11.15 kW, the power constraint is also satisfied. The calculated interface temperature is 1180 K. Since it is above 1000 K, B.U.E. constraint is also satisfied. The specific cost of machining at this grid point is 26198 $/m^3$. The grid points at which the calculations are performed are clearly labelled in Fig.5-3; the specific cost corresponding to these grid points are shown in Fig. 5-4(b). The encircled

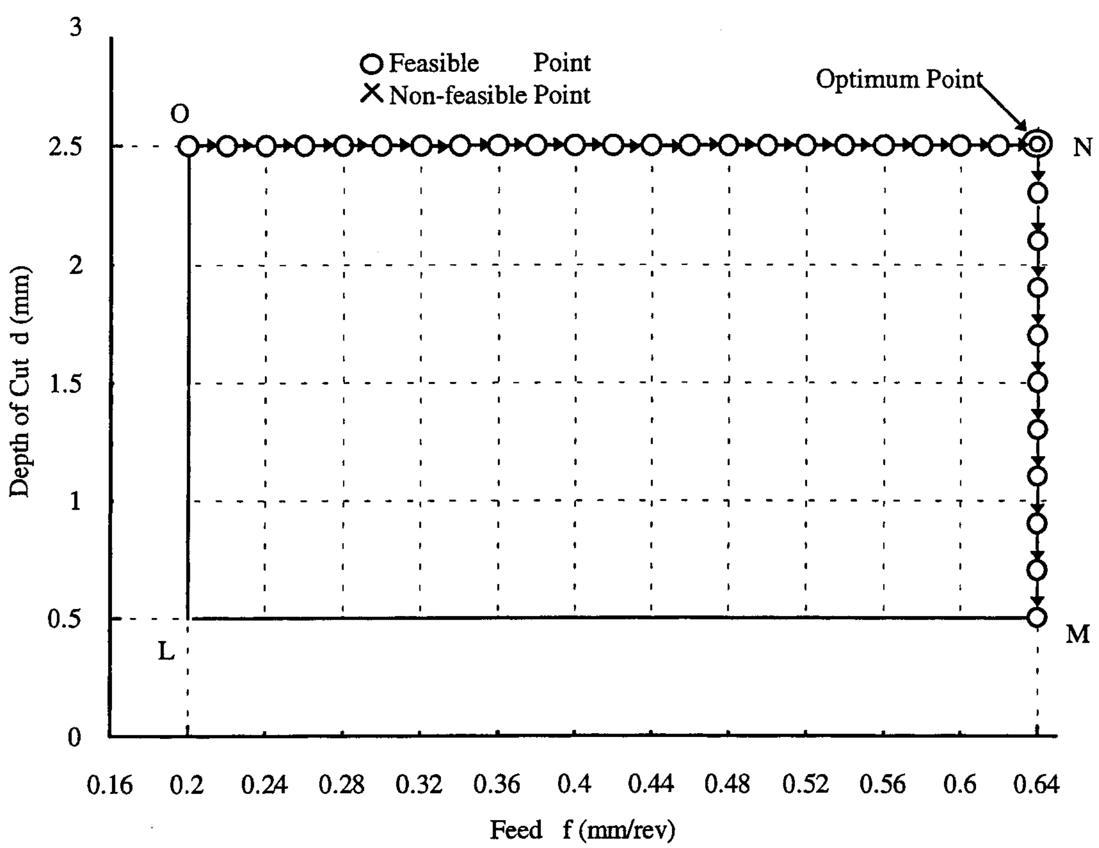

Fig. 5-3 Worked Example 1: Feasible and Non-feasible Grid Points on the Search Boundary

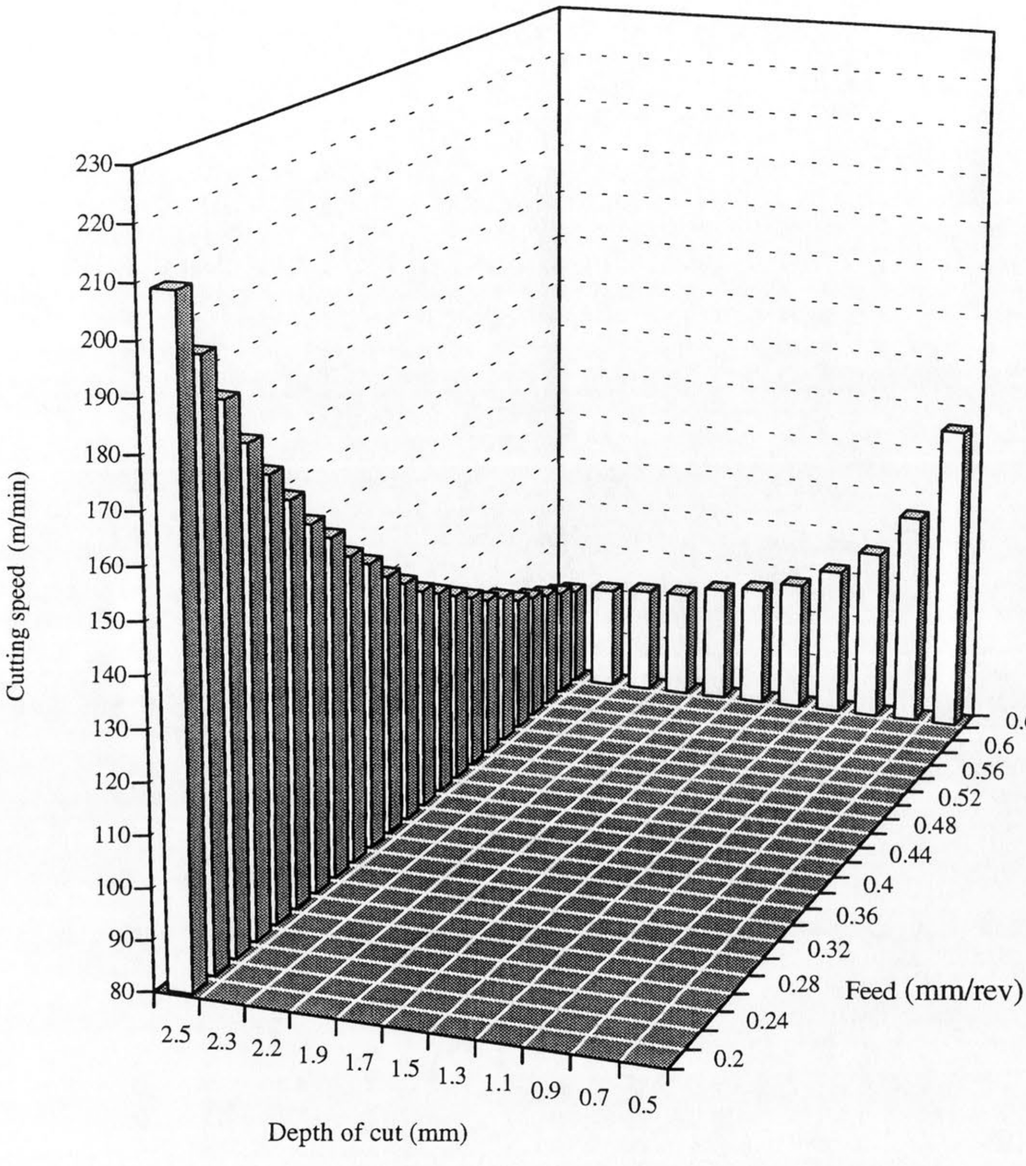

Fig.5-4(a) Worked Example 1: Optimum Cutting Speeds at Feasible Points for Specific Production Cost

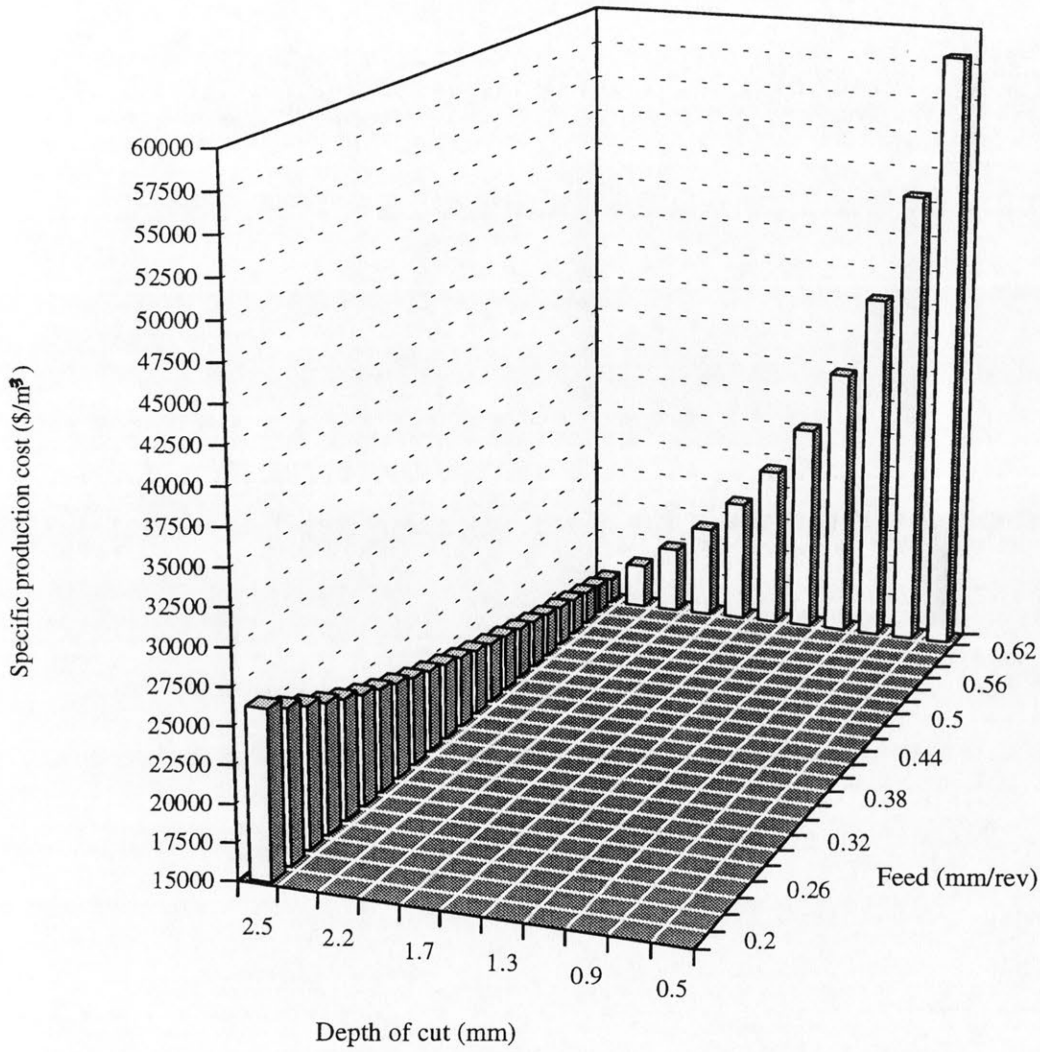

Fig.5-4(b) Worked Example 1: Specific Production Cost Values at Feasible Points

point results in the optimum depth/feed/speed combination, that is the position at which the specific production cost is a minimum. It can also be seen that for grid points from O to N (Fig.5-3) depth remains constant at 2.5 mm and feed increases from 0.2 to 0.64 mm/rev. With increase in feed both the unconstrained optimum cutting speed (Fig.5-4(a)) and the specific cost of machining (Fig.5-4(b)) decreases continuously. This clearly shows that, at a given depth, it is much more economical to machine using a high-feed/low-speed combination than a low-feed/high-speed combination.

Figs.5-5(a) and 5-5(b) show the results obtained using the optimisation program discussed above using maximum production rate as the economic criterion. The optimum tool life calculated is 3.126 min. Since this is lower than the minimum preset value (5 min), a tool life of 5 min is selected. Once again none of the grid points lying on the boundary ONM (Fig.5-3) were found to violate any of the constraints considered. The encircled grid point at which depth and feed are maximum and speed is minimum represents the optimum point since these cutting conditions result in the minimum production time (Fig.5-5(b)). For grid points from O to N with increase in feed both the unconstrained optimum cutting speed (Fig.5-5(a)) and specific production time (Fig.5-5 (b)) decrease continuously. This confirms that, at a given depth, it is much more economical to machine using a high-feed/low-speed combination than a low-feed/high-speed combination. Note that at a given grid point (depth/feed combination) the optimum speed for minimum cost criterion is lower than that for maximum production rate criterion. This is due to the fact that tool life for minimum cost criterion is greater than the tool life for maximum production rate criterion.

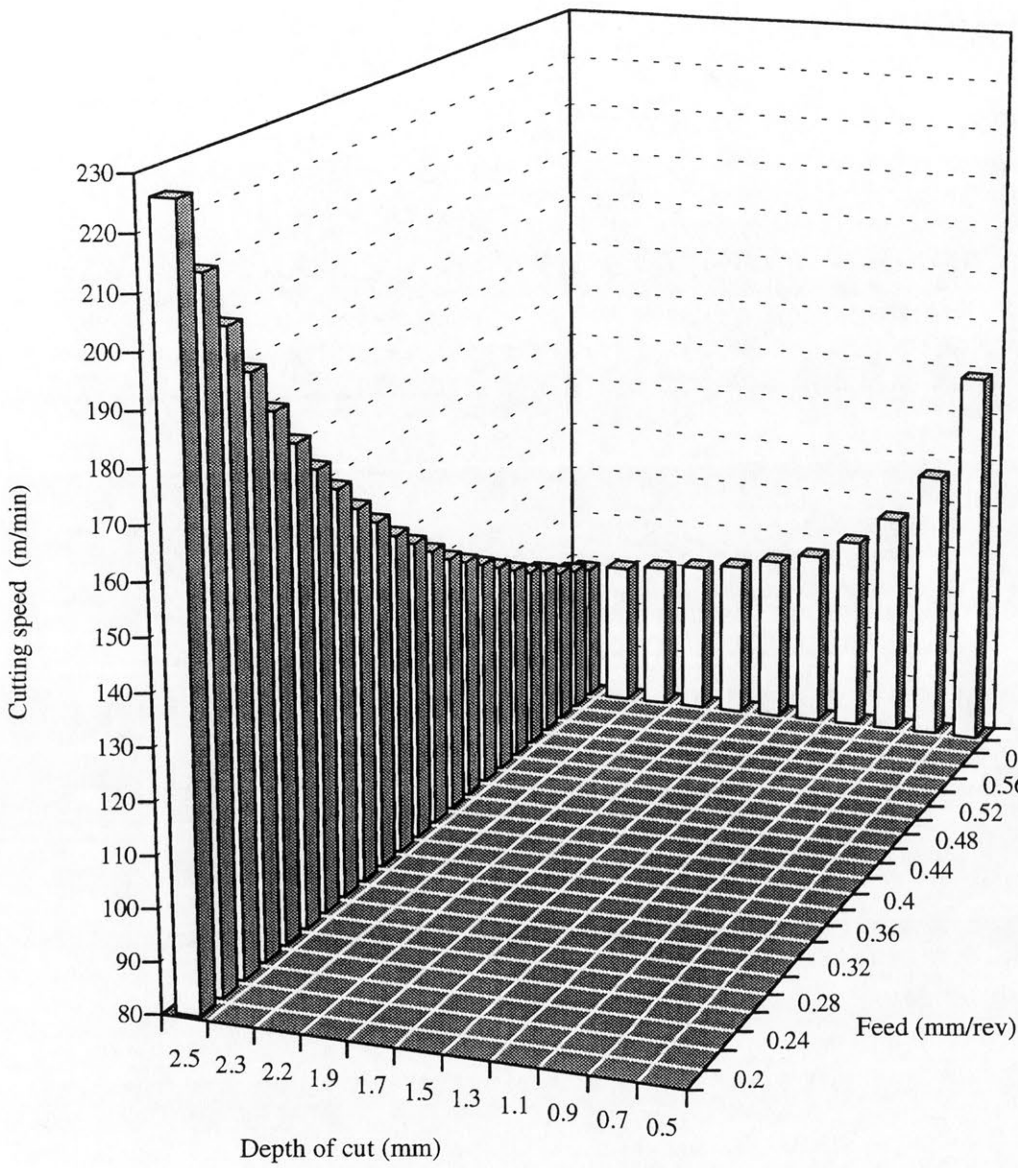

Fig.5-5 (a) Worked Example 1: Optimum Cutting Speed at Feasible Points for Specific Production Time

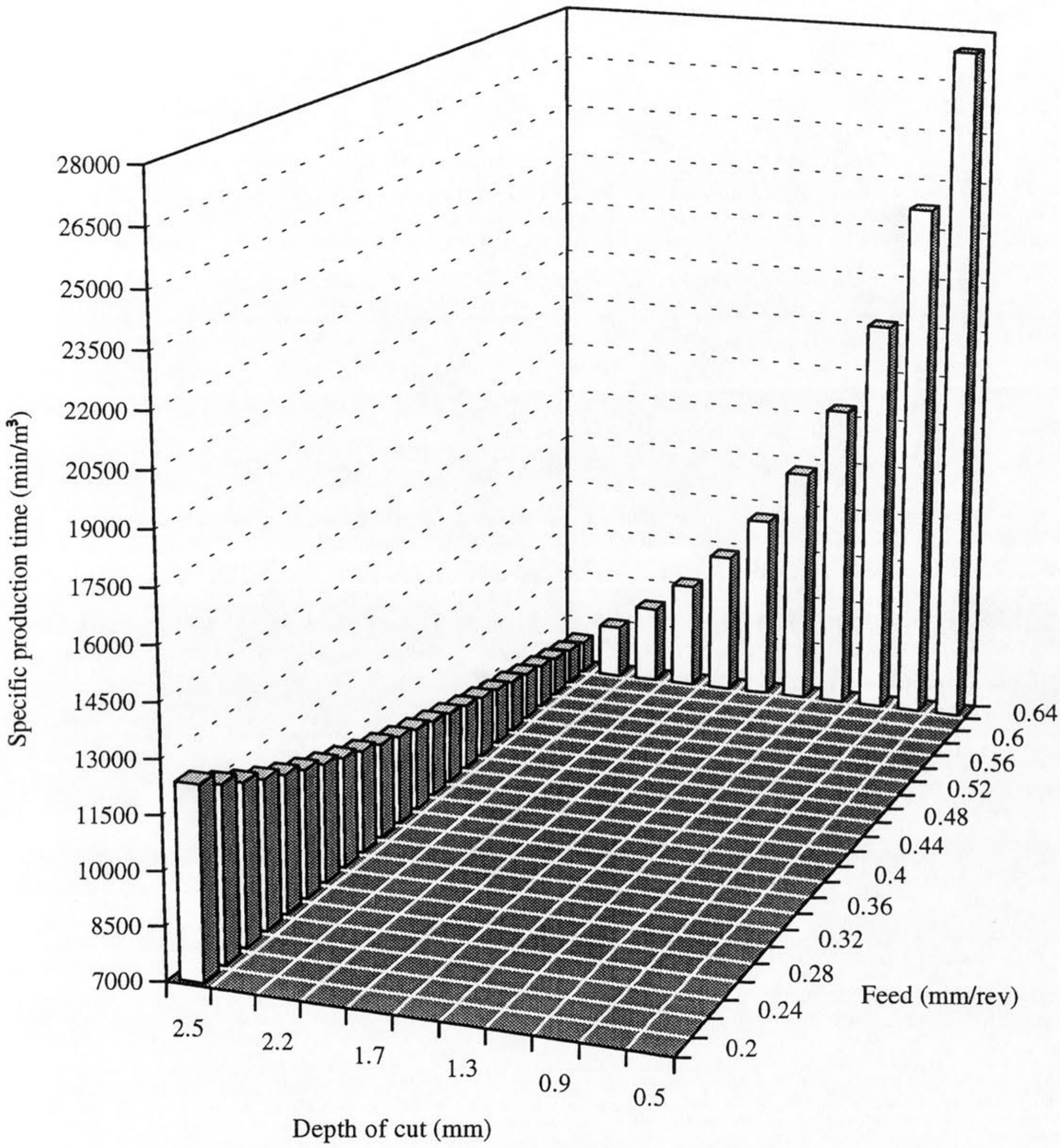

Fig.5-5(b) Worked Example 1: Specific Production Time Values at Feasible Points

Example 2

It is assumed that a 200 mm diameter AISI-1045 steel bar has to be machined using a tool with a P15 grade coated carbide insert (Holder: PCLNR2525; Insert: CNMG120408). The d-f plane used in the search for the optimum cutting conditions is shown in Fig.5-6.

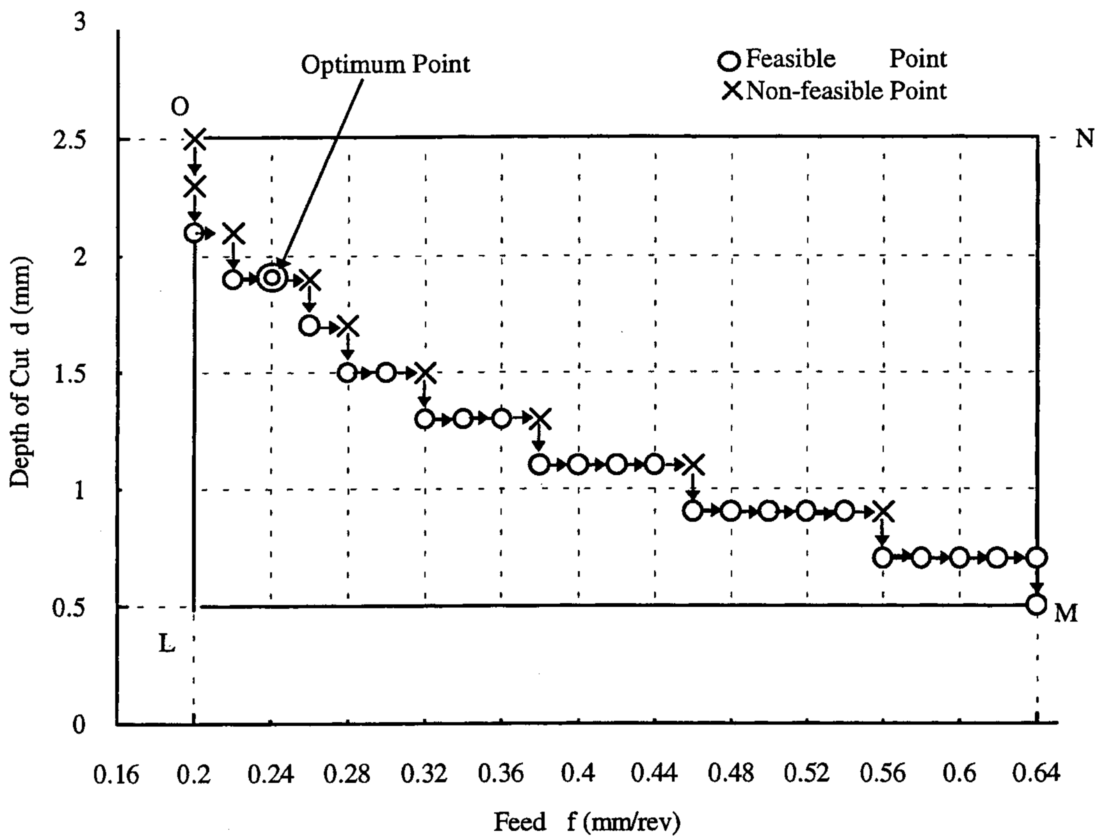

Fig. 5-6 Worked Example 2: Feasible and Non-feasible Grid Points on the Search Boundary

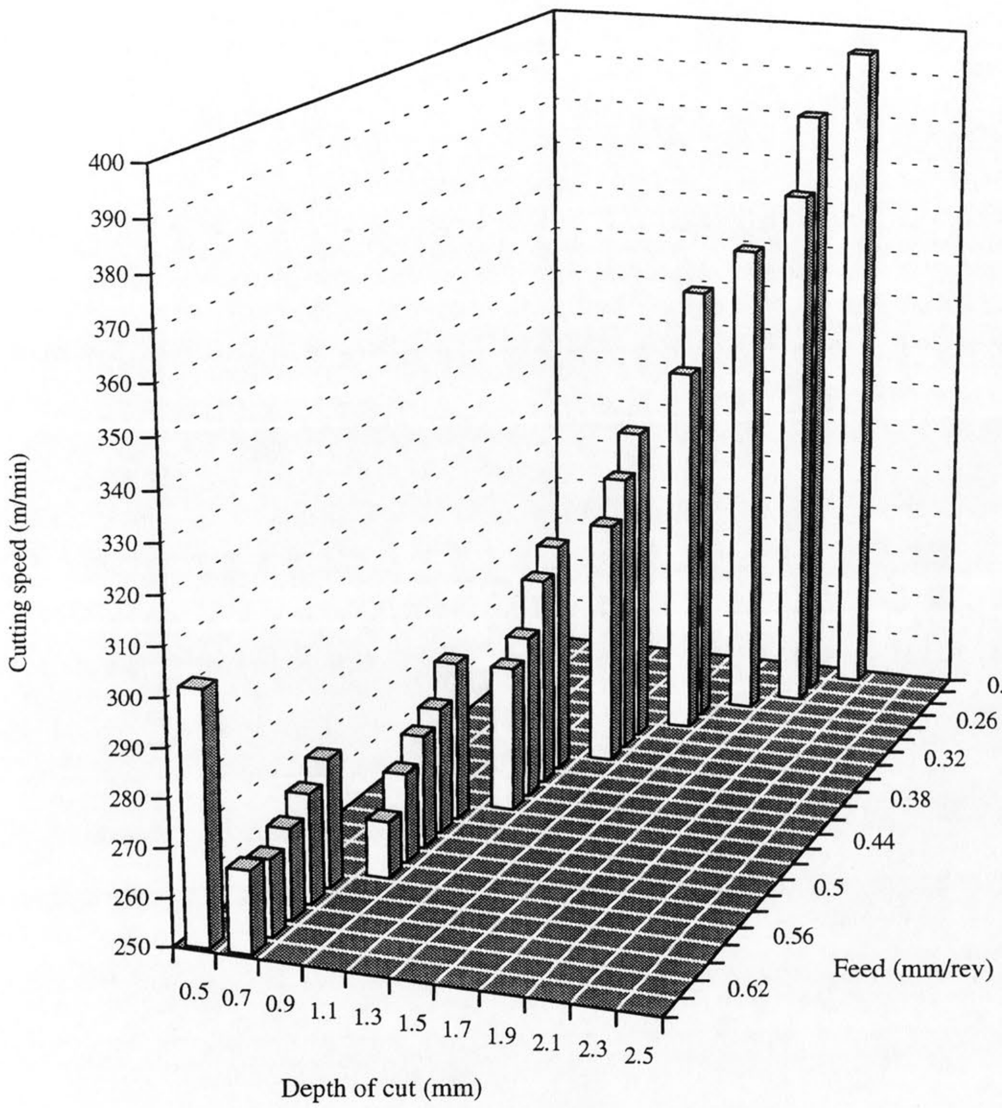

Fig. 5-7(a) Worked Example 2: Optimum Cutting Speeds at Feasible Points for Specific Production Time

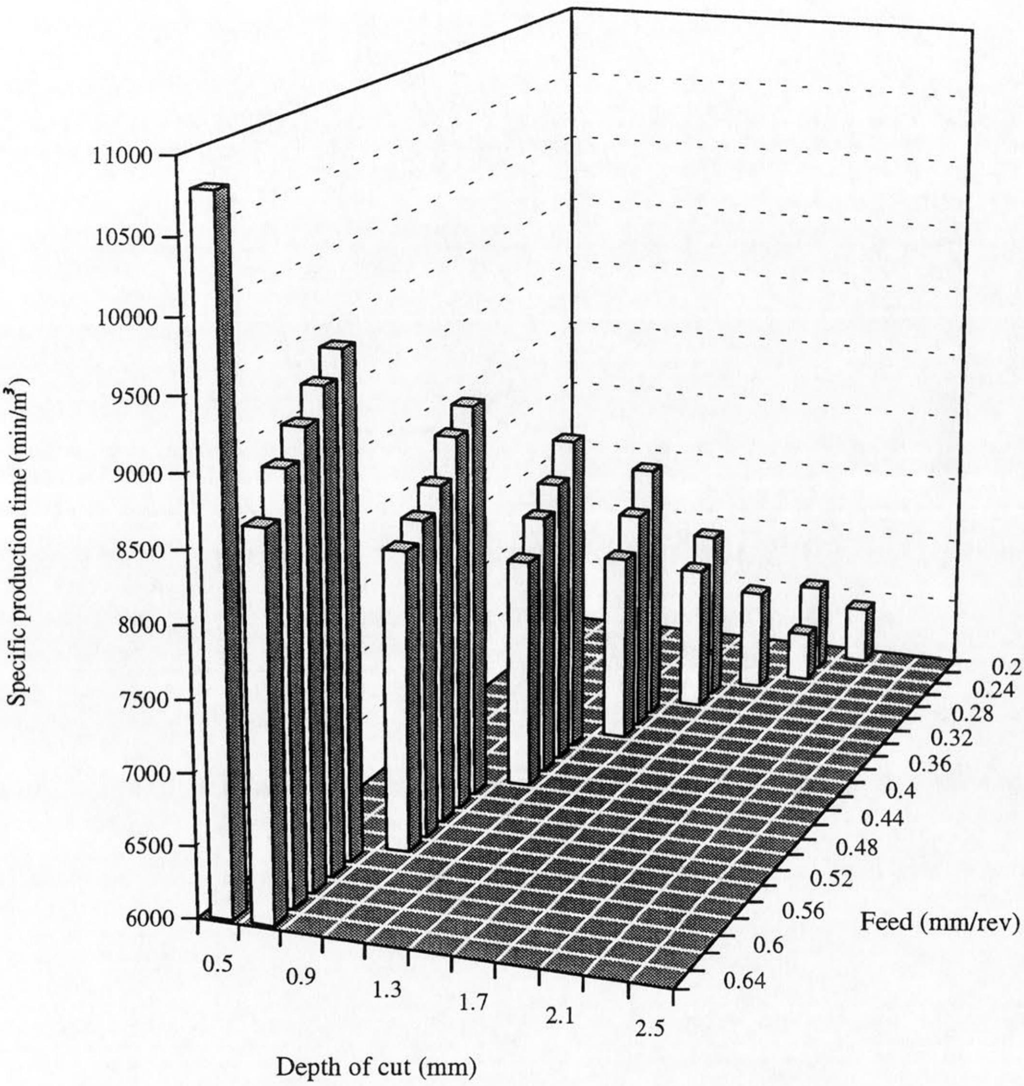

Fig. 5-7(b) Worked Example 2: Specific Production Time Values at Feasible Points

Fig.5-7(a) and Fig.5-7(b) show the results obtained using the optimisation program with maximum production rate as the economic criterion. The optimum tool life calculated is 3.9 min. Since this is lower than the minimum preset value (5 min), a tool life of 5 min is selected. At the first grid point (d = 2.5 mm and f = 0.2 mm/rev) the optimum cutting speed corresponding to a 5 min tool life is 699 m/min. The maximum speed that can be used without violating the plastic deformation constraint is 390 m/min. Therefore, the optimum speed cannot be used; instead the sub-optimum value of 390 m/min is selected. With this relatively low sub-optimum value still the power constraint cannot be satisfied. Therefore the grid point becomes unfeasible. The grid point corresponding to the next lower depth is also unfeasible due to power constraint. At the third grid point considered power constraint can be satisfied. All the grid points that are considered by the optimisation program and the point corresponding to the optimum depth/feed combination are shown in Fig.5-6. In this example all the unfeasible points are due to power constraint. At each feasible point the corresponding optimum cutting speed and specific production time are given in Fig.5-7(a) and 5-7(b). Note that, at a given depth, the optimum cutting speeds are much higher due to superior wear characteristics of the coated tool used in this example than the speeds for the previous one (Fig.5-5(a)) which are for an uncoated P25 grade tool.

Example 3

In order to investigate the effect of radius of cutting (workpiece diameter) on the machining process, a 200 mm diameter (instead of the 50 mm diameter bar in example 1) AISI-1045 steel bar is assumed to be machined using the same machining parameters (except the radius of cutting) as that in example 1. The d-f plane used in the search for the optimum cutting conditions is shown in Fig.5-8. Due to the increase of the radius of cutting, the shape of the search boundary is different to that in example 1. The reason is that some of the grid points violate certain process constraints.

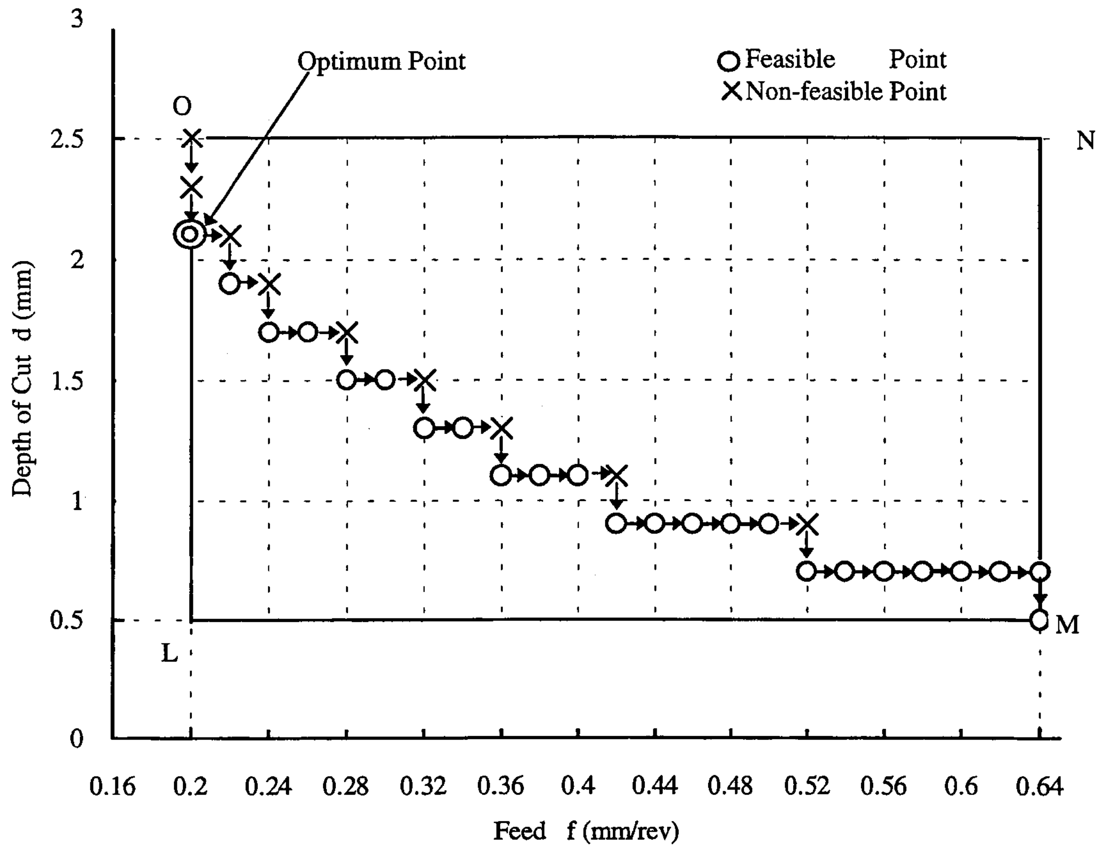

Fig. 5-8 Worked Example 3: Feasible and Non-feasible Grid Points on the Search Boundary

Figs.5-9(a) and 5-9(b) show the results obtained using the optimisation program discussed above with minimum production cost as the economic criterion. Similar to example 1, the optimum tool life calculated is still 6.12 min because the tool life equation constants are the same as that in example 1. At the first grid point (d = 2.5 mm and f = 0.2 mm/rev) the optimum cutting speed corresponding to a 6.12 min tool life is still 209 m/min.. The maximum speed that can be used without violating plastic deformation constraint is still 390 m/min. Therefore this constraint is satisfied. But this grid point is found to violate the power constraint. Therefore the optimum speed cannot be used. Since a sub-optimum speed cannot be found to satisfy the power constraint this grid point becomes unfeasible. The grid point corresponding to the next lower depth is also unfeasible due to power constraint. At the third grid point considered power

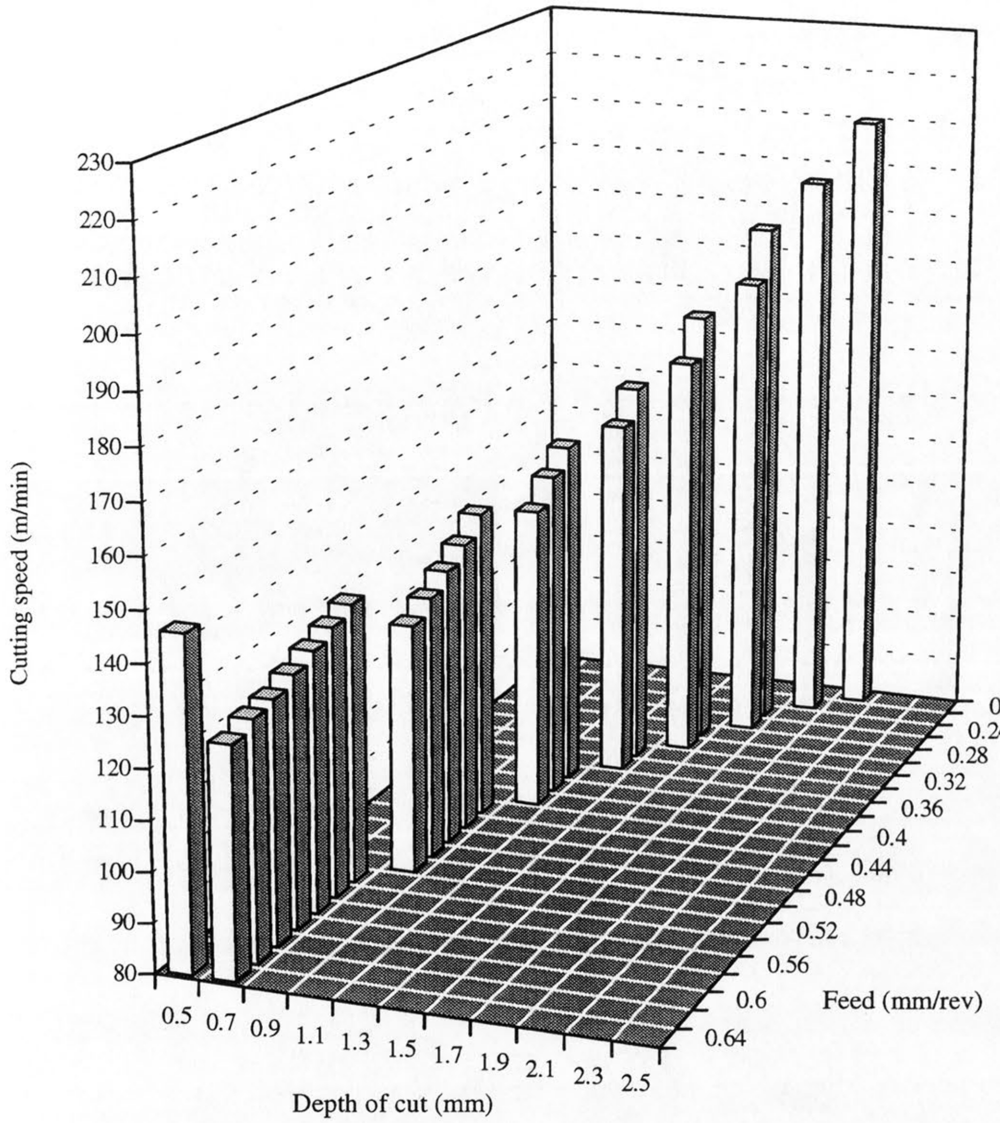

Fig. 5-9(a) Worked Example 3: Optimum Cutting Speeds at Feasible Points for Specific Production Cost

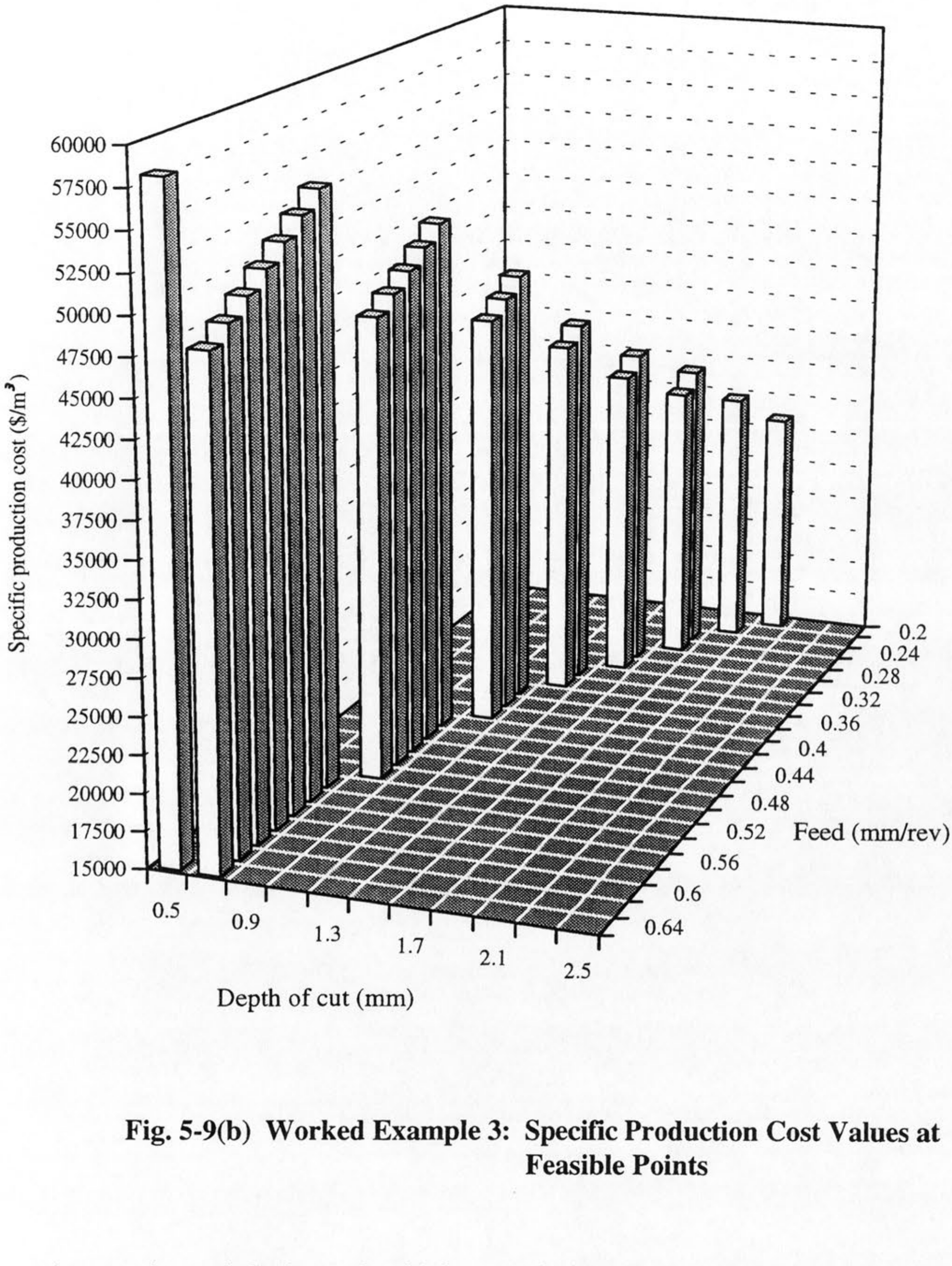

Fig. 5-9(b) Worked Example 3: Specific Production Cost Values at Feasible Points

constraint can be satisfied. It should be noted that the grid point corresponding to the minimum specific production cost is no longer the grid point with the maximum depth, maximum feed and the lowest speed (101 m/min); instead the third grid point with a depth 2.1 mm, the minimum feed and a speed 210 m/min is the optimum point. The corresponding minimum specific production cost is 30999 $\$/m^3$ which is nearly two times that of 16866 $\$/m^3$ in example 1.

Figs.5-10(a) and Fig.5-10(b) show the results obtained using the optimisation program discussed above with maximum production rate as the economic criterion. Once again the third grid point (Fig.5-8) is the optimum point for this economic criterion. The corresponding specific production time is 14645 min/m^3 which is also nearly two times that of 7968 min/m^3 in example 1.

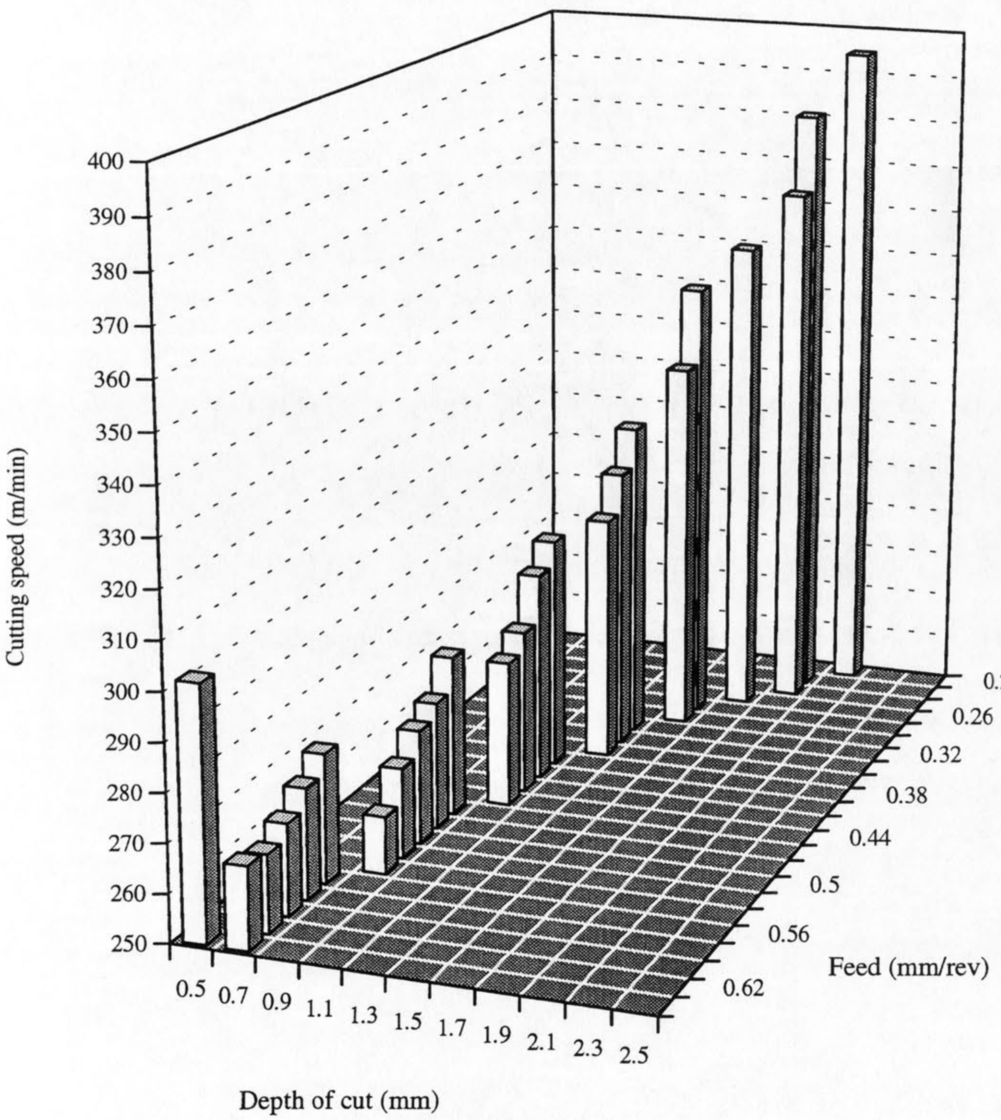

Fig. 5-10(a) Worked Example 3: Optimum Cutting Speeds at Feasible Points for Specific Production Time

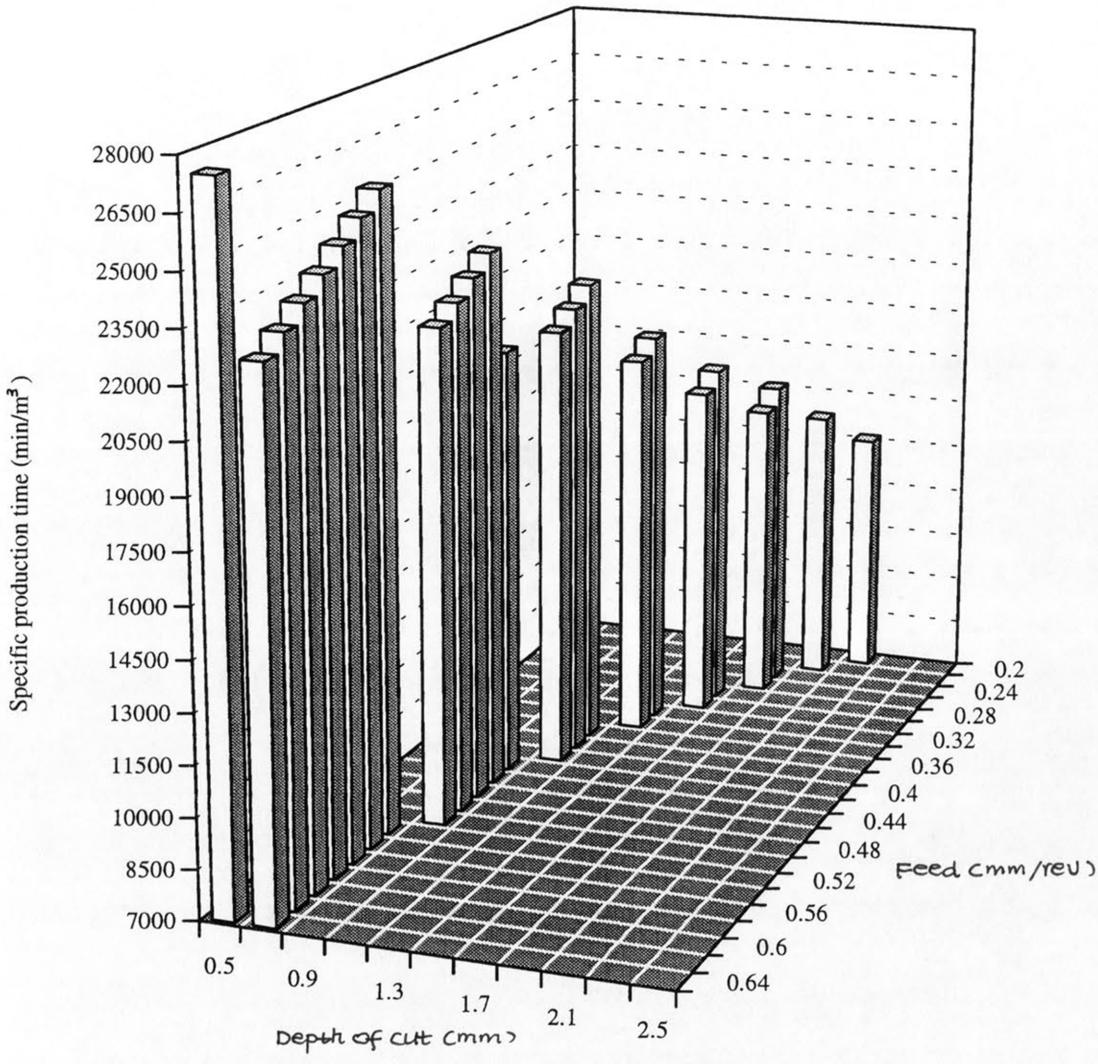

Fig. 5-10(b) Worked Example 3: Specific Production Time Values at Feasible Points

In example 1 the grid point corresponding to the maximum depth/feed combination was the optimum which was also unconstrained. In this example the larger work diameter (200 mm compared to 50 mm in example 1) has made the above grid point unfeasible due to power constraint. The optimum grid points corresponding to minimum cost and maximum production rate economic criteria have been obtained using the search procedure developed. However, it can be seen that the production cost and time corresponding to these optimum points are approximately twice as much as those obtained in example 1.

Example 4

In a production situation the carbon content of incoming steel can vary around the nominal amount recommended. To consider the effect of varying carbon content in work material on the optimum cutting conditions, example 1 was considered again but this time the carbon content of the work material (AISI-1045) was changed from 0.45%C to 0.52%C (the maximum allowable variation was 0.07%C), while the rest of machining parameters were kept the same as those in example 1. Since the chemical composition of work material is changed, the constants for tool life equation (Eq.(3-4)) are recalculated using the procedure described in section 5.21. These new constants are given below.

$A_t = 320181.3$ $b_t = 2.63$ $c_t = 1.67$ $d_t = 0.0007$.

Using the above constants, the optimum tool life calculated is 6.33 min, which is greater than that (6.12 min) in example 1. Therefore the optimum cutting speeds at the grid points on the boundary are now lower than those in example 1. Although the optimum grid point corresponding to the minimum specific production cost/time is still the point with maximum depth, maximum feed and the lowest speed, the value of minimum specific production cost/time is slightly different.

Table 5-1 shows the differences of these optimum results with changing carbon content in the work material. From the results given in Table 5-1, it can been seen that with the carbon content is increased from 0.45% to 0.52%, for minimum cost objective criterion the optimum cutting speed has decreased from 101 m/min to 95.4 m/min. This decrease in optimum cutting speed has resulted in a 4.99% increase in the specific production cost. For the maximum production rate criterion, with the above increase in carbon content, the optimum cutting speed has decreased from 109 m/min to 104 m/min. This decrease in optimum cutting speed has resulted in a 5.17% increase in the specific production time. The calculated results for the above examples were also given in the tables in Appendix C.

Table 5-2 Comparison of Optimum Results with Changing Carbon Content (Work Material: AISI 1045)

	Optimum cutting conditions				Economic values	
Carbon content (%C)	Depth of cut (mm)	Feed (mm/rev)	Optimum speed for cost (m/min)	Optimum speed for time (m/min)	Specific production cost ($\$/m^3$)	Specific production time (min/m^3)
0.45 (C1)	2.5	0.64	101	109	16866	7968.4
0.52 (C2)	2.5	0.64	95.4	104	17707.7	8380.6
% Difference with respect to C1	-	-	-5.54	-4.59	4.99	5.17

Note that the optimum cutting conditions given in the above examples compare favourably with those recommended by the tool manufacturers for the tool/workpiece combination considered. Theses results show that the described optimisation procedure using the machining theory can be used to determine the optimum cutting conditions in rough turning.

CHAPTER SIX - Conclusions and Suggestions for Further Work

Chapter 6 Conclusions and Suggestions for Further Work

6.1 Concluding Remarks

Since the cost of machining on the expensive advanced machines is sensitive to the cutting conditions, optimum values have to be determined before a part is put into production. The optimum cutting conditions in this context are those that do not violate any of the constraints that may apply on the process and satisfy the economic criterion.

Since many of the constraints are influenced by parameters such as tool life and cutting forces, one has to estimate these parameters with a reasonable degree of accuracy. In most of the optimisation procedures investigated, the prediction of these parameters has to be done using empirical equations. But the required empirical data for a given job are not readily available. In addition it is extremely time consuming and expensive to obtain and manage these data. This has resulted in a limited application of these optimisation procedures. Therefore an alternative to the above empirical approach that can be used to predict cutting forces, tool life, etc. is of great value.

The variable flow stress machining theory which has been extended to the more general case of oblique machining with nose radius tools using the concept of equivalent cutting edge, was used in the described work to predict cutting forces, temperatures, stresses, tool life, etc.. This minimised the empirical data required in determining optimum cutting conditions for oblique machining with nose radius tools. In addition, it was shown that a modified form of extended Taylor tool life equation can be used to predict the tool life with good accuracy. The required constants for this equation were determined using a method which used the machining theory. This approach greatly reduced the amount of experimental work needed in collecting tool life data as it allows variations in work material properties and tool geometry to be allowed for independently of experiments.

Since plastic deformation of tool has adverse effects on the machining process, it has to be incorporated in determining the optimum cutting conditions. An analytical model developed to calculate the stresses inside the cutting edge of a tool has been proven to be effective. Using this model, a method has been developed in the present work which has been successfully used to predict cutting conditions at which the cutting edge starts to deform plastically when machining with oblique nose radius tools. It has been shown that tool stresses and temperatures determined from the machining theory could be used together with experimental high temperature compressive strength data for the tool material to make these predictions. Experiments were carried out to check the accuracy of this method. The comparison made between predicted and experimental results obtained for two plain carbon steel work material and a range of cutting conditions shows good agreement.

The optimisation procedure incorporating the above methodologies has been presented in this work for determining the optimum cutting conditions for turning operations. A number of worked examples were given to demonstrate and validate the optimisation procedure. Based on the results of these worked examples, the following have been noted:

(i) At a given depth, it is much more economical to machine using a high-feed/low-speed combination than a low-feed/high-speed combination when none of the process constraints are violated.

(ii) At a given depth/feed combination, the optimum speed for minimum cost criterion is lower than that for maximum production rate criterion due to the fact that tool life for minimum cost criterion is greater than the tool life for maximum production rate criterion.

(iii) Due to superior wear characteristics of the coated tool, the optimum cutting speeds for this tool are much higher than the corresponding speeds for an uncoated tool used.

(iv) Due to the power constraint, the *d-f* plane grid point corresponding to the maximum feed/depth combination might be unfeasible when a work material with larger diameter is machined. When that happened, the production cost/time was found to increase considerably.

(v) The effect of varying carbon content in work material on the optimum cutting conditions should be considered in practice. It has been shown that the differences of the optimum cutting conditions and the resulting production cost/time due to the maximum allowable variation of carbon content is about 5%.

(vi) The optimum cutting conditions given in the above examples compared favourably with those recommended by the tool manufacturers for the tool/workpiece combination considered. The results indicated that the optimisation procedure developed in this work is capable of selecting the appropriate cutting conditions.

There is no need to emphasise that the computer program is valuable in the obtaining of optimum cutting conditions. The need for this is, for instance, increasingly being recognised during the last twenty years or so by the management of small workshops and particularly those who operate CNC-lathes.

6.2 Suggestions for Further Work

The optimisation procedure presented in this thesis has been successfully applied in single pass turning. It is recommended that the present method would be extended to the multi-pass turning situation and for that purpose an approach similar to the one described by Arsecularatne et al (1992) could be used. The strength of the described method lies in the use of fundamental thermal and flow stress properties of the work material in making machining predictions. At this stage analysis has to be restricted to plane face tools which may limit the practical value of the work. In particular chip breaking constraint needs to be incorporated into the optimisation procedure so that the method can have wider application. This will require the machining theory to be extended so that cutting forces, tool life, etc. for chip breaker tools can be predicted. As a first step towards the prediction of cutting forces for these tools a method has been developed (Arsecularatne and Oxley, 1997) by which the cutting forces can be predicted in orthogonal machining with restricted contact tools. The method uses orthogonal machining theory (Oxley, 1989) to predict the cutting forces and natural tool-chip contact length for the equivalent plane face tool. These parameters are then used together with suitable empirical equations to predict forces under restricted contact conditions. It is recommended that further work be done to extend this approach to predict cutting forces, tool life, etc. where machining with commercial chip breaker tools. Once completed, this work should offer an alternative, far more efficient approach to selecting cutting conditions when using tools with chip breakers than the empirical methods widely used at present for this purpose.

It is also recommended that the method used to predict tool plastic deformation be extended to tools with chip-breakers in the near future for wider applications.

REFERENCES

Agapiou, J.S., 1992, *The Optimisation of Machining Operations based on a Combined Criterion, Part 1: The Use of Combined Objectives in Single-Pass Operations,* Trans. ASME, v114, Nov., pp500-513.

Armarego, E.J.A. and Russel, J.K., 1966, *Maximum Profit Rate as a Criterion for the Selection of Machining Conditions,* Int. J. Prod. Res., v6, pp15-23.

Armarego, E.J.A. and Brown, R.H., 1969, *The Machining of Metals,* Prentice-Hall.

Armarego, E.J.A. and Chia, 1980, *The Influence of Constraints on Maximum Production Rate cutting Conditions Selection for Rough Turning,* International Conference on Manufacturing Engineering, August, Melbourne, Australia.

Arsecularatne, J.A., 1990, *A Process Monitoring System to Optimize Cutting Conditions in Turning*, PhD thesis, University of Manchester Institute of Science and Technology.

Arsecularatne, J.A., Hinduja, S. and Barrow, G., 1992, *Optimum cutting conditions for turned components,* Proceedings of the Institution of Mechanical Engineers, v206, pp15-30.

Arsecularatne, J.A., 1993, *Prediction of the Radial Force in Turning Using Feed Force Data,* International Journal of Machine Tools Manufacture, v33, n6, pp827-840.

Arsecularatne, J.A., Mathew, P. and Oxley P.L.B., 1995, *Prediction of Chip Flow Direction and Cutting Forces in Oblique Machining with Nose Radius Tools*, Proc. Inst. Mech. Engrs., Part B, v209, pp305-315.

Arsecularatne, J.A., Fowle, R.F., Mathew, P. and Oxley, P.L.B., 1996, *Prediction of Cutting Forces and Built-up Edge Formation Conditions in Machining with Oblique Nose Radius Tools*, Proceedings of the Institution of Mechanical Engineers, v210(B), pp457-469.

Arsecularatne, J.A., Fowle, R.F., Mathew, P. and Oxley, P.L.B., 1996, *Prediction of Tool Life in Oblique Machining with Nose Radius Tools*, Wear, 198, pp 220-228.

Arsecularatne, J. A., 1997, *On Tool-chip Interface Stress Distributions, Ploughing Force and Size Effect in Machining*, International Journal of Machine Tools Manufacture, v37, n7, pp885-899.

Arsecularatne J.A. and Oxley P. L. B., 1997, *Prediction of Cutting Forces in Machining with Restricted Contact Tools*, Machining Science and Technology, v1, n1, pp95-112.

Arsecularatne, J. A., 1998, *Private Discussion.*

Brewer, R.C., 1958, *On the Economics of the Basic Turning Operation,* Trans. ASME, 80, pp1479-1489.

Brewer, R.C. and Reuda, R., 1963, *A Simplified Approach to the Optimum Selection of Machining Parameters,* Engineer's Digest, September, v24, n9, pp133-150.

Brown, R.H., 1962, *On the Selection of Economical Machining Rates,* Int. Jnl. Prod. Res., v1, n2, March, pp1-22.

Broothroyd, G., 1963, *Temperatures in Orthogonal Metal Cutting,* Proc. Instn. Mech. Engrs. 177, p789-802.

Chen, L. and Rao, S.S., 1997, *Manipulation of uncertainties in the Determination of Optimal Machining Conditions Under Multiple Criteria,* Journal of Manufacturing Science and Engineering, Transactions of the ASME, v119, pp186-192.

C.I.R.P., 1976, *Reports: International Directory of Machining and Production Information Centres.*

Colding, B.N., 1969, *Machining Economics and Industrial Data Manuals,* Annals of the C.I.R.P., v17, pp279-288.

Cook, N.H. and Goldberger, D.S., 1982, *Machining Parameter Selection Using On-Line Adaptive Control, in On the Art of Cutting Metals -75 years later: A Tributer to F. W. Taylor,* ASME. PED 7, pp159-166.

Crookall, J.R., 1969, *The Performance-Envelope Concept in the Economics of Machining,* Int. J. Mach. Tool Des. Res., v9, pp261-278.

Crookall, J.R. and Venkataramani, N., 1971, *When It Pays to Machine in More than One Pass,* Metalworking Production, January, pp148-155.

Cus, F., Sokovic, M. and Balic, J., 1997, *Model of Complex Optimization of Cutting Conditions,* Journal of Materials Processing Technology 64, pp41-52.

Da, Z.J., Sadler, J.P. and Jawahir, I.S., 1996, *Multiple Criteria Optimization of Finish Turning Operations based on a Hybrid model,* Proceedings, The 1996 ASME Design Engineering Technical Conferences, Computers in Engineering Conference, August, Irvine, Ca., USA, pp1-10.

DeGarmo, E.P., Black, J.T. and Kohser, R.A., 1990, *Materials and Processes in Manufacturing, 7th ed.,* Macmillan, New York.

Erner, D.S. and Patel, D.C., 1974, *Maximization of the Production Rate with Constraints by Linear Programming and Sensitive Analysis,* Second North American Metalworking Research Conference, Madison, Wisc., USA.

Ernst, H. And Merchant, M.E., 1941, *Chip Formation, Friction and High Quality Machined Surfaces,* Trans. Am. Soc. Met. 29, pp299-378.

Gilbert, W.W., 1950, *Economics of Machining, Machining -Theory and Practice,* Anne. Soc. Metals, pp465-473.

Gupta, R., Batra, J.L. and Lal, G.K., 1994, *Profit Rate Maximazation in Multipass Turning with Constraints: a Geometric Programming Approach,* Int. J. Prod. Res., v32, n7, pp1557-1569.

Hinduja, S., Petty, D.J., Tester, M. And Barrow, G., 1985, *Calculation of Optimum Cutting Conditions for Turning Operations,* Proc Instn Mech Engrs, v199, nB2, pp81-92.

Hitomi, K. and Nakamura, N., 1971, *Optimization of Machining : Concept of Optimum-Seeking Machining and Experimental Results,* Annals of the CIRP, v20, n1, pp101-104.

Hu, R.S., Mathew, P. Oxley, P.L.B. and Young, H.T., 1986, *Allowing for End Cutting Edge Effects in Predicting Forces in Bar turning with Oblique Machining Conditions,* Proc. Instn Mech. Engrs, Part C, 200(C2), pp89-99.

Kaczmarek, J., 1976, *Principles of Machining by Cutting, Abrasion and Erosion,* Peter Peregriuus limited, Stevenage, Wydawnictwa Naukowo -Techniczne, Warsaw.

Kals, H.J.J. and Higink, J.A.W., 1978, *A Computer Aid in the Optimisation of Turning Conditions in Multicut Operations,* Annals of the CIRP, v27, pp465-470.

Kee, P.K., 1995, *Alternative Optimisation Strategies and CAM Software for Multipass Rough Turning Operations,* Int J Adv Manuf Technol 10, pp287-298.

Kegg, R.C. and Zdeblick, W.J., 1983, *High Speed Milling of Aluminium - Research vs Todas's Practices,* Paper Presented to the Numerical Control Society Conference, USA.

Kilic, S.E., Cogun, C. And Sen, D.T., 1993, *A Computer-aided Graphical Technique for the Optimization of Machining Conditions,* Computers in Industry 22, pp3319-326.

Kobayashi, S. and Thomsen, E.G., 1962, Tyrans. Am. Soc. Mech. Engrs B 84, p71.

Kronenberg, M., 1966, *Machining Science and Application: Theory and Practice for Operation and Development of Machining Process,* Pergamon Press, Oxford.

Kuljanic, E., 1992, *Macro Plastic Deformation of Cutting Edge--A Method for Maximum Utilization of Cutting Tool,* Annals of the CIRP v41(1), pp151-154.

Lee, E.H. and Shaffer, B.W., 1951, *The Theory of Plasticity Applied to a Problem of Machining,* J. Appl. Mech., 18, pp405-413.

Lee, Y.H., Shin, H.M. and Yang, B.H., 1996, *An Approach for Multiple Criteria Simulation Optimization with Application to Turning Operation,* Computers ind. Engng v30,n3, pp375-386.

Loladze, T. N., 1975, *Nature of Brittle Failure of Cutting Tool,* Ann. CIRP 24, pp13-15.

Li, Xiaoping, 1991, *A Computer-based Numerical Study of the Role of Cooling in Machining*, Ph.D. thesis, UNSW.

Li, Xiaoping, 1997, *Development of a predictive model for stress distributions at the tool-chip interface in machining*, J. Materials Processing Technology 63, pp169-174.

Lin, G.C., Mathew, P., Oxley, P.L.B. and Watson, A.R., 1982, *Predicting Cutting Forces for Oblique Machining Conditions,* Proc Instn Mech Engrs, v196, pp141-148.

Mathew, P., 1983, *A Theoretical and Experimental Investigation of the Mechanics of Machining*, PhD Thesis, The University of New South Wales.

Meng, Q., Arsecularatne, J.A. and Mathew, P., 1998, *Prediction of the Cutting Conditions Giving Plastic Deformation of the Tool in Oblique Machining,* International Journal of Machine Tools & Manufacture, 38, pp1165-1182.

Meng, Q., Arsecularatne, J.A. and Mathew, P., *Calculation of Optimum Cutting Conditions for Turning Operations Using a Machining Theory,* under preparation.

Mesquita, R., Krasteva, E. and Doytchinov, S., 1995, *Computer-Aided Selection of Optimum Machining Parameters in Multipass Turning,* Int J Adv Manuf Technol 10, pp19-26.

Metcut Research Associates, 1980, *Machining Data Handbook,* Ohio.

Nachev, V.I., 1983, *Obtaining a Machinablity Chart Using a Mechanics of Mechining Approach,* BE thesis, UNSW.

Nachev, V.I. and Oxley, P.L.B., 1985, *Predicting Cutting Conditions Giving Plastic Deformation of the Cutting Edge in Terms of Tool and Work Material Properties,* Proceedings of the 25th International MTDR Conference, Macmillan, London, pp225-230.

Nash, W.A., 1994, *Schaum's Outline of Theory and Problems of Strength of Materials ,3rd ed.,* McGraw-Hill, New York.

Nee, A.Y.C., 1983, *The Optimization of Machining Conditions with a Programmable Calculator,* 11 NAMRC Proceedings, May, Madison, Wisc., USA, pp111-116.

Norusis, M.J., 1992, *SPSS for Windows: Base System User's Guide, Release 5.0,* SPSS Inc.

Okushima, K. and Hitomi, K., 1964, *A Study of Economical Machining: An Analysis of the Maximum Profit Cutting Speed,* Int. J. Prod. Res., v3, pp73-78.

Oxley, P.L.B. and Hastings, W.F., 1976, *Minimum Work as a Possible Criterion for Determining the Frictional Condition at the Tool/Chip Interface in Machining,* A. Mathematical and Physical Sciences, v282, pp565-584.

Oxley, P.L.B., 1989, *Mechanics of Machining: An Analytical Approach to Assessing Machinability,* Ellis Horwood, Chichester.

Petropoulos, P.G., 1973, *Optimum Selection of Machining Rate Variables by Geometric Programming,* Int. J. Prod. Res. V11, pp305-314.

Sampath, W.S., Lee, Y.M. and Shaw, M.C., 1984, *Tool Fracture Probability Under Steady State Cutting Conditions,* J. Engineering for Industry, May, Trans. Of the ASME, v106, pp161-167.

Schey, J.A., 1984, *Introduction to Manufacturing Processes, 2rd ed.,* McGrow-Hill, New York.

Shaw, M.C., Cook, N.H. and Finnie, I., 1953, *Shear Angle Relationships in Metal Cutting,* Trans. Am. Soc. Mech. Engrs 75, pp273-288.

Shaw, M.C., 1984, *Metal Cutting Principles,* Clarendon Press, Oxford.

Timoshenko, S.P. and Goodier, J.N., 1987, *Theory of Elasticity, 3rd,* McGraw-Hill Publishing Company, New York.

Tlusty, J. and Masood, Z., 1978, *Chipping and Breakage of Carbide Tools*, Trans. ASME, J. Eng. Ind. v100, pp403-412.

Trent, E. M., 1968, *Hot Compressive Strength of Cemented Carbides*, Proceedings of the 8th International MTDR Conference, Manchester, pp629-642.

Venkatesh, V.C., 1986, *Computerized Machinability Data,* AUTOMACH Australia'86 Conference Proceedings, Sydney, Australia, May.

White, B. and Houshyar, A., 1992, *Quality and Optimum Parameter Selection in Metal Cutting,* Computer in Industry 20, pp87-98.

Wu, S.M. and Ermer, D.S., 1966, *Maximum Profit as the Criterion in the Determination of the Optimum Cutting Conditions,* Journal of Engineering for Industry, Trans. ASME, November, pp435-442.

Yakowitz, S. And Szidarovszky, F., 1990, *An Introduction to Numerical Computations, 2nd ed.,* Macmilian-Collier.

Young, H.T., Mathew, P. And Oxley, P.L.B., 1987, *Allowing for Nose Radius Effects in Predicting the Chip flow Direction, and Cutting forces in Bar Turning,* Proc. Instn. Mech. Engrs, Part C, 201(C3), pp213-226.

Zhou, J. M., Sturesson, P. O., Sandqvist, H. and Stahl, J. E., 1994, *An Approach for On-Line Cutting Edge Stress Estimation*, Int. J. Mach. Tools Manufact. v34, n5, pp741-75.

APPENDIXES -

Appendix A Data for Prediction of Tool Life for Seco S4 Tool Material and AISI 1022 Steel Work Material

(i) *Tool*: Seco S4 (rake angle = 10 deg; inclination angle = 10, -10 deg; side cutting edge angle = 10, 20 deg; tool nose radius = 0.4, 0.8 mm).

(ii) *Work material*: AISI 1022 carbon steel (0.19%C, 0.88%Mn, 0.27%Si, 0.085%Cr, 0.021%P, 0.02%S, 0.02%Ni, 0.02%Cu, 0.02%Ti and 0.05%Mo).

(iii) *The constants* for Eq.(5-1): A = 52.97, B = -16.997 (Arsecularatne, 1998)

(iv) Cutting conditions and corresponding temperatures from the machining theory and the predicted values of tool life from Eq.(5-1):

w (mm)	tc (mm)	U (m/min)	Tint (deg)	T_f (K)	T (min)
1.5	0.2	150	832.7	995.13	107.05
1.5	0.2	190	874.4	1032.66	57.52
1.5	0.2	250	928.7	1081.53	26.22
3.5	0.3	170	894.3	1050.57	42.95
3.5	0.3	210	937.8	1089.72	23.07
3.5	0.3	260	985.1	1132.29	12.03
4.5	0.5	160	947.9	1098.81	20.03
4.5	0.5	200	998.6	1144.44	10.03
4.5	0.5	240	1043.6	1184.94	5.56
5	0.25	155	861	1020.6	70.23
5	0.25	195	905	1060.2	36.78
5	0.25	255	962	1111.5	16.48
2	0.45	150	916	1070.1	31.41
2	0.45	190	966.7	1115.73	15.45
2	0.45	250	1031.5	1174.05	6.50

(iii) Calculated constants for tool life equation (Eq.(3-4)):

$A_t = 10^{7.313356}$ $b_t = 2.9502$ $c_t = 1.6899$ $d_t = 0.0206$.

Appendix B Input Data for Worked Examples

Example 1:

(i) *Work material*: AISI-1045 plain carbon steel bars of chemical composition 0.45%C, 0.01%P, 0.66%Mn, 0.053%Si, 0.031%S, 0.01%Ni, 0.02%Cr, 0.01%Mo, 0.01%Cu and 0.001%Al.

(ii) *Tool material*: chemical composition of P25 grade carbide tool insert was 7.6-8.4%TiC + 3.5%Co + 11-12%TaC. Tool geometrical data were: rake angle = -6 deg, inclination angle = -6 deg, side-cutting edge angle = 27 deg and nose radius = 0.8 mm.

(iii) *Economic data*: x = 1.67 \$/min, y = 3.2 \$, $t_3 = 2$ min.

(iv) *Tool life equation data* (constants for Eq.(3-4)):

$A_t = 281104$ $b_t = 2.56319$ $c_t = 1.66511$ $d_t \approx 0.0$.

The minimum and maximum tool life values were assumed to be: T_{min} = 5 min, T_{max} = 100 min.

(v) *The high temperature shear strength curve* for P25 carbide tool was obtained using the method described in chapter 4. It is given by $\tau = 2.248\times10^{33}\ T^{-10.135}$.

(vi) *Machine tool's power- speed characteristics* was given by Fig.3-2.

N_{break1} = 1000 rev/min, P_{break1} = 11.3 kW; $N_{break12}$= 3000 rev/min, P_{break2} = 10.4 kW; N_{break3} = 4500 rev/min, P_{break3} = 6.9 kW.

Example 2:

(i) *Work material*: AISI-1045 plain carbon steel bars of chemical composition 0.45%C, 0.01%P, 0.66%Mn, 0.053%Si, 0.031%S, 0.01%Ni, 0.02%Cr, 0.01%Mo, 0.01%Cu and 0.001%Al.

(ii) *Tool material*: P15 grade carbide tool insert was used in this example. Its chemical composition was assumed as the same as that of P25 grade tool insert used in example 1. Tool geometrical data were: rake angle = -6 deg, inclination angle = -6 deg, side-cutting edge angle = 27 deg and nose radius = 0.8 mm.

(iii) *Economic data*: x = 1.67 \$/min, y = 3.2 \$, $t_3 = 2$ min.

(iv) *Tool life equation data* (constants for Eq.(3-4)):

$A_t = 278351778$ $b_t = 3.0$ $c_t = 1.2$ $d_t = 0.22$.

The minimum and maximum tool life values were assumed to be: T_{min} = 5 min, T_{max} = 100 min.

(v) *The high temperature shear strength curve* for P25 carbide tool was obtained using the method described in chapter 4. It is given by $\tau = 2.248 \times 10^{33}\ T^{-10.135}$.

(vi) *Machine tool's power- speed characteristics* was given by Fig.3-2.

N_{break1} = 1000 rev/min, P_{break1} = 11.3 kW; $N_{break12}$= 3000 rev/min, P_{break2} = 10.4 kW; N_{break3} = 4500 rev/min, P_{break3} = 6.9 kW.

Appendix C Additional Results of Worked Examples

Table C-1 Example 1: Calculated Results

Grid Point No.	Search points		Initial cutting speed (m/min)		Check constraints			Grid point available or unavailable	Optimum cutting speed (m/min)		Optimum tool life (min)		Specific production cost	Specific production time
	depth (mm)	feed (mm/rev)	for cost	for time	$U_{plastic}$ (m/min)	Power OK/N ?	BUE Ok/N ?		for cost	for time	for cost	for time	(A$/m^3)	(min/m^3)
1	2.5	0.2	209	226	390	OK	OK	Available	209	226	6.12	5	26197.8	12376.1
2	2.5	0.22	196	212	372	OK	OK	Available	196	212	6.12	5	25313.2	11959.4
3	2.5	0.24	186	201	356	OK	OK	Available	186	201	6.12	5	24529.9	11588.9
4	2.5	0.26	176	191	342	OK	OK	Available	176	191	6.12	5	23827.4	11257.3
5	2.5	0.28	168	182	325	OK	OK	Available	168	182	6.12	5	23193.1	10957.4
6	2.5	0.3	161	174	310	OK	OK	Available	161	174	6.12	5	22614.1	10684.2
7	2.5	0.32	154	167	300	OK	OK	Available	154	167	6.12	5	22084.3	10433.8
8	2.5	0.34	149	161	291	OK	OK	Available	149	161	6.12	5	21595.2	10202.7
9	2.5	0.36	143	155	283	OK	OK	Available	143	155	6.12	5	21142.3	9988.5
10	2.5	0.38	139	150	276	OK	OK	Available	139	150	6.12	5	20719.7	9788.9
11	2.5	0.4	134	145	265	OK	OK	Available	134	145	6.12	5	20324.3	9602.1
12	2.5	0.42	130	141	259	OK	OK	Available	130	141	6.12	5	19952.8	9426.5
13	2.5	0.44	126	137	254	OK	OK	Available	126	137	6.12	5	19602.3	9261.1
14	2.5	0.46	123	133	249	OK	OK	Available	123	133	6.12	5	19271.1	9104.1
15	2.5	0.48	120	130	241	OK	OK	Available	120	130	6.12	5	18956.3	8955.9
16	2.5	0.5	117	127	236	OK	OK	Available	117	127	6.12	5	18657	8814.4
17	2.5	0.52	114	124	229	OK	OK	Available	114	124	6.12	5	18370.9	8679.2
18	2.5	0.54	112	121	222	OK	OK	Available	112	121	6.12	5	18096.9	8549.7
19	2.5	0.56	109	118	215	OK	OK	Available	109	118	6.12	5	17833	8425.3
20	2.5	0.58	107	116	212	OK	OK	Available	107	116	6.12	5	17580.2	8305.5

Table C-1 (continued) Example 1: Calculated Results

Grid Point No.	Search points		Initial cutting speed (m/min)		Check constraints			Grid point available or unavailable	Optimum cutting speed (m/min)		Optimum tool life (min)		Specific production cost (A$/m^3)	Specific production time (min/m^3)
	depth (mm)	feed (mm/rev)	for cost	for time	$U_{plastic}$ (m/min)	Power OK/N ?	BUE Ok/N ?		for cost	for time	for cost	for time		
21	2.5	0.6	105	113	206	OK	OK	Available	105	113	6.12	5	17335	8189.8
22	2.5	0.62	103	111	200	OK	OK	Available	103	111	6.12	5	17097.5	8077.4
23	2.5	0.64	101	109	196	OK	OK	Available	101	109	6.12	5	16866	7968.4
24	2.3	0.64	102	110	196	OK	OK	Available	102	110	6.12	5	18221.9	8608.8
25	2.1	0.64	102.8	111	201	OK	OK	Available	102.8	111	6.12	5	19809.8	9358.9
26	1.9	0.64	103	112	203	OK	OK	Available	103	112	6.12	5	21649	10249.2
27	1.7	0.64	105	113	211	OK	OK	Available	105	113	6.12	5	23963.1	11321.2
28	1.5	0.64	106	115	212	OK	OK	Available	106	115	6.12	5	26742.9	12634.4
29	1.3	0.64	108	117	221	OK	OK	Available	108	117	6.12	5	30216.7	14275.1
30	1.1	0.64	112	121	230	OK	OK	Available	112	121	6.12	5	34657.3	16373.4
31	0.9	0.64	117	127	245	OK	OK	Available	117	127	6.12	5	40468.1	19118.8
32	0.7	0.64	126	137	263	OK	OK	Available	126	137	6.12	5	48204.2	22773.8
33	0.5	0.64	146	159	302	OK	OK	Available	146	159	6.12	5	58219.1	27505.1

Table C-2 Example 2: Calculated Results

Grid Point No.	Search points		Initial cutting speed (m/min)		Check constraints			Grid point available or unavailable	Optimum cutting speed (m/min)		Optimum tool life (min)		Specific production cost (A$/m³)	Specific production time (min/m³)
	depth (mm)	feed (mm/rev)	for cost	for time	$U_{plastic}$ (m/min)	Power OK/N ?	BUE Ok/N ?		for cost	for time	for cost	for time		
1	2.5	0.2	602	699	390	N		Unavailable						
2	2.3	0.2	607	705	389.8	N		Unavailable						
3	2.1	0.2	612	711	395	OK	OK	Available	395	395	29	29	11414	6434
4	2.1	0.22	590	686	381	N		Unavailable						
5	1.9	0.22	596	692	382	OK	OK	Available	382	382	29.6	29.6	11818	6677
6	1.9	0.24	577	670	367	OK	OK	Available	367	367	30.3	30.35	11256	6362
7	1.9	0.26	559	650	353	N		Unavailable						
8	1.7	0.26	566	657	355	OK	OK	Available	355	355	31.6	31.6	11948	6763
9	1.7	0.28	550	639	338	N		Unavailable						
10	1.5	0.28	558	648	347	OK	OK	Available	347	347	32.5	32.5	12833	7280
11	1.5	0.30	543	631	331	OK	OK	Available	331	331	34.4	34.45	12450	7089
12	1.5	0.32	530	616	320	N		Unavailable						
13	1.3	0.32	539	626	325	OK	OK	Available	325	325	35.8	35.85	13695	7923
14	1.3	0.34	527	613	316	OK	OK	Available	316	316	36.4	36.4	13236	7649
15	1.3	0.36	517	600	303	OK	OK	Available	303	303	38.8	38.8	12953	7408
16	1.3	0.38	507	588	297	N		Unavailable						
17	1.1	0.38	518	601	306	OK	OK	Available	306	306	37.9	37.9	14391	8219
18	1.1	0.40	508	590	295	OK	OK	Available	295	295	39.9	39.9	14101	8073
19	1.1	0.42	500	580	291	OK	OK	Available	291	291	39.7	39.7	13641	7808
20	1.1	0.44	492	571	282	OK	OK	Available	282	282	41.5	41.5	13381	7682

Table C-2 (continued) Example 2: Calculated Results

Grid Point No.	Search points		Initial cutting speed (m/min)		Check constraints			Grid point available or unavailable	Optimum cutting speed (m/min)		Optimum tool life (min)		Specific production cost (A$/m^3)	Specific production time (min/m^3)
	depth (mm)	feed (mm/rev)	for cost	for time	Uplastic (m/min)	Power OK/N ?	BUE Ok/N ?		for cost	for time	for cost	for time		
21	1.1	0.46	484	562	273	N		Unavailable						
22	0.9	0.46	500	580	284	OK	OK	Available	284	284	42.5	42.5	15487	8890
23	0.9	0.48	493	572	282	OK	OK	Available	282	282	41.7	41.7	14983	8599
24	0.9	0.50	486	565	274	OK	OK	Available	274	274	43.4	43.4	14720	8464
25	0.9	0.52	480	558	268	OK	OK	Available	268	268	44.7	44.7	14436	8187
26	0.9	0.54	475	551	263	OK	OK	Available	263	263	46	46	14165	8038
27	0.9	0.56	469	545	262	N		Unavailable						
28	0.7	0.56	494	574	278	OK	OK	Available	278	278	44	44	16685	9603
29	0.7	0.58	490	569	273	OK	OK	Available	273	273	45	45	16350	9398
30	0.7	0.60	485	564	269	OK	OK	Available	269	269	45	45	16004	9211
31	0.7	0.62	481	559	266	OK	OK	Available	266	266	46	46	15666	9025
32	0.7	0.64	478	555	263	OK	OK	Available	263	263	46.7	46.7	15313	8841
33	0.5	0.64	526	611	302	OK	OK	Available	302	302	41	41	18870	10830

Table C-3 Example 3: Calculated Results

Grid Point No.	Search points		Initial cutting speed (m/min)		Check constraints			Grid point available or unavailable	Optimum cutting speed (m/min)		Optimum tool life (min)		Specific production cost (A$/m^3)	Specific production time (min/m^3)
	depth (mm)	feed (mm/rev)	for cost	for time	$U_{plastic}$ (m/min)	Power OK/N ?	BUE Ok/N ?		for cost	for time	for cost	for time		
1	2.5	0.2	209	226	390	N		Unavailable						
2	2.3	0.2	209	226	395	N		Unavailable						
3	2.1	0.2	210	227	395	OK	OK	Available	186	201	6.12	5	30999.2	14645.2
4	2.1	0.22	197	214	382	N		Unavailable						
5	1.9	0.22	198	215	383	OK	OK	Available	168	182	6.12	5	32956.7	15570.1
6	1.9	0.24	188	203	367	N		Unavailable						
7	1.7	0.24	189	204	373	OK	OK	Available	154	167	6.12	5	35477.4	16761.2
8	1.7	0.26	179	194	354	OK	OK	Available	149	161	6.12	5	34442.1	16271
9	1.7	0.28	171	185	338	N		Unavailable						
10	1.5	0.28	173	187	347	OK	OK	Available	139	150	6.12	5	37667.5	17795
11	1.5	0.3	165	179	332	OK	OK	Available	134	145	6.12	5	36695.9	17336.7
12	1.5	0.32	159	172	314	N		Unavailable						
13	1.3	0.32	161	174	324	OK	OK	Available	126	137	6.12	5	40825.5	19287.6
14	1.3	0.34	155	168	311	OK	OK	Available	123	133	6.12	5	39866.9	18834.8
15	1.3	0.36	150	162	303	N		Unavailable						
16	1.1	0.36	152	165	312	OK	OK	Available	117	127	6.12	5	45227.2	21367.5
17	1.1	0.38	148	160	305	OK	OK	Available	114	124	6.12	5	44231.6	20896.6
18	1.1	0.40	143	155	295	OK	OK	Available	112	121	6.12	5	43292.5	20453.2
19	1.1	0.42	139	151	291	N		Unavailable						
20	0.9	0.42	144	147	301	OK	OK	Available	107	116	6.12	5	50231.2	20033.8

Table C-3 (continued) Example 3: Calculated Results

Grid Point No.	Search points		Initial cutting speed (m/min)		Check constraints			Grid point available or unavailable	Optimum cutting speed (m/min)		Optimum tool life (min)		Specific production cost (A$/m^3)	Specific production time (min/m^3)
	depth (mm)	feed (mm/rev)	for cost	for time	$U_{plastic}$ (m/min)	Power OK/N ?	BUE Ok/N ?		for cost	for time	for cost	for time		
21	0.9	0.44	140	152	292	OK	OK	Available	140	152	6.12	5	49181.1	23235.4
22	0.9	0.46	137	148	284	OK	OK	Available	137	148	6.12	5	48178.2	22761.5
23	0.9	0.48	134	145	277	OK	OK	Available	134	145	6.12	5	47216.1	22306.9
24	0.9	0.50	131	142	275	OK	OK	Available	131	142	6.12	5	46289.9	21869.3
25	0.9	0.52	128	139	268	N		Unavailable						
26	0.7	0.52	137	148	288	OK	OK	Available	137	148	6.12	5	54804.2	25891.8
27	0.7	0.54	135	146	282	OK	OK	Available	135	146	6.12	5	53648.4	25345.7
28	0.7	0.56	133	143	277	OK	OK	Available	133	143	6.12	5	52521.3	24813.2
29	0.7	0.58	131	141	273	OK	OK	Available	131	141	6.12	5	51418.0	24292.3
30	0.7	0.60	129	140	274	OK	OK	Available	129	140	6.12	5	50333.9	23779.9
31	0.7	0.62	128	138	266	OK	OK	Available	128	138	6.12	5	49264.2	23274.1
32	0.7	0.64	126	137	263	OK	OK	Available	126	137	6.12	5	48204.5	22773.8
33	0.5	0.64	146	159	302	OK	OK	Available	146	159	6.12	5	58219.7	27505.1

Table C-4 Example 4: Calculated Results

Grid Point No.	Search points		Initial cutting speed (m/min)		Check constraints			Grid point available or unavailable	Optimum cutting speed (m/min)		Optimum tool life (min)		Specific production cost	Specific production time
	depth (mm)	feed (mm/rev)	for cost	for time	$U_{plastic}$ (m/min)	Power OK/N ?	BUE Ok/N ?		for cost	for time	for cost	for time	(A$/m^3)	(min/m^3)
1	2.5	0.2	193	212	361	OK	OK	Available	193	212	6.33	5	27903	13205.8
2	2.5	0.22	182	199	344	OK	OK	Available	182	199	6.33	5	26928	12744.6
3	2.5	0.24	172	189	331	OK	OK	Available	172	189	6.33	5	26065.7	12336.2
4	2.5	0.26	164	179	315	OK	OK	Available	164	179	6.33	5	25293.8	11970.9
5	2.5	0.28	156	171	300	OK	OK	Available	156	171	6.33	5	24596	11641.2
6	2.5	0.3	150	164	286	OK	OK	Available	150	164	6.33	5	23962	11340.9
7	2.5	0.32	144	158	278	OK	OK	Available	144	158	6.33	5	23381.9	11065.9
8	2.5	0.34	139	152	269	OK	OK	Available	139	152	6.33	5	22846.7	10812.7
9	2.5	0.36	134	147	263	OK	OK	Available	134	147	6.33	5	22350	10578.1
10	2.5	0.38	129	142	256	OK	OK	Available	129	142	6.33	5	21889.3	10359.6
11	2.5	0.4	125	127	250	OK	OK	Available	125	127	6.33	5	21457.9	10155.5
12	2.5	0.42	122	133	241	OK	OK	Available	122	133	6.33	5	21053.3	9963.8
13	2.5	0.44	118	130	233	OK	OK	Available	118	130	6.33	5	20671.1	9783.3
14	2.5	0.46	115	126	228	OK	OK	Available	115	126	6.33	5	20311.2	9612.7
15	2.5	0.48	112	123	220	OK	OK	Available	112	123	6.33	5	19969.2	9450.9
16	2.5	0.5	110	120	217	OK	OK	Available	110	120	6.33	5	19643.9	9296.9
17	2.5	0.52	107	117	210	OK	OK	Available	107	117	6.33	5	19333.6	9150.1
18	2.5	0.54	105	115	203	OK	OK	Available	105	115	6.33	5	19036.7	9009.6
19	2.5	0.56	102	112	201	OK	OK	Available	102	112	6.33	5	18751.8	8874.7
20	2.5	0.58	100	110	195	OK	OK	Available	100	110	6.33	5	18477.3	8744.9

Table C-4 (continued) Example 4: Calculated Results

Grid Point No.	Search points		Initial cutting speed (m/min)		Check constraints			Grid point available or unavailable	Optimum cutting speed (m/min)		Optimum tool life (min)		Specific production cost	Specific production time
	depth (mm)	feed (mm/rev)	for cost	for time	$U_{plastic}$ (m/min)	Power OK/N ?	BUE Ok/N ?		for cost	for time	for cost	for time	(A\$/m^3)	(min/m^3)
21	2.5	0.6	98.9	108	189	OK	OK	Available	98.9	108	6.33	5	18213	8619.7
22	2.5	0.62	97	106	184	OK	OK	Available	97	106	6.33	5	17956.7	8498.4
23	2.5	0.64	95.4	104	180	OK	OK	Available	95.4	104	6.33	5	17707.7	8380.6
24	2.3	0.64	95.9	105	184.4	OK	OK	Available	95.9	105	6.33	5	19128.5	9052.9
25	2.1	0.64	96	105.9	185	OK	OK	Available	96	105.9	6.33	5	20793.3	9840.8
26	1.9	0.64	97	106.8	187	OK	OK	Available	97	106.8	6.33	5	22768.5	10775.7
27	1.7	0.64	98	108	191	OK	OK	Available	98	108	6.33	5	25147.2	11901.8
28	1.5	0.64	100	109	200	OK	OK	Available	100	109	6.33	5	28064.1	13282.1
29	1.3	0.64	102	112	204	OK	OK	Available	102	112	6.33	5	31711.5	15008.2
30	1.1	0.64	105	115	212	OK	OK	Available	105	115	6.33	5	36278.2	17217.2
31	0.9	0.64	110	120	226	OK	OK	Available	110	120	6.33	5	42498.0	20113.6
32	0.7	0.64	119	130	243	OK	OK	Available	119	130	6.33	5	50678.5	23984.9
33	0.5	0.64	137	150	277	OK	OK	Available	137	150	6.33	5	61367.2	29043.5

Appendix D A Published Paper

Meng, Q., Arsecularatne, J.A. and Mathew, P., 1998, *Prediction of the Cutting Conditions Giving Plastic Deformation of the Tool in Oblique Machining,* International Journal of Machine Tools & Manufacturing, 38, pp1165-1182.

INTERNATIONAL JOURNAL OF
MACHINE TOOLS
& MANUFACTURE
DESIGN, RESEARCH AND APPLICATION

Pergamon International Journal of Machine Tools & Manufacture 38 (1998) 1165–1182

Prediction of the cutting conditions giving plastic deformation of the tool in oblique machining

Q. Meng, J.A. Arsecularatne, P. Mathew*

School of Mechanical and Manufacturing Engineering, The University of New South Wales, Sydney 2052, Australia

Received 1 December 1997; in final form 22 December 1997

Abstract

A method is described for predicting cutting conditions at which the cutting edge starts to deform plastically when machining with oblique nose radius tools. It is shown how tool stresses and temperatures determined from machining theory can be used together with experimental high temperature compressive strength data for the tool material to make these predictions. A comparison made between predicted and experimental results for two plain carbon steel work materials and a range of cutting conditions shows good agreement. © 1998 Elsevier Science Ltd. All rights reserved.

Keywords: Plastic deformation; Oblique machining; Nose radius tools; Hot compressive strength; Stress analysis

Nomenclature

C_s	side cutting edge angle (deg)
d	depth of cut (mm)
f	feed (mm/rev)
F	frictional force at tool–chip interface (N)
F_C	orthogonal force component in direction of cutting (N)
F_T	orthogonal force component normal to F_C acting in plane normal to cutting edge (N)
F_S	shear force on AB (N)
F_R	force component normal to F_C and F_T (N)
i	inclination angle (deg)
k_{AB}	shear flow stress on AB (N/mm²)

* Corresponding author.

PII: S0890-6955(98)00011-X

k_{chip}	shear flow stress in chip at tool–chip interface (N/mm^2)
N	normal force at tool–chip interface (N)
r	radial distance of element from cutting edge (mm)
r_ϵ	tool nose radius (mm)
R	resultant force in orthogonal chip formation model (N)
t_1	undeformed chip thickness (mm)
t_2	chip thickness (mm)
T_{int}	average temperature along tool–chip interface (°C)
U	cutting speed (m/min)
w	width of cut measured along cutting edge (mm)
α	tool rake angle (deg)
α_n	tool normal rake angle (deg)
ϕ	shear angle (deg)
η_c	chip flow angle (deg)
η_0	chip flow angle due to the effect of the nose radius measured from the normal to the side cutting edge on the reference plane (deg)
θ	angle made by the tool element with the tool rake face (rad)
σ_f	average normal stress on tool flank–work interface (N/mm^2)
σ_N	average normal stress on tool rake face (N/mm^2)
σ_r	normal stress component in the radial direction (N/mm^2)
σ_θ	normal stress component in the circumferential direction (N/mm^2)
τ_f	average shear stress on tool flank–work interface (N/mm^2)
τ_{int}	average shear stress on the tool–chip interface (N/mm^2)
τ_{max}	maximum shear stress in the tool (N/mm^2)
$\tau_{r\theta}$	shear stress component (N/mm^2)
ψ	stress function
*	star sign to indicate angles associated with equivalent cutting edge

1. Introduction

The tendency of cutting tools to deform plastically under the influence of the high compressive stresses and temperatures encountered during machining at high speeds and feeds has been discussed by a number of researchers. Plastic deformation of the tool changes the geometry of the cutting edge which in turn causes accelerated rates of tool wear, resulting in a decrease in tool life and in the machined surface quality. Plastic deformation can also cause catastrophic tool failure which can damage the component, the tool and/or machine tool and thus interrupt the machining process substantially. In obtaining the optimum cutting conditions it is important to determine the conditions that cause tool plastic deformation and avoid them.

This paper presents a method by which the tool temperatures, stresses and subsequently tool deformation conditions can be predicted in turning with oblique nose radius tools using as a basis the orthogonal machining theory developed by Oxley [1] and his co-workers. This theory, which takes account of variations in work material flow stress with strain, strain-rate and temperature, has been applied with considerable success in predicting cutting forces, temperatures, etc. from a knowledge of the work material properties and the cutting conditions.

2. Review of previous work

In recent years there has been a rapid development and implementation of advanced machining systems designed to manufacture components efficiently and at low cost. Since the efficiency and operating cost are sensitive to the cutting conditions, optimum values have to be determined before a part is put into production. Procedures reported so far to determine the optimum cutting conditions are based on various nomograms, graphical techniques, performance envelope, linear programming, geometrical programming, and search procedures [2]. In calculating the optimum cutting conditions (speed, feed and depth of cut) it is important to avoid the conditions that cause built-up edge (BUE) formation and accelerated rates of tool wear as these have a major negative influence on surface finish, tool life and dimensional accuracy. In this connection the so called machining charts prepared by Trent [3] which show the ranges of feeds and speeds for a given combination of work and tool material under which BUE, rapid cratering and plastic deformation of the tool cutting edge can occur are useful.

Cook and Goldberger [4] have outlined a method of selecting the feed to give maximum metal removal rate using the results obtained from tool life tests when machining 4340 steel using carbide (Carbaloy 370) tools. For a given feed, tests were made at a number of cutting speeds and the results were cross-plotted to determine the speed which would give a flank wear land width of 0.25 mm after 10 min of cutting. When plotted on a log(speed) versus log(feed) graph they were able to represent the tool life results by two straight lines with the line for the higher feed range steeper than that for the lower feed range. It was also shown that the feed corresponding to the maximum metal removal rate is given by the feed value at the intersection of the two lines (referred to as f_{max}). Cook and Goldberger have shown how this f_{max} value decreases as the hardness of the 4340 steel is increased. They also carried out a series of tool-life tests to determine the feed required to actually break the tool-tip. It was found that the value of f_{max} (based on wear) was substantially less than the feed required for fracture. Cook and Goldberger offered no explanation of why their results show that it is necessary to reduce the cutting speed far more rapidly with increase in feed above f_{max} in order to maintain the same tool life. Nachev and Oxley [5] in considering this observation suggested that f_{max} corresponds to those conditions where the cutting edge starts to deform plastically. This is also consistent with the experimental results of Trent [3] and Kuljanik [6] which show that accelerated rates of flank wear can occur when the flank face is bulged outwards by the high stresses acting on the rake face. Trent found that carbide tools could be plastically deformed by 5–10% without visible fracture damage to the structure. He also suggested that the high rates of metal removal attainable with carbide tools results mainly from their ability to resist plastic deformation of the cutting edge at high temperatures.

The empirical approach given in [4] or the machinability charts [3] are useful in determining the cutting conditions for maximum metal removal rate without affecting surface finish, tool life, etc. However these methods require a huge amount of empirical data which can be extremely costly in terms of time, work material and tool requirements. In order to overcome this problem Nachev and Oxley [5] presented a method to predict those cutting conditions giving plastic deformation of the cutting edge using the tool stresses and temperatures predicted from machining theory together with the high temperature compressive strength data of the tool material given by Trent [3]. Their approach is now considered.

In predicting those conditions which will cause plastic deformation of the cutting edge the factors of interest are the tool stresses and temperatures. The machining theory used, assumes a perfectly sharp tool with no forces acting on the clearance face and provides values of average stresses and temperatures on the tool rake face. Nachev and Oxley assumed that the average tool–chip interface temperature, T_{int} can be taken to represent the cutting edge temperature and that the average normal stress at the interface σ_{N} would be the stress that causes deformation of the cutting edge. They calculated the values of σ_{N} and T_{int} from the machining theory for two plain carbon steels (0.19%C and 0.48%C) for feeds in the range 0.2–0.5 mm/rev and cutting speeds in the range 100–500 m/min. Calculations were made for only one rake angle, i.e. $\alpha = 5°$, which was the rake angle of the tips used in the subsequent tests. The predicted results for σ_{N} and T_{int} were then plotted (Fig. 1) together with the curve which was assumed to represent the hot compressive strength properties of the tool material. The σ_{N} lines given in Fig. 1 are lines of constant feed with cutting speed increasing along the lines from left to right. The intersection of the σ_{N} curves with the curve representing the compressive strength of the tool material were assumed to give the feed/speed combinations at which the tool starts to deform plastically. In order to determine the accuracy of these predictions Nachev and Oxley carried out bar turning tests using similar work and tool materials as used in making the predictions. In the tests the feeds used were the same as those used in making predictions and the starting cutting speed in each test was selected to be approximately the same as the speed at which deformation was predicted to occur. By varying the speed in subsequent tests they were able to determine the speed at which the tool starts to deform plastically within 50 m/min. When the predicted results were compared with the experimental results reasonable agreement was found to exist.

In the work described in [5] the shear stress acting on the tool rake face and the normal and shear stresses on the flank face were not taken into account and it was assumed that the average normal stress on the rake face σ_{N} was the stress that causes deformation of the cutting edge. Attention was also limited to approximately orthogonal conditions.

In this paper more realistic account is taken of the mode of cutting edge failure under the action of all of the stresses acting by considering a criterion of failure based on the maximum shear stress at the cutting edge. The analysis is also extended to oblique conditions for a tool having a nose radius.

3. Failure of cutting tools

The starting point for predicting the conditions giving plastic deformation of the cutting edge is to make a stress analysis for the region of the tool adjacent to the cutting edge. Kronenberg [7] has done this previously but limited his attention to a wedge under the action of a single load acting at the wedge apex. In the present work account is taken of the stress distributions at the rake and flank faces of the tool rather than reducing these to a single force.

Figure 2 shows the stresses assumed to act at the cutting edge in the analysis. For the sake of simplicity the rake and clearance angles of the tool have been assumed to be zero which is reasonable for carbide tools. The normal and shear stress distributions on the rake face have been assumed to be uniform. In support of this it should be noted that Arsecularatne [8] who reviewed the experimental methods used to determine rake face stress distributions and the reported results concluded that, for a sharp tool, shear and normal stresses reach constant values as the cutting

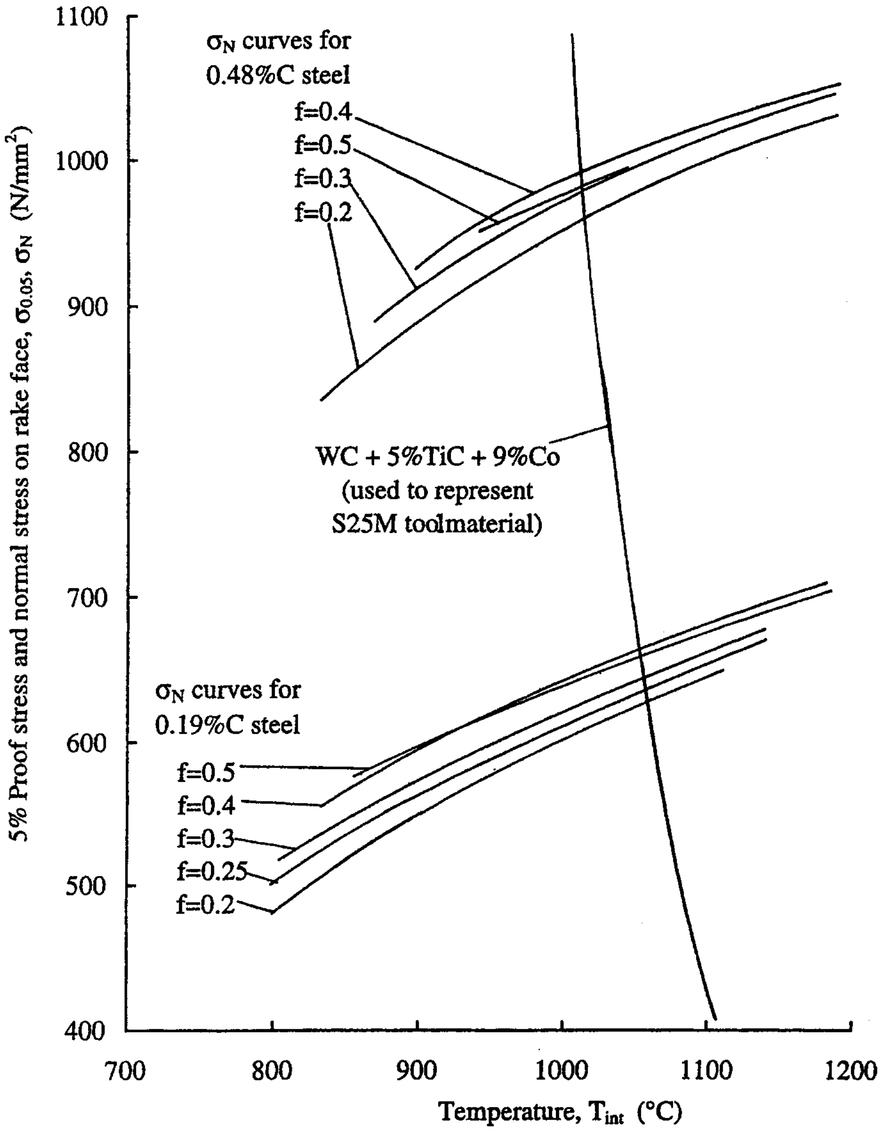

Fig. 1. Curves of tool material (S25M) hot compressive strength and predicted tool stresses and temperatures (after Nachev and Oxley [5]).

edge is approached. At this stage, and lacking more detailed information it also seems reasonable to assume uniform stress distributions at the flank face.

Consider the equilibrium of the element P at r, θ (Fig. 2). The normal stress components in the radial and circumferential directions are denoted by σ_r and σ_θ while the shear stress component is denoted by $\tau_{r\theta}$. From the equilibrium of the element P in the circumferential and radial directions (neglecting the body force) the general form of relations for the stress components can be obtained as shown by Timoshenko and Goodier [9] in the form

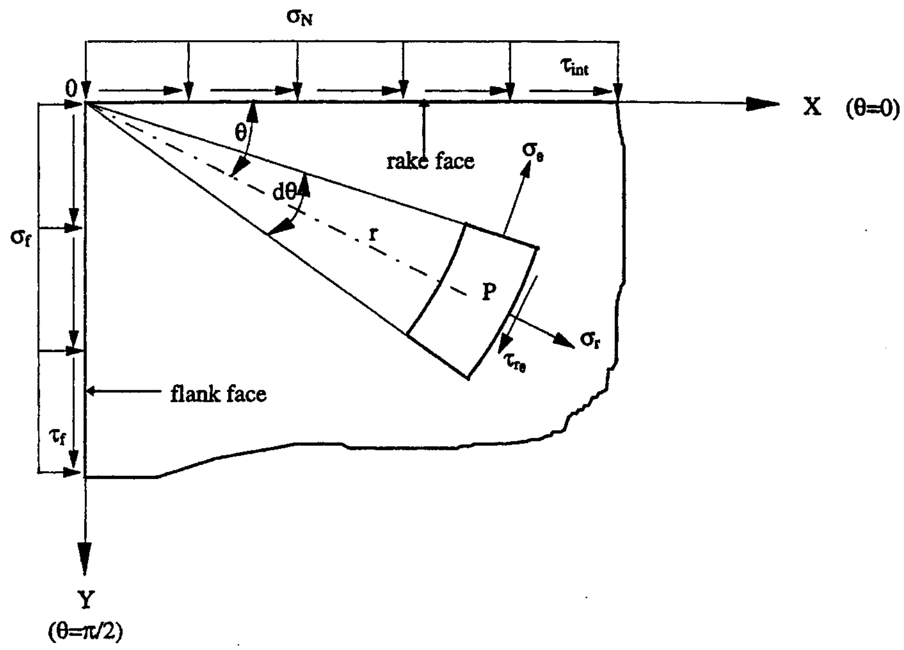

Fig. 2. Stresses acting on an element and on rake and flank faces of a tool.

$$\sigma_r = \frac{1}{r}\frac{\partial\psi}{\partial r} + \frac{1}{r^2}\frac{\partial^2\psi}{\partial\theta^2}$$
$$\sigma_\theta = \frac{\partial^2\psi}{\partial r^2} \tag{1}$$
$$\tau_{r\theta} = \frac{1}{r^2}\frac{\partial\psi}{\partial\theta} - \frac{1}{r}\frac{\partial^2\psi}{\partial r\partial\theta}$$

where ψ is the appropriate stress function.

For the boundary conditions given in Fig. 2, the following equations for these stress components can be obtained using the expression for ψ given in [9]

$$\sigma_r = \frac{1}{2}\Big[(\cos 2\theta - 1)\sigma_N - (\cos 2\theta + 1)\sigma_f - \left(\sin 2\theta + \frac{\pi}{2}\cos 2\theta - 2\theta + \frac{\pi}{2}\right)\tau_{int} - \left(\sin 2\theta - \frac{\pi}{2}\cos 2\theta + 2\theta - \frac{\pi}{2}\right)\tau_f\Big]$$
$$\sigma_\theta = \frac{1}{2}\Big[-(\cos 2\theta + 1)\sigma_N + (\cos 2\theta - 1)\sigma_f + \left(\sin 2\theta + \frac{\pi}{2}\cos 2\theta + 2\theta - \frac{\pi}{2}\right)\tau_{int} + \left(\sin 2\theta - \frac{\pi}{2}\cos 2\theta - 2\theta + \frac{\pi}{2}\right)\tau_f\Big] \tag{2}$$

$$\tau_{r\theta} = \frac{1}{2}\left[(\sin 2\theta)\sigma_N + (\sin 2\theta)\sigma_f + \left(\frac{\pi}{2}\sin 2\theta - \cos 2\theta - 1\right)\tau_{int} - \left(\frac{\pi}{2}\sin 2\theta + \cos 2\theta - 1\right)\tau_f\right]$$

The maximum shear stress at P, τ_{max} can be obtained in terms of the above stress components as

$$\tau_{max} = \sqrt{\tau_{r\theta}^2 + \left(\frac{\sigma_\theta - \sigma_r}{2}\right)^2} \tag{3}$$

The maximum value of τ_{max} occurs at a value of θ given by

$$\tan 2\theta = -\frac{(\sigma_f - \sigma_N) + \frac{\pi}{2}(\tau_{int} - \tau_f)}{\tau_f + \tau_{int}} \tag{4}$$

with τ_{max} then given by

$$\tau_{max} = \frac{1}{2}(\tau_f - \tau_{int}) + \frac{1}{2}\frac{\left[(\sigma_f - \sigma_N) + \frac{\pi}{2}(\tau_{int} - \tau_f)\right]^2}{\sqrt{\left[(\sigma_f - \sigma_N) + \frac{\pi}{2}(\tau_{int} - \tau_f)\right]^2 + (\tau_{int} + \tau_f)^2}} + \frac{1}{2}\frac{(\tau_{int} + \tau_f)^2}{\sqrt{\left[(\sigma_f - \sigma_N) + \frac{\pi}{2}(\tau_{int} - \tau_f)\right]^2 + (\tau_{int} + \tau_f)^2}}, \text{ when } \left[(\sigma_f - \sigma_N) + \frac{\pi}{2}(\tau_{int} - \tau_f)\right] \geq 0 \tag{5}$$

$$\tau_{max} = \frac{1}{2}(\tau_f - \tau_{int}) - \frac{1}{2}\frac{\left[(\sigma_f - \sigma_N) + \frac{\pi}{2}(\tau_{int} - \tau_f)\right]^2}{\sqrt{\left[(\sigma_f - \sigma_N) + \frac{\pi}{2}(\tau_{int} - \tau_f)\right]^2 + (\tau_{int} + \tau_f)^2}} - \frac{1}{2}\frac{(\tau_{int} + \tau_f)^2}{\sqrt{\left[(\sigma_f - \sigma_N) + \frac{\pi}{2}(\tau_{int} - \tau_f)\right]^2 + (\tau_{int} + \tau_f)^2}}, \text{ when } \left[(\sigma_f - \sigma_N) + \frac{\pi}{2}(\tau_{int} - \tau_f)\right] < 0$$

Note that the maximum shear stress in the tool τ_{max} does not depend on r. This is due to the assumption of uniform shear and normal stress distributions on the rake and flank faces of the tool near the cutting edge. Beyond this region τ_{max} will depend on r. However, since deformation is mainly restricted to the cutting edge region, as will be seen later, it is sufficient to consider τ_{max} in the region where constant boundary stresses apply.

When considering plastic deformation of a tool working at high temperatures, the failure criterion can be taken as [10]

$$|\tau_{max}| \geq \left|\frac{\sigma_{comp}}{2}\right| \tag{6}$$

where σ_{comp} is the uniaxial compressive strength of the tool material at the onset of plastic deformation. In practice, it is assumed that when τ_{max} reaches a value of $\sigma_{0.05}/2$, i.e. when

$$|\tau_{max}| \geq \left|\frac{\sigma_{0.05}}{2}\right| \tag{7}$$

the tool starts to deform plastically where $\sigma_{0.05}$ is the 5% proof stress for the tool material determined from high temperature uniaxial compression test data such as that given by Trent [3].

Thus τ_{max} and hence the cutting edge plastic deformation conditions can be determined if σ_N, τ_{int}, σ_f, τ_f and T_{int} are known. The following sections describe the methods used to obtain these parameters.

4. Tool temperatures and stresses in oblique machining

Using extensive experimental results it has been shown that the orthogonal machining theory [1] can be extended to predict the chip flow direction and cutting forces in oblique machining with nose radius tools by introducing the concept of an equivalent cutting edge [11]. It has also been shown that predicted tool temperatures can be used to determine the built-up edge formation range [12] and tool life [13] with reasonable accuracy. The method used in the present work to determine the tool temperature and stresses in oblique machining, which is based on this previous work, is now described.

4.1. Chip flow direction and equivalent cutting edge

In order to predict the chip flow direction the method adopted for nose radius tools with non-zero rake and inclination angle tools is as follows. The chip flow angle due to the effect of the nose radius is determined first by assuming a tool with zero rake and inclination angles irrespective of their actual values. The equivalent cutting edge for this case is taken to be at right angles to the chip flow direction. The line representing this equivalent cutting edge is now projected onto the face of the tool with non-zero rake and inclination angles with the projected line assumed to represent the equivalent cutting edge for the actual tool. Since this method is discussed in detail in reference [11] what follows is only a brief review of the method.

4.2. Chip flow angle due to the effect of nose radius

In the method described in [11] the chip is treated as a series of elements of infinitesimal width. The frictional force component for each element changes in magnitude as well as direction. These frictional force components are summed up in order to find the resultant and it is assumed that this resultant coincides with the chip flow direction. In this way the resultant chip flow angle due to the nose radius effect, $\overline{\Omega_0}$ can be determined from the relation

$$\overline{\Omega_0} = \tan^{-1}\left(\frac{\int \sin \Omega_0 \, dA}{\int \cos \Omega_0 \, dA}\right) \tag{8}$$

where dA is the area of the undeformed chip element and Ω_0 is the angle a chip element makes with the outward radial direction. By integrating the numerator and denominator of Eq. (8) over the entire area of undeformed chip section, the chip flow angle $\overline{\Omega_0}$ is determined. These relations are given in reference [11].

It is also possible to define the chip flow angle with reference to the normal to the straight side cutting edge of the tool. As depicted in Fig. 3, if this angle is denoted by η_0, it can be related to $\overline{\Omega_0}$ by the relationship

$$\eta_0 = \frac{\pi}{2} - C_s - \overline{\Omega_0} \tag{9}$$

4.3. Modified tool angles and equivalent cutting edge

Using three dimensional geometric analysis the equation for η_0' , which is the projection of η_0 on the tool rake face plane as shown in Fig. 3, is obtained as follows

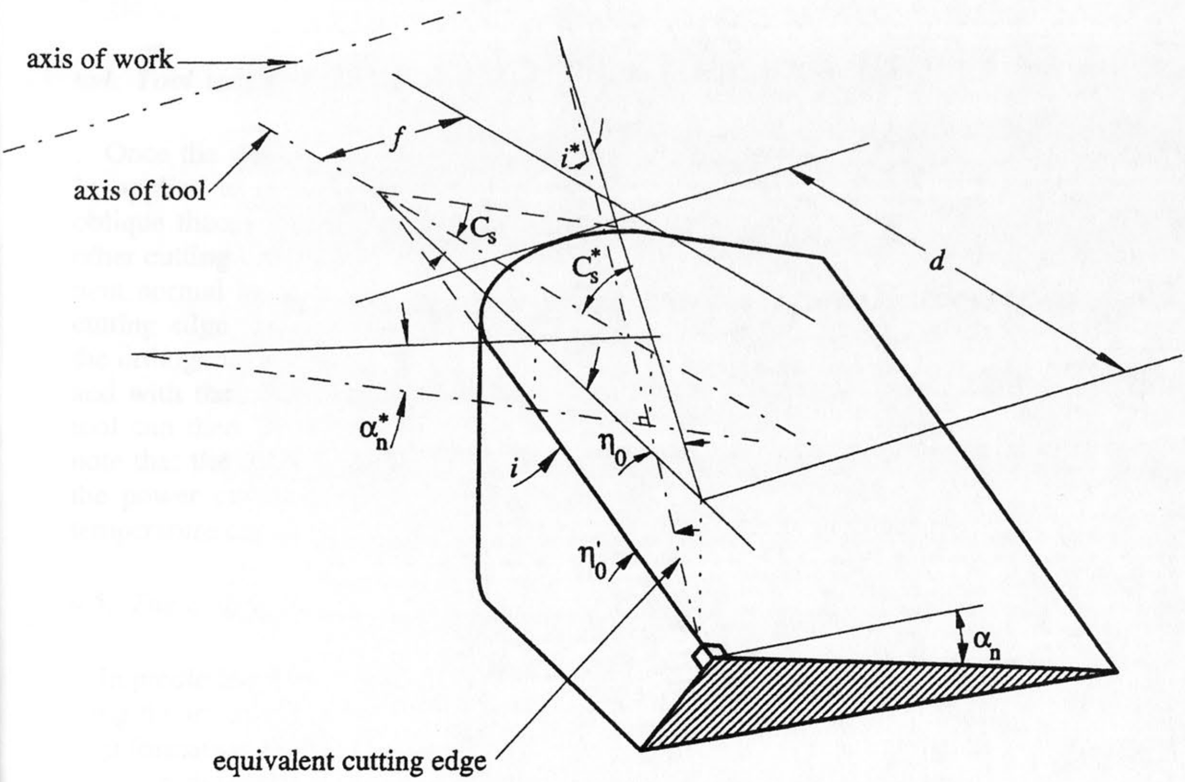

Fig. 3. Equivalent cutting edge and tool angles.

taken as the value which makes $\tau_{int} = k_{chip}$ as the assumed model of chip formation is then in equilibrium.

So far the machining theory has mainly been applied to making predictions for steel work materials with the required flow stress properties obtained from high speed compression tests made over a wide range of temperatures. The thermal properties used in calculating temperatures have been determined from well established empirical equations. The theory has been applied to the prediction of cutting forces, temperatures, stresses etc. for wide ranges of cutting conditions and steels [1]. Good agreement has been shown between predicted and experimental results.

4.6. Stresses on the tool flank–work interface

As mentioned earlier when the cutting edge radius is small enough to be neglected, it is reasonable to assume uniform shear and normal stress distributions on the tool flank–work interface as shown in Fig. 2. Based on an investigation on the contribution of the tool flank wear to cutting forces in orthogonal machining, Li [15] pointed out that the tool flank–work interface shear stress τ_f and normal stress σ_f can be obtained using the empirical relations:

$$\sigma_f = \frac{0.0528F_T}{t_1} \qquad (12)$$

$$\tau_f = \frac{0.0671F_C}{t_1}$$

where t_1, F_C and F_T are undeformed chip thickness, cutting force and feed force, respectively.

5. The prediction of cutting conditions giving plastic deformation of cutting edge

In predicting the conditions which give plastic deformation of the tool the maximum shear stress in the tool was determined from Eq. (5). In making the calculations the following three cases of tool loading were initially considered:

Case I, when $\sigma_N \neq 0$, $\tau_{int} \neq 0$, $\sigma_f \neq 0$, and $\tau_f \neq 0$
Case II, when $\sigma_N \neq 0$, $\tau_{int} \neq 0$, and $\sigma_f = \tau_f = 0$
Case III, when $\sigma_N \neq 0$ and $\tau_{int} = \sigma_f = \tau_f = 0$

It can be seen that Case III is that considered by Nachev and Oxley [5] in which case as shown by Eq. (5),

$$\tau_{max} = \frac{\sigma_N}{2} \qquad (13)$$

It should be noted that in considering cutting edge deformation only the stresses acting on element P as shown in Fig. 2 have been taken into account. This neglects the possible influence of the stresses normal to the plane in Fig. 2. Preliminary calculations show that this will only introduce an error in Case II and that this error is relatively small.

In order to determine which of the above three cases is the most appropriate in predicting cutting conditions giving plastic deformation of the cutting edge, the predicted results for each case were compared with the experimental results of Nachev [16] and Nachev and Oxley [5] obtained from approximately orthogonal machining tests. These workers determined the experimental plastic deformation conditions for two plain carbon steel work materials (0.19%C and 0.48%C) using P25 grade (Seco-Titan S25M with chemical composition WC + 6.5%TiC + 9.5%Co + 14.5%(TaC + NbC)) TPGN-220408 carbide tools. Although the S25M carbide tool has 6.5%TiC, it was considered by Nachev and Oxley to be near enough to the alloy of chemical composition WC + 5%TiC + 9%Co tested by Trent to justify using Trent's curve for this material to represent the hot strength properties of the S25M carbide used in their machining tests. In what follows this was again assumed to be the case.

In applying the above three cases to predict the cutting speeds which will cause plastic deformation of the cutting edge the method used was basically the same as that depicted in Fig. 1 and described earlier in the paper. However, as the maximum shear stress τ_{max} was now used as the failure criterion Trent's curve was plotted in terms of maximum shear strength which was taken as half the value of the corresponding hot compressive strength. The predicted cutting speeds giving plastic deformation were then taken to be the values at the intersections of this curve with the τ_{max} curves calculated from the machining theory and Eq. (5). A computer program written in C-language was used in the present work to make all of the necessary calculations. The input data to the program includes: work material composition, tool geometrical data (rake angle, inclination angle, side-cutting edge angle and nose radius), high temperature shear strength of tool material, feed and depth of cut and an assumed initial cutting speed value. The steps involved are:

1. Determine the equivalent cutting edge geometry for the given oblique nose radius tool, depth of cut and feed.
2. For this equivalent cutting edge and the assumed cutting speed, determine the forces F_C, F_T, temperature T_{int} and tool stresses using the machining theory.
3. Calculate the maximum shear stress τ_{max} for the appropriate case from Eq. (5).
4. Determine the cutting speeds corresponding to the intersections of the two curves using a bisection search method [17].

The experimental results of Nachev and Oxley [5] are given in Fig. 5(a) and Fig. 5(b) for the 0.19 and 0.48% carbon steel respectively with the filled in symbols indicating the cutting speeds for which plastic deformation was observed and the open symbols indicating cutting speeds 50 m/min lower for which no plastic deformation was observed. The predicted results for the three cases discussed above are given by the lines.

From Fig. 5, it can be seen that the predicted plastic deformation speeds show the same trends as the experimental results with reasonably good quantitative agreement. However, the predicted results can be seen to overestimate the cutting edge's ability to resist plastic deformation with the smallest overestimation corresponding to Case I which takes into account the shear and normal stresses acting on both the rake and flank faces of the tool. Case I represents the most realistic tool edge loading conditions and it is not surprising that this gives the best predictions. Experiments are now described which were made to check the effectiveness of the proposed method when extended to oblique machining conditions.

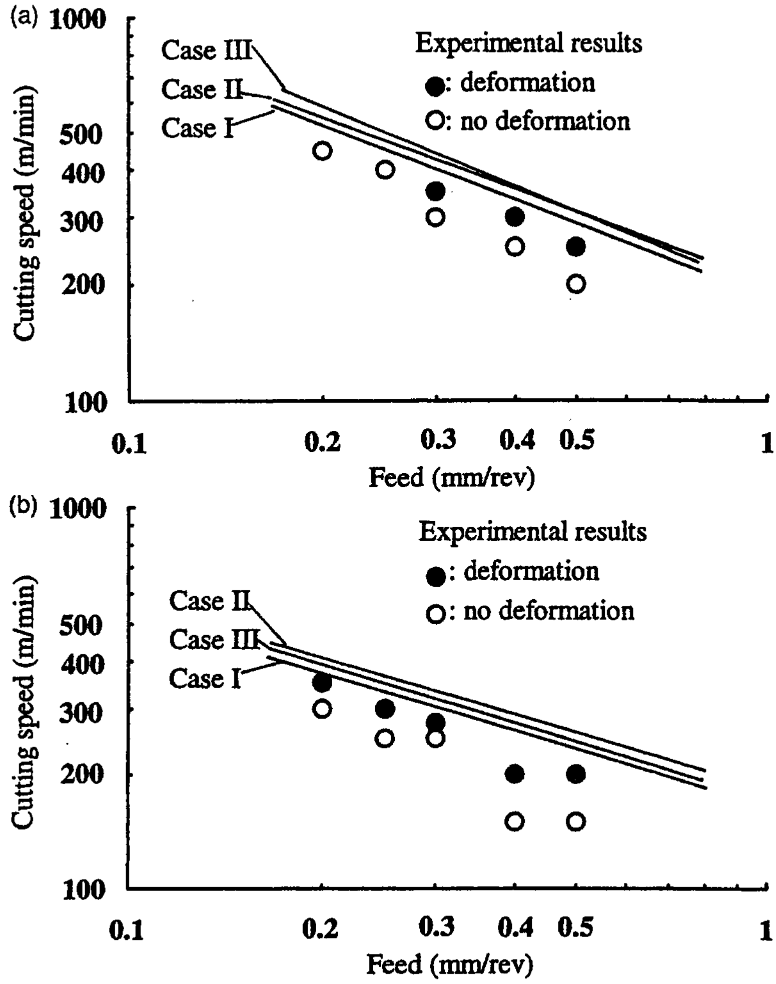

Fig. 5. Comparison between predicted and experimental plastic deformation cutting conditions: (a) 0.19%C steel; (b) 0.48%C steel.

6. Experimental procedure

The experiments were made on a lathe using a bar turning process under dry conditions. For each test condition, it was necessary to measure the plastic deformation of the cutting edge after machining for a predetermined time interval. Tool plastic deformation is affected by the work material, tool material, tool geometrical parameters, cutting conditions, etc. In order to keep the experiments to a manageable number priority was placed on the parameters having greatest relevance to the present investigation. The selected ranges of each parameter are given below.

1. *Work materials*. A nominal AISI-1045 plain carbon steel bar of chemical composition 0.45%C, 0.01%P, 0.66%Mn, 0.053%Si, 0.031%S, 0.01%Ni, 0.02%Cr, 0.01%Mo, 0.01%Cu and 0.001%Al was used as one work material. The other material used was a nominal AISI-1030

plain carbon steel bar with a chemical composition of 0.30%C, 0.013%P, 0.68%Mn, 0.26%Si, 0.011%S, 0.02%Ni, 0.01%Mo, 0.02%Cu and 0.025%Al.

2. *Tool material and tool geometry.* Uncoated P25 grade DNGA-150408 carbide inserts (without chipbreaker groove) with a chemical composition 7.6–8.4%TiC + 3.5%Co + 11–12%TaC were used on a PDNNR2525 tool holder. The tool geometrical parameters were normal rake angle $\alpha_n = -6°$, inclination angle $i = -6°$, nose radius $r_\varepsilon = 0.8$ mm, side cutting edge angle $C_s =$ 27° and clearance angle 6°.
3. *Cutting conditions.* Feeds $f = 0.2$, 0.25, 0.315, 0.4 and 0.45 mm/rev and depth of cut $d =$ 2.5 mm were used. The initial cutting speed in each test was selected to be approximately the same as the speed at which deformation was predicted to occur.

The machine tool used for the tests was a 37 kW Heidenreich and Harbeck VDF precision lathe having a variable speed motor with speeds 0–5600 rev/min. The available feed range was 0.01 to 0.71 mm/rev. The original DNGA-150408 inserts were provided with all faces ground by the manufacturer. The flank face of each cutting edge was checked for flatness using the same method adopted for checking plastic deformation which is to be described later in this section. Finally each cutting edge was numbered and randomly assigned to a test in order to minimise the influence of variations in work and tool material properties, etc.

For each test machining was carried out at a cutting speed which was selected to be approximately the same as the speed at which deformation was predicted to occur. If in this initial test no deformation was observed further tests were made with the speed increased in increments of 40 m/min until deformation was observed. If deformation was observed further tests were made with the speed decreased in increments of 40 m/min until no deformation was observed. In all tests it was found that 20 s machining time was sufficient for steady state conditions to be achieved.

A number of methods were tried for measuring the plastic deformation of the cutting edge, and the following method, although one of the simplest, gave the best results. The flank face of the tool which was expected to bulge outwards when plastic deformation has occurred was carefully cleaned to remove any adhering steel, etc. The flank face was then held firmly on a polished surface and the two surfaces were placed in front of a strong light and examined from the front. If deformation had not occurred the flank surface was flat and in close contact along its length with the polished surface thus there was no gap between the two surfaces and hence no light could be seen. If deformation had occurred then light could be seen through the resulting gap between the two surfaces which was formed due to the bulged out flank face near the cutting edge. With this method it was possible to detect even small amounts of plastic deformation occurring in the nose radius part of the tool flank face.

When the deformed inserts were further examined it was found that bulging out of the flank face had occurred in a small region near the cutting edge. This justifies the use of the equation for τ_{max} (Eq. (5)) which was derived for the region where uniform boundary stresses were assumed to apply.

7. Results and discussion

7.1. Determination of high temperature shear strength data for the tool material

In order to determine the predicted deformation conditions it was first necessary to determine the high temperature shear strength curve for the P25 grade carbide tools used in the experiments.

From the data given by Trent [3] it is clear that the hot compressive strength is directly related to the TiC content of the tool material with, at a given temperature, the 5% proof stress increasing with increase in TiC content. Since the P25 grade carbide used in the tests had 7.6–8.4%TiC, it was assumed that the curve representing its hot compressive strength would lie in the middle of the curves given by Trent [3] for tool materials of chemical composition WC + 5%TiC + 9%Co and WC + 12%TiC + 7%Co.

7.2. Comparison of predicted and experimental results

The lines given in Fig. 6(a) and (b) represent predicted speed/feed combinations for the 0.30%C and 0.45%C steels respectively at which the tool starts to deform plastically. The predictions were made using the procedure described above with the tool stresses corresponding to Case I assumed.

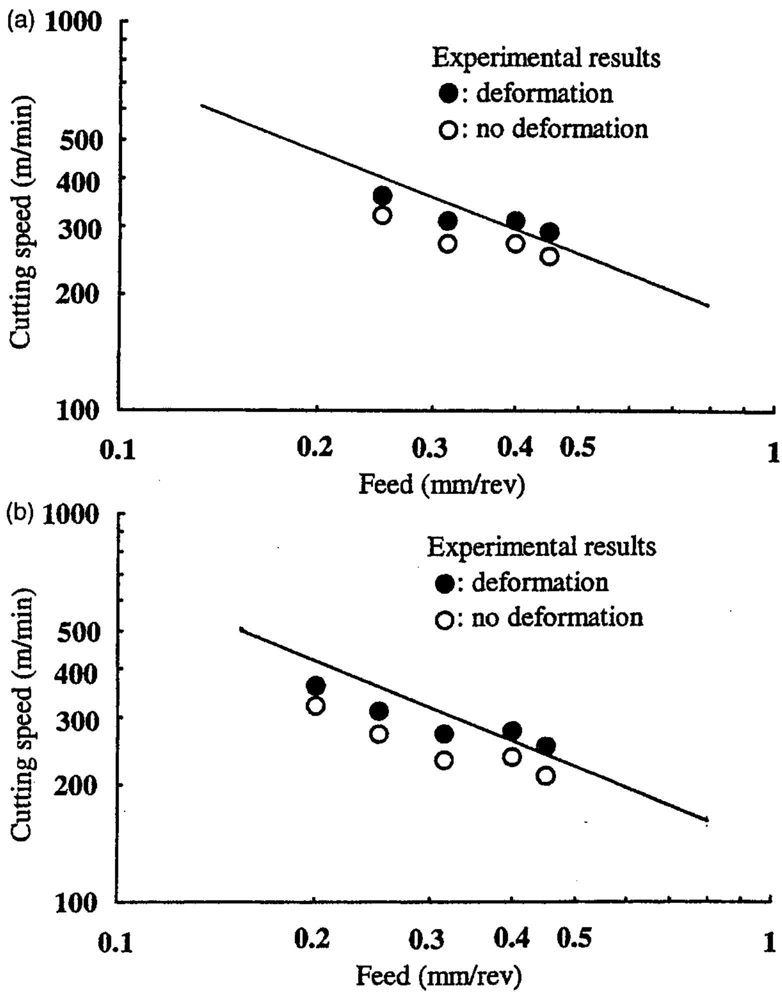

Fig. 6. Comparison between predicted and experimental plastic deformation cutting conditions: (a) 0.30%C steel; (b) 0.45%C steel.

Considering the relatively small inclination angles used with carbide tools it was also assumed that the two-dimensional stress analysis (Section 3) is applicable to oblique machining. The experimental results are given by the symbols with the filled in symbols indicating the cutting speeds at which plastic deformation was observed and the open symbols indicating cutting speeds 40 m/min lower at which no plastic deformation was observed. From Fig. 6 it can be seen that the predicted plastic deformation speeds show the same trends as the experimental results with reasonably good quantitative agreement. In particular the speeds which cause tool deformation can be seen to decrease with increase in feed and, at a given feed the speed which causes tool deformation can be seen to decrease with increase in carbon content of the steel work material. However the predictive method tends to overestimate cutting edge's resistance to plastic deformation, particularly at feeds below 0.4 mm/rev. One reason for this overestimation of the plastic deformation cutting speed is due to possible underestimation of the stresses acting on the tool flank face. Another reason is that the actual high temperature shear strength of the tool material could have been lower than that given by the assumed curve, which is for a tool material with approximately 8.5%TiC while the P25 grade tool material used in the tests had 7.6–8.4%TiC. The results given in Fig. 6 also confirm that it is necessary to take into account the stresses acting on both the rake and flank faces (Case I) of the tool in determining the plastic deformation conditions as Case II and Case III were found to result in greater overestimations. It is expected that the present level of agreement between predicted and experimentally observed deformation conditions will be sufficiently accurate for most practical applications including the prediction of optimum cutting conditions.

8. Concluding remarks

It has been shown how the cutting conditions that cause tool cutting edge plastic deformation can be predicted for oblique nose radius tools from a knowledge of the hot compressive strength of the tool material using machining theory combined with an analysis of the tool stresses. It is hoped to extend the method to tools with chip-breakers in the near future.

Acknowledgements

The authors gratefully acknowledge the valuable help rendered by Professor P.L.B. Oxley during the course of this work. Thanks are also due to BHP (Long Products Division in Newcastle) for providing some of the steels and the Australian Research Council for financial support.

References

[1] P.L.B. Oxley, The Mechanics of Machining: An Analytical Approach to Assessing Machinability, Ellis Horwood, Chichester, 1989.

[2] J.A. Arsecularatne, S. Hinduja, G. Barrow, Optimum cutting conditions for turned components, Proceedings of the Institution of Mechanical Engineers 206 (1992) 15–30.

[3] E.M. Trent, Hot compressive strength of cemented carbides, Proceedings of the 8th International MTDR Conference, Manchester, 1968, pp. 629–642.
[4] N.H. Cook, D.S. Goldberger, Machining parameter selection using on-line adaptive control, in On the Art of Cutting Metals —75 Years Later: A Tribute to F.W. Taylor, A.S.M.E. PED 7 (1982) 159–166.
[5] V.I. Nachev, P.L.B. Oxley, Predicting cutting conditions giving plastic deformation of the cutting edge in terms of tool and work material properties, Proceedings of the 25th International MTDR Conference, Macmillan, London, 1985, pp. 225–230.
[6] E. Kuljanic, Macro plastic deformation of cutting edge — a method for maximum utilisation of cutting tool, Annals of the CIRP 41 (1) (1992) 151–154.
[7] M. Kronenberg, Machining Science and Application: Theory and Practice for Operation and Development of Machining Process, Pergamon Press, Oxford, 1966.
[8] J.A. Arsecularatne, On tool–chip interface stress distributions, ploughing force and size effect in machining, International Journal of Machine Tools Manufacture 37 (7) (1997) 885–899.
[9] S.P. Timoshenko, J.N. Goodier, Theory of Elasticity, 3rd ed., McGraw-Hill, New York, 1987.
[10] William A. Nash, Schaum's Outline of Theory and Problems of Strength of Materials, 3rd ed., McGraw-Hill, New York, 1994.
[11] J.A. Arsecularatne, P. Mathew, P.L.B. Oxley, Prediction of chip flow direction and cutting forces in oblique machining with nose radius tools, Proceedings of the Institution of Mechanical Engineers 209B (1995) 305–315.
[12] J.A. Arsecularatne, R.F. Fowle, P. Mathew, P.L.B. Oxley, Prediction of cutting forces and built-up edge formation conditions in machining with oblique nose radius tools, Proceedings of the Institution of Mechanical Engineers 210B (1996) 457–469.
[13] J.A. Arsecularatne, R.F. Fowle, P. Mathew, P.L.B. Oxley, Prediction of tool life in oblique machining with nose radius tools, Wear 198 (1996) 220–228.
[14] P. Mathew, A theoretical and experimental investigation of the mechanics of machining. Ph.D. thesis, The University of New South Wales, 1983.
[15] Xiaoping Li, A computer-based numerical study of the role of cooling in machining, Ph.D. thesis, UNSW, 1991.
[16] V.I. Nachev, Obtaining a machinablity chart using a mechanics of machining approach, BE thesis, UNSW, 1983.
[17] S. Yakowitz, F. Szidarovszky, An Introduction to Numerical Computations, 2nd ed., Macmillan-Collier, 1990.